R-10-38

Preliminary Hydrogeochemical Site Description SFR (version 0.2)

Ann-Chatrin Nilsson, Geosigma AB

Eva-Lena Tullborg, Terralogica AB

John Smellie, Conterra AB

May 2010

Svensk Kärnbränslehantering AB
Swedish Nuclear Fuel
and Waste Management Co

Box 250, SE-101 24 Stockholm
Phone +46 8 459 84 00

ISSN 1402-3091
SKB R-10-38

Preliminary Hydrogeochemical Site Description SFR (version 0.2)

Ann-Chatrin Nilsson, Geosigma AB

Eva-Lena Tullborg, Terralogica AB

John Smellie, Conterra AB

May 2010

Keywords: SKBdoc id 1243511.

Abstract

The final repository for low and intermediate level radioactive operational waste, SFR, located about 150 km north of Stockholm, is to undergo a future extension. The present on-going project, scheduled from 2007 to 2011, is to define and characterise a suitable bedrock volume for the extended repository. This will include the drilling and geoscientific evaluation of seven core-drilled and four percussion boreholes as well as subsequent interpretation and modelling based on the obtained results in order to provide the necessary information for safety assessment and repository design. This report presents a preliminary hydrogeochemical site description for the SFR site and should be considered as an early progress report rather than a complete hydrochemical site descriptive model.

The completed hydrogeochemical field investigations have yielded chemical data from a total of 12 borehole sections in five boreholes and additional data from the entire length of two open boreholes in connection with hydraulic tests. These data, together with data from a total of 18 early boreholes in the present SFR tunnel system, were used in the interpretation work. The main part of the data consisted of basic groundwater analyses including major ions and isotopes. Some sporadic gas, microbe and measured redox data are available, but these are either not treated in this report, or are only briefly discussed. This was due to time constraints since special care is needed when interpreting few data of varying quality.

The groundwaters in the SFR dataset cover a maximum depth down to about –400 masl and represent a relatively limited salinity range (1,500 to 5,500 mgL^{-1}chloride). However, the $\delta^{18}O$ values show a wide variation (–15.5 to –7.5‰ V-SMOW) similar to that reported from the Forsmark site investigations /Laaksoharju et al. 2008/. At the SFR, marine indicators such as Mg/Cl, K/Cl and Br/CL also show relatively large variations considering the limited salinity range. From very few measured Eh values, and in accordance with the chemistry of Fe, Mn, S and U, it is concluded that mildly reducing conditions (–140 to –190 mV) generally prevail in the investigated groundwaters. This is in line with measured Eh values in brackish marine waters of Littorina type from the site investigations in Forsmark and Laxemar (PLU) /Auqué et al. 2008/.

Hydrogeochemical observations together with palaeoclimatic considerations were used to differentiate the groundwaters into four major types; 1) local Baltic Sea water type, 2) Littorina type water with a glacial component, 3) brackish glacial water type, and 4) mixed brackish water (transition type). Explorative analyses using traditional geochemical approaches have been performed to describe groundwater conditions (origin and evolution) and other properties (mixing and reactions) in more detail.

The division into groundwater types has facilitated interaction and integration with the hydrogeological models making it possible to construct a hydrogeochemical site descriptive model for the SFR site. The distribution of the different groundwater types shows that the major deformation zones have served as important groundwater flow pathways over long periods of geological time while single fractures in rock volumes between zones generally contain older and more isolated groundwater. Presently, the steeply dipping structures in particular have facilitated the drawdown of modern Baltic Sea water which has been observed since excavation and construction of the SFR some twenty years ago.

Understanding the evolution of the groundwater system over time, i.e. since the last glaciation and more recently since excavation and construction of the SFR repository, shows that: 1) present-day hydraulic conditions have preserved groundwater patterns which replicate to a large extent what will occur during the next deglaciation (long-term perspective), and 2) the future impact of extended excavations and underground construction on groundwater chemistry can be predicted from past to present-day observations at the SFR site (short-term perspective).

Sammanfattning

Vid slutförvaret för låg- och medelaktivt radioaktivt driftavfall, SFR, lokaliserat ca 150 km norr om Stockholm, planeras för en utbyggnad. Syftet med platsundersökningsprojektet, som omfattar tiden 2007–2011, är att definiera och karakterisera en lämplig bergvolym för denna utbyggnad. Detta inbegriper borrning och geovetenskaplig utvärdering av sju kärnborrhål och fyra hammarborrhål samt efterföljande tolknings- och modelleringsarbete baserat på erhållna resultat för att leverera nödvändig information för säkerhetsanalys och projektering. Denna rapport presenterar en preliminär hydrogeokemisk platsbeskrivning som omfattar SFR och aktuellt område för utbyggnaden och ska betraktas som en tidig lägesrapport snarare än en fullständig platsbeskrivande modell.

De avslutade hydrogeokemiska fältundersökningarna har bidragit med kemiska data från totalt 12 borrhålssektioner i fem borrhål samt ytterligare kemiska data från provtagningar i två öppna hela borrhål i samband med hydrauliska tester. Dessutom har data från totalt 18 tidiga borrhål i nuvarande SFR använts i tolkningsarbetet. Huvuddelen av datamängden består av vanliga grundvattenanalyser inkluderande huvudkomponenter och isotoper. Ett fåtal gas-, mikrob- och mätta redoxdata finns tillgängliga men är inte behandlade, eller är endast kortfattat diskuterade i rapporten. Detta på grund av tidsbrist eftersom tolkningen av dessa få data med varierande kvalitet kräver speciella insatser, bl a kompletterande geokemisk modellering.

Datasetet från SFR täcker ett maximalt djup ner till knappt –400 masl. och representerar ett relativt begränsat salinitetsintervall (1500 to 5500 mgL^{-1}klorid). Värdena för $\delta^{18}O$ däremot visar en större variation (–15.5 to –7.5 ‰ V-SMOW) vilket är samma intervall som har rapporterats från platsundersökningarna i Forsmark /Laaksoharju et al. 2008/. Marina indikatorer som Mg/Cl, K/Cl och Br/CL visar också relativt stora variationer med tanke på det begränsade intervallet i salinitet. Från ett fåtal uppmätta Eh värden och i överensstämmelse med kemin avseende Fe, Mn, S och U, görs ett generellt antagande att det råder måttligt reducerande förhållanden (–140 to –190 mV) i de undersökta grundvattnen. Detta är helt i linje med uppmätta Eh värden i bräckta marina vatten av Littorinatyp från platsundersökningarna i Forsmark och Laxemar (PLU) /Auqué et al. 2008/.

Hydrogeokemiska observationer tillsammans med beaktande av palaeoklimatet har använts för att differentiera grundvattnen i fyra huvudgrupper; 1) vatten av lokal Östersjötyp, 2) vatten av Littorina typ med en glacial komponent, 3) bräckt glacialt vatten, och 4) blandat bräckt vatten (övergångstyp). Det hydrokemiska datasetet har analyserats med hjälp av etablerade geokemiska metoder för att beskriva grundvattenförhållanden (ursprung och utveckling) och andra egenskaper (blandning och reaktioner) mer i detalj. Uppdelningen i vattentyper har underlättat samverkan och integration med de hydrogeologiska modellerna och möjliggjort konstruktionen av den hydrogeokemiska platsbeskrivningen för SFR. Distributionen av de olika vattentyperna i bergvolymen visar att de större deformationszonerna har tjänat som viktiga flödesvägar för grundvattnet under långa geologiska tidsperioder medan enstaka sprickor i bergvolymer mellan zoner generellt innehåller ett äldre och mer isolerat grundvatten. I nutid underlättar i synnerhet de brantstående zonerna för den inträngning av modernt Östersjövatten som har observerats sedan utsprängningen och konstruktionen av SFR, för cirka tjugu år sedan.

Förståelsen för utvecklingen av grundvattensystemet över tid, sedan den sista deglaciationen och fram till modern tid inkluderande utsprängningen och konstruktionen av SFR förvaret, visar att; 1) dagens hydrauliska förhållanden har bevarat grundvattenmönster som replikerar till stor del vad som förväntas bli resultatet av nästa deglaciation (långtidsperspektiv), och 2) framtida påverkan på grundvattenkemin från utgrävning och underjordskonstruktioner kan förutsägas från tidiga och senare observationer från nuvarande SFR (korttidsperspektiv).

Contents

1 Introduction

1.1 Background

During 2008, the Swedish Nuclear Fuel and Waste Management Company (SKB) initiated an investigation programme for a future expansion of the final repository for low and medium level radioactive operational waste, SFR, located about 150 km north of Stockholm. The repository was inaugurated in April 1988 and, at present, the stored waste volume is about 30,000 m^3 (total capacity is 63,000 m^3) consisting of operational waste from the Swedish nuclear power plants and radioactive waste from hospitals. The purpose of the investigations was to define and characterise a bedrock volume large enough to allow further storage of operational waste from existing Swedish nuclear power plants and future waste from the decommissioning and dismantling of nuclear power plant reactors /SKB 2008a/. Of several alternatives, a selected location was investigated southwest of the present SFR tunnel system, cf. Figure 1-1.

The geoscientific investigation programme for the SFR extension project is clearly less extensive than the previous PLU programme at Forsmark (henceforth referred to as the 'Forsmark site investigations' or 'PLU' /SKB 2008b/) and the number of drilled boreholes is comparatively few. The stated reasons are: 1) The candidate area is relatively small. 2) The investigation and construction phase as well as the operational phase have already provided a rather detailed understanding of the repository area and its vicinity. 3) The issues to consider in the safety assessment are somewhat different from PLU. The implication for the hydrogeochemical part of the investigation programme is, besides the more limited analytical protocol, that the number of new sampling locations (borehole sections) amounts to less than fifteen. However, when already available hydrogeochemical data from early SFR boreholes are included, and considering the small area, the data density for the SFR extension site turns out to be quite high.

The SFR site investigation, including also the interpretation and modelling work to follow, is based to a large extent on methodologies that were established during the preceding Forsmark site investigations (2002 to 2007) for a deep repository for high level radioactive waste. However, some aspects differ from PLU: 1) It is intended that the new storage capacity will connect with the existing SFR facility and thus the target area for the location of the extension is already defined, 2) Due to the differences in the waste inventory (e.g. the heterogeneous nature of the waste materials compared with spent fuel) and the probable absence of any engineered barrier (i.e. copper canister and bentonite backfill), the requirements on the rock mass and the groundwater chemistry may be somewhat greater for the SFR repository compared to the final repository for high level radioactive waste. 3) Assuming, therefore, that the bedrock itself will serve as the only barrier to radionuclide transport, which is not finally decided yet, the hydrochemical stability of the groundwaters both present and in the future will be a critical factor for long-term safety assessment. 4) The potential importance of colloids, microbes and gases in the mobility and transport of radionuclides given in the PLU will be of less significance for the SFR due to the short transport pathways and consequently have not been fully included in the analytical protocol.

The regional and local SFR model areas as well as the Forsmark site investigation local model area are shown in Figure 12. The SFR local model volume extends from elevation +100 masl (metres above sea level) to –300 masl, while the regional model volume extends from +100 masl to –1,100 masl. The coordinates defining the model areas are provided in Table 1-1.

Table 1-1. Coordinates defining the model areas for SFR in metres. RT90 (RAK) coordinate system.

Regional model volume		Local model volume	
Easting	Northing	Easting	Northing
1631920.0000	6701550.0000	1632550.0000	6701880.0000
1633111.7827	6702741.1671	1633059.2484	6702388.9854
1634207.5150	6701644.8685	1633667.2031	6701780.7165
1633015.7324	6700453.7014	1633157.9547	6701271.7311

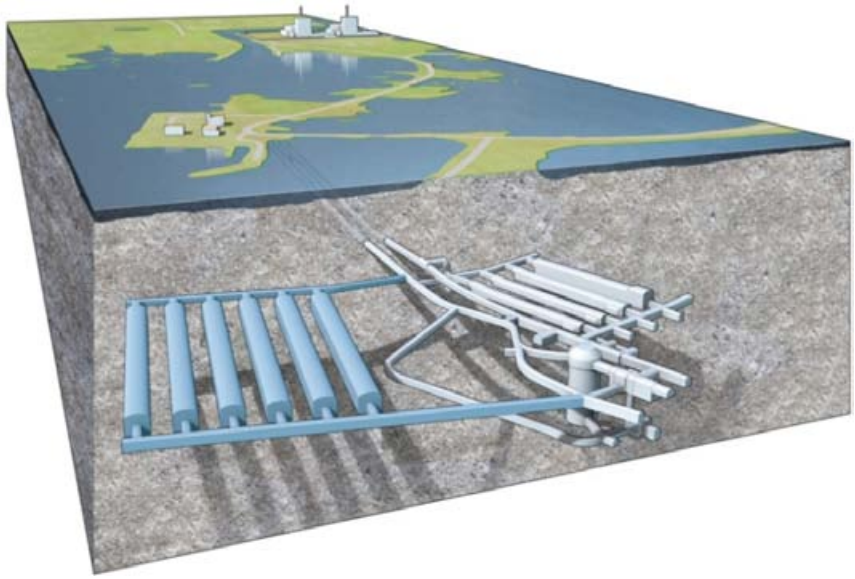

Figure 1-1. *One of several lay out proposals for the extension of the SFR repository. The present SFR repository is located to the right (light blue colour) while the planned new tunnel system is shown to the left (darker blue colour).*

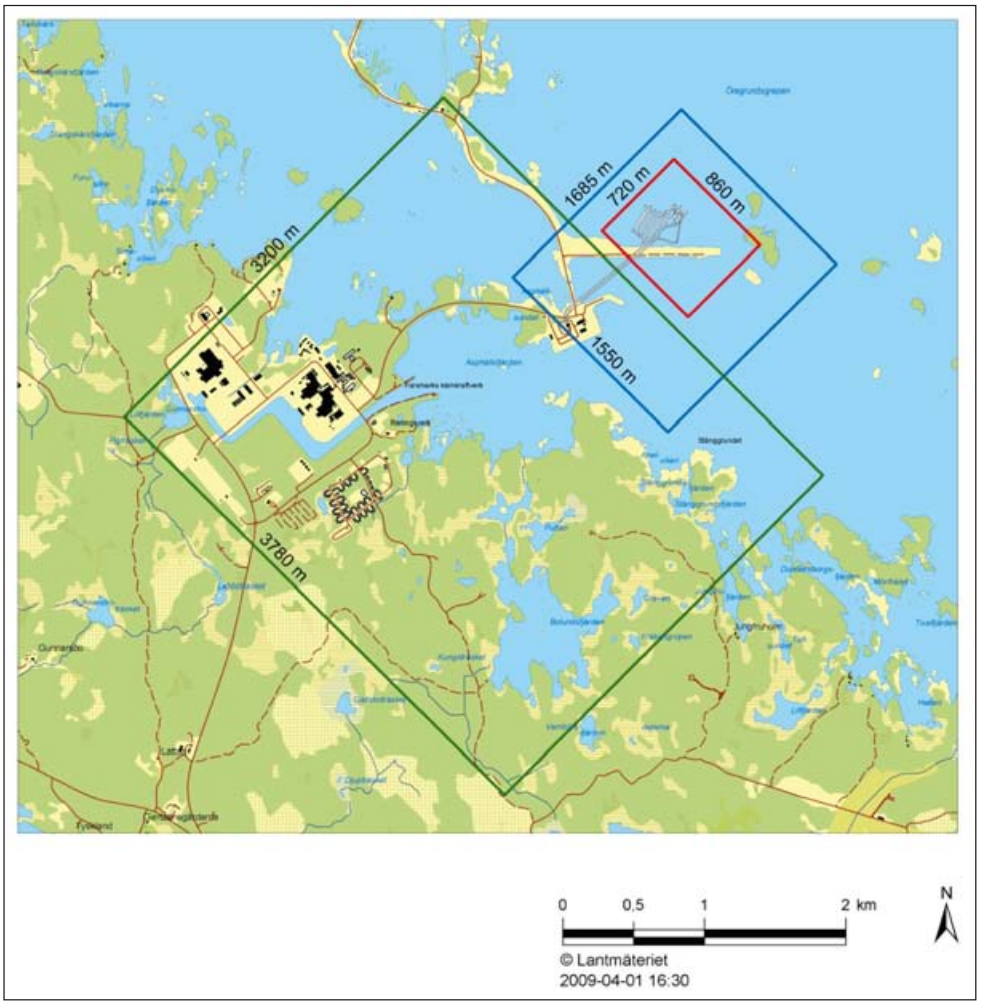

Figure 1-2. *Regional (blue) and local (red) model domains for SFR model v. 0.1, in relation to the local model area of the Forsmark Site Investigation, model v. 2.2 (green).*

1.2 Objectives and scope

The overall objectives of the hydrochemical interpretation and modelling work for the SFR site are to establish a detailed understanding of the hydrogeochemical conditions at the site, and to develop models to describe and visualise the site. The focus is to describe the chemistry, origin and the distribution of groundwaters in the bedrock and the hydrogeochemical processes involved in the evolution of the groundwaters. Hydrogeochemical information, for example, salinity distribution, groundwater residence time and palaeohydrogeochemical input are of concern also for the hydrogeology in order to constrain the hydrogeological descriptive model. The hydrogeochemical modelling work is to be performed in three steps, resulting in three model versions (0.1, 0.2 and 1.0).

Version 0.1, presented in SFR P-09-45 /Nilsson A-C 2009/, comprised a systematic data evaluation and retrospective QA of data from the early SFR boreholes, see Table 4-1, including the period 1984 to 2007, rather than the construction of a hydrogeochemical model. The hydrogeochemical data were extracted from the database Sicada (Sicada-08-200 0:1). A simple initial check of both borehole information and data was performed by comparison with corresponding SKB documentation in earlier reports from the SFR. Further evaluation was performed by using trend plots, different x-y scatter plots, charge balance calculations, and 3D visualisations of a few selected parameters/components (e.g. Cl, Mg and $\delta^{18}O$) etc. The main purpose was to become acquainted with the dataset and groundwater variability, as well as to discover inconsistencies and outliers among the data. The revealed errors were subsequently corrected in Sicada and questionable data were highlighted in the report.

The specific aim with this present version 0.2 interpretation and modelling work is to produce a preliminary hydrogeochemical site description model based on both the early SFR data and most of the new data from the SFR extension project (i.e. data deliveries Sicada-09-182 (0:1), Sicada-09-189 (0:1) and a few complementary data available in April 2010). Explorative analyses using traditional geochemical approaches have been performed to describe the data and to provide an early insight and understanding of the site, i.e. to construct a preliminary conceptual model. The groundwaters are interpreted in relation to their origin, evolution and composition, and the conceptual model is used to describe and visualise the site.

The final hydrogeochemical model version 1.0 will include also subsequent data from the SFR extension project and then all data will be further evaluated using additional modelling approaches and techniques. Model versions 1.0 from each discipline (Geology, Hydrogeology and Hydrochemistry) will be documented in background reports prior to being finally integrated into the SFR Site Descriptive Model version 1.0. The purpose of the final SFR SDM will be to fulfil the needs of the repository design and safety assessment groups.

1.3 Report structure

This report should be considered as an early progress report, documenting the initial achievements in the interpretation and modelling work, rather than a complete hydrogeochemical site description for the SFR site. Several important modelling approaches (e.g. geochemical equilibrium and M3 modelling) will be treated in report version 1.0.

Following the introduction, the geological and hydrogeological input is outlined in Chapter 2 and the evolutionary effects which have influenced the SFR site area from beyond and including the Holocene are presented in Chapter 3. This includes a preliminary palaeohydrogeochemical conceptual model adapted for the SFR site, based on the recent PLU conceptual model for the Forsmark site. The model forms the basis for the explorative analyses and especially for the identification/definition of the four different groundwater types, i.e. Local Baltic, Littorina type, Mixed transition type and Brackish glacial type. Chapter 4 focuses on the hydrogeochemical data, i.e. data availability, the databases, the quality assured and categorised data etc. and Chapter 5 describes data and information from other disciplines (geology and hydrogeology) that have been used to understand different water sampling aspects, or to construct the hydrogeochemical conceptual model presented in this report. Chapter 6 addresses the explorative analysis of the data, mainly centred on the four main groundwater types described in Chapter 3, by means of: a) scatter plots illustrating depth trends and the evolutionary relationships between major ion-ion/isotopes using cross plots, b) Eh and redox sensitive elements, c) groundwater

residence times, and d) changes in groundwater composition since construction of the SFR. The constructed preliminary conceptual hydrogeochemical SDM model is visualised and described in Chapter 7, and the main conclusions and future issues to be addressed are outlined in Chapter 8.

Besides necessary improvements and modifications, complementary interpretation and modelling work remains to be done and some important topics and issues are left to be treated in the Hydrogeochemical SFR Site description version 1.0, see Section 8.2.

1.4 Nomenclature and abbreviations

Table 1-1. Explanation of symbols, subscripts and abbreviations used in this report.

Symbol/abbreviation	Description
CCC	Complete Chemical Characterisation
CDT	Cañon Diablo Troilite (standard used for $\delta^{34}S$)
EC	Electrical Conductivity
^{13}C	Heavy stable carbon isotope
pmC	Percent Modern Carbon
Deuterium or ^{2}H	The heavy stable isotope for hydrogen
DOC	Dissolved Organic Carbon
Eh	Redox potential
Fe(II)	Ferrous iron
Fe(III)	Ferric iron
Tritium or ^{3}H	Radioactive hydrogen isotope, half-life=12.43 years
$^{14}C_{TIC}$	Radiocarbon in Total Inorganic Carbon
TIC	Total Inorganic Carbon
TOC	Total Organic Carbon
TDS	Total Dissolved Solids
^{32}S	Light Stable Sulphur Isotope
^{34}S	Heavy Stable Sulphur Isotope
Early SFR boreholes	Boreholes drilled between 1984 and 1987 from the present SFR tunnel system, see Figure 4-2.
Initial section water	Water present in the borehole section prior to pumping from the section.
Formation groundwater	Groundwater originating directly from fracture system in the bedrock
Forsmark site investigation	Site investigation in Forsmark (2002–2007)
PLU	Site investigation projects carried out in Forsmark and Oskarshamn (2002–2007) to select locations for the planned repository for radioactive waste. The PLU data notation in x/y scatter plots is restricted to data from the Forsmark site.
PFL logging	Flow logging using Posiva Flow Log equipment
BIPS	Borehole Image Processing System
Secup, Secmid, Seclow	Upper, midpoint and lower borehole section limit (mbl)
mbl	Metre borehole length (length measured from top of casing, the zero point, along the borehole)
masl	Metres above sea level. Coordinate system RT90- RHB 70
RHB 70	An improvement of the elevation reference system RH 70.
Silo	Silo shaped storage facility
BLA	*(Bergssalar för Lågativt Avfall)* Rock gallery for low level radioactive waste
BMA	*(Bergsalar för Medelaktivt Avfall)* Rock gallery for intermediate level radioactive waste
BTF1 and BTF2	*(Bergssalar för betongtankar)* Rock galleries to host concrete containers

Table 1-2. Zone nomenclature used in the SFR investigations, based on the system established during the Forsmark site investigation.

SFR terminology	Forsmark site investigation terminology
Singö zone	ZFMWNW0001
Zone H2	ZFM871
Zone 3	ZFMNNE0869
Zone 6	ZFMNNW1209
Zone 8	ZFMNW0805A
Zone 9a	ZFMNE0870A
Zone 9b	ZFMNE0870B

2 Geological and hydrogeological input

2.1 Geological setting

2.1.1 General

The geology of the Forsmark area has been described in /Olofsson et al. 2007, Stephens et al. 2007/ and the bedrock evolution from the Palaeoproterozoic through to the Quaternary in /Söderbäck 2008 /. The interplay between structural geological and hydrogeological features at Forsmark has been addressed in /Follin et al. 2007a, b, 2008a, b/. The geology of the SFR locality, lying just to the north-east of the Forsmark candidate site, is shown in Figure 2-1 and has been described by /Curtis et al. 2009/.

Summarised by /Curtis et al. 2009/, the SFR locality is situated within a high strain belt that forms the north-easterly margin to the so-called Forsmark tectonic lens, and is separated from the Forsmark area by the regionally significant Singö deformation zone which dips steeply and strikes WNW-ENE. The bedrock is dominated by different types of metamorphosed granitoid with subordinate felsic to intermediate metavolcanic rocks, metamorphosed diorite or gabbro, and pegmatite or pegmatitic granite (Figure 2-1). These rocks formed between 1.89 and 1.85 billion years ago (1.89–1.85 Ga).

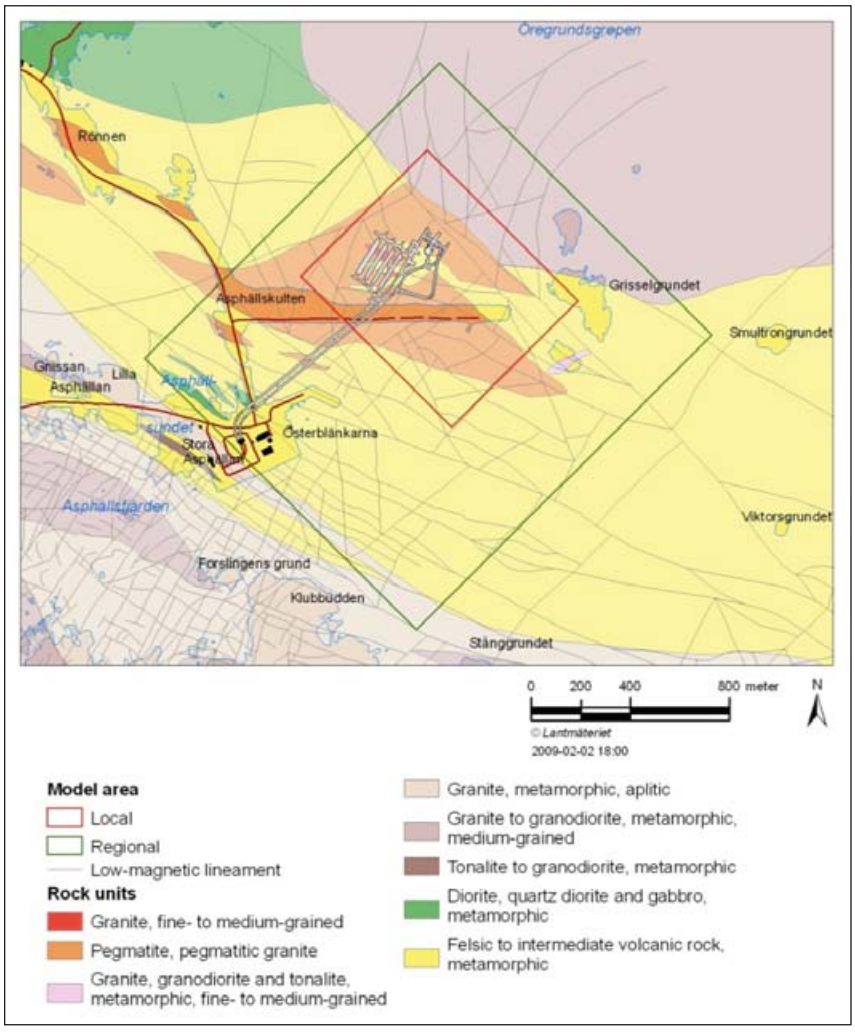

Figure 2-1. *Bedrock geological map of the area around SFR produced during the Forsmark site investigation. The inferred low magnetic lineaments in the area, based on model stage 2.3 in the Forsmark site investigation, and the local and regional SFR model areas, are also shown. The paler shades for each colour on the map indicate that the corresponding rock unit is under water /Curtis et al. 2009/.*

A penetrative, ductile tectonic fabric developed between 1.87–1.85 Ga during the Svecokarelian orogeny, when temperatures exceeded 600°C and the rocks were situated at mid-crustal depths. After 1.85 Ga, the rocks started to cool below 500°C. Areas where the bedrock is banded and/or affected by a strong, ductile tectonic foliation can be separated from areas where the bedrock is folded and more lineated in character (Figure 2-2). The former are inferred to have been affected by higher ductile strain. They anastomose around the more folded and lineated bedrock with lower ductile strain that is restricted to several tectonic lenses /Curtis et al. 2009/.

Following these early developments, ductile-brittle and brittle deformation occurred several times during the Proterozoic, related to major tectonic activity probably during the later part of the Svecokarelian (1.80–1.70 Ga), Gothian (1.70–1.60 Ga) and Sveconorwegian (1.10–0.90 Ga) orogenies. This has resulted in the activation and subsequent reactivation of the different fracture systems. A second geological process has also affected the bedrock at several times during the Proterozoic and Phanerozoic. This process involved loading by sedimentary rocks or by ice during cold, glacial periods and, subsequently, unloading related to denudation of this younger material. This process has occurred at several times during the long geological history of the bedrock and each unloading phase resulted in exhumation of the Proterozoic crystalline bedrock.

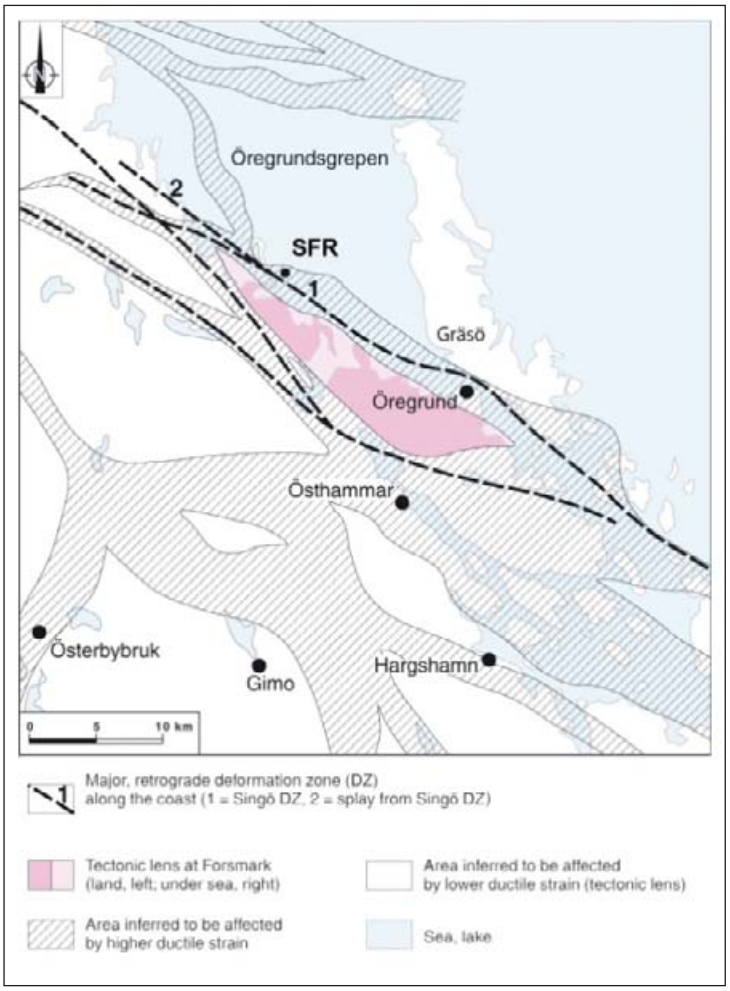

Figure 2-2. *Map showing the structural framework in the Forsmark area with ductile highstrain belts that anastomose around tectonic lenses of lower ductile strain. The major retrograde deformation zones surrounding the Forsmark tectonic lens are also shown /Curtis et al. 2009/.*

2.1.2 Major deformation zones

An earlier three-dimensional visualisation (Figure 2-3) of the most important deformation zones has been modified by including Forsmark site terminology and input from the Forsmark site investigations (PLU).

The modelled 0.1 version of major deformation zones (high confidence), i.e. those inferred to be 300 m or longer at the surface, as well as possible minor zones (low and medium confidence) within the local model area are shown in Figure 2-4. Three-dimensional visualisations of the vertical and steeply dipping deformation zones present at different strike directions are shown in Figures 2-5 and 2-6, and the gently dipping deformation zones in Figure 2-7 /Curtis et al. 2009/.

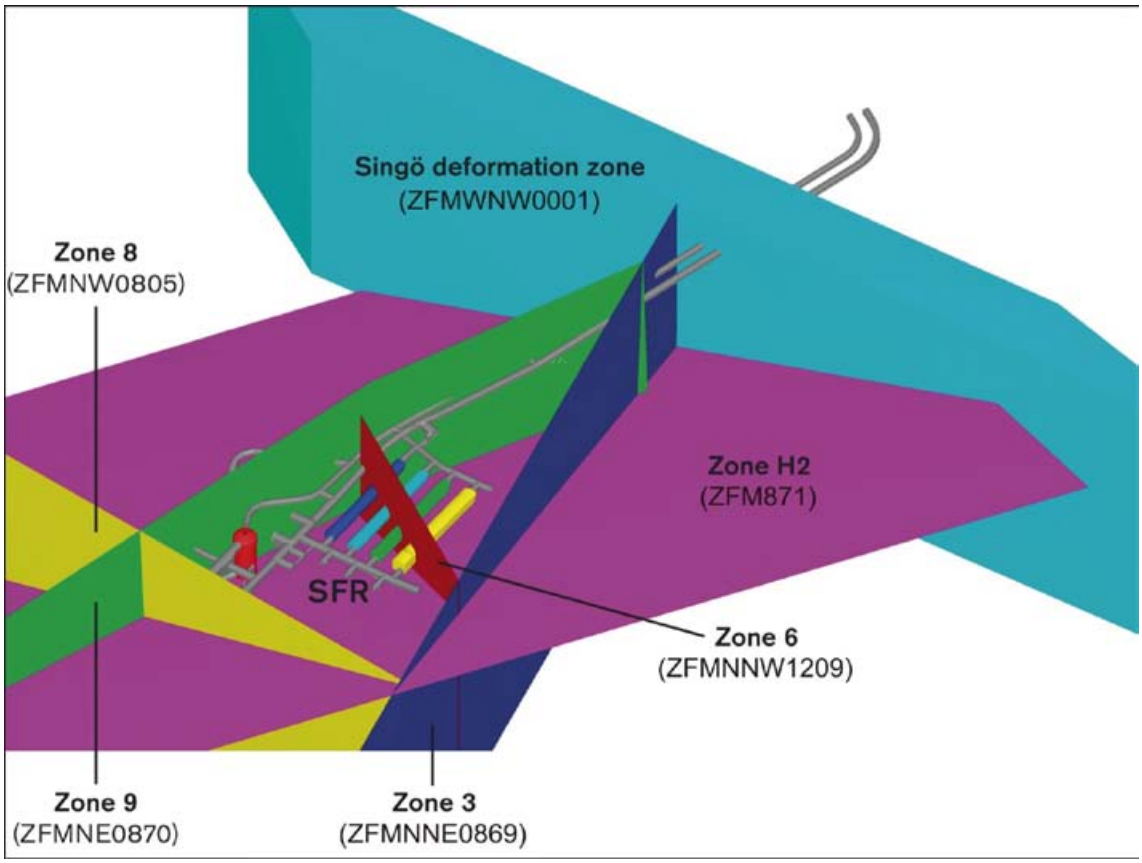

Figure 2-3. *Deformation zones and the general layout of the SFR tunnel systems in the local structural model updated by /Axelsson and Mærsk Hansen 1997/ and modified by including Forsmark site terminology and input from the Forsmark site investigations (PLU) after /Curtis et al. 2009/. View towards south. The deformation zone colour codings refer to Purple = H2, Dark Red = 6, Green = 9, Turquoise = Singö zone and Dark Blue = 3, and the tunnel coding to Grey = Access, Red = Silo, Dark Blue = BTF1, Light Blue = BTF2, Green = BLA and Yellow = BMA.*

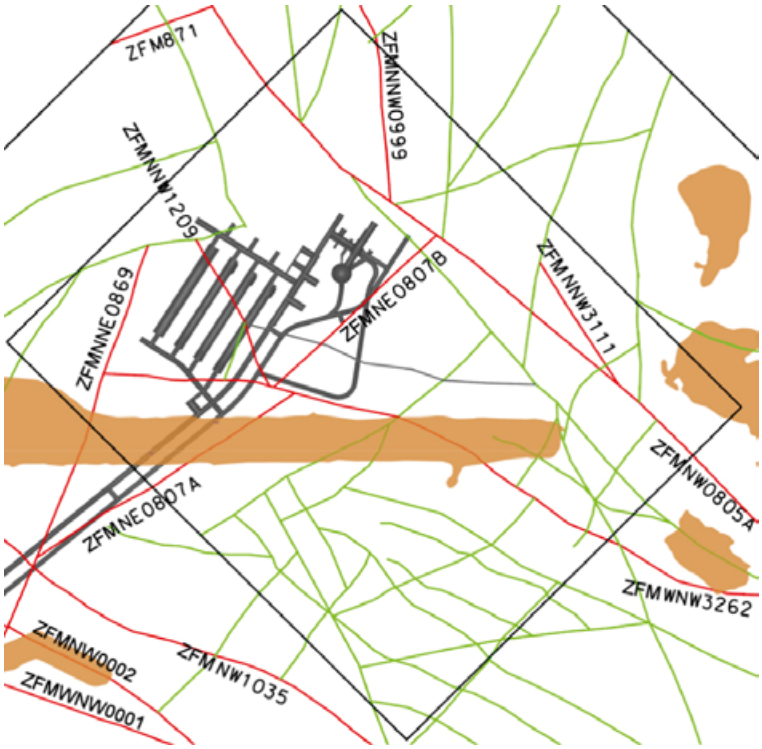

Figure 2-4. *Local model area (version 0.1) showing the intersection at the current ground surface of deformation zone traces. Degree of confidence: high=red, medium=green, low=grey /Curtis et al. 2009/. Light brown=Land, White=Sea.*

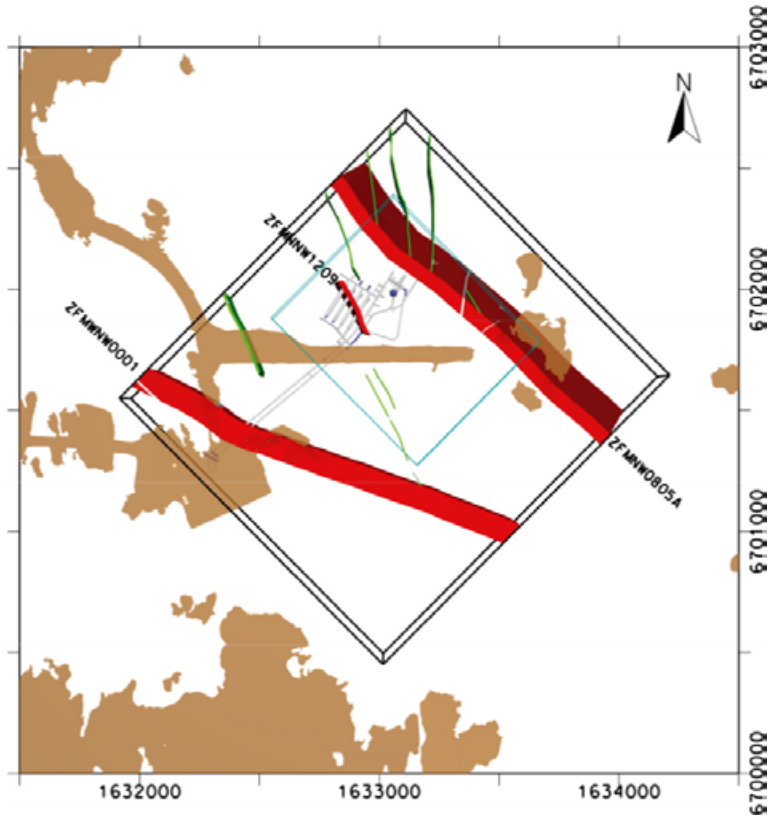

Figure 2-5. *Three dimensional model (version 0.1) of the steeply dipping deformation zones that strike NNW-SSE and N–S (NNW set) inside the local and regional model volumes. ZFMWNW0001 (Singö deformation zone) and ZFMNW0805A are included as reference. The colours of the zones refer to the degree of confidence where red = high and green = medium. /Curtis et al. 2009/. Light brown=Land, White=Sea.*

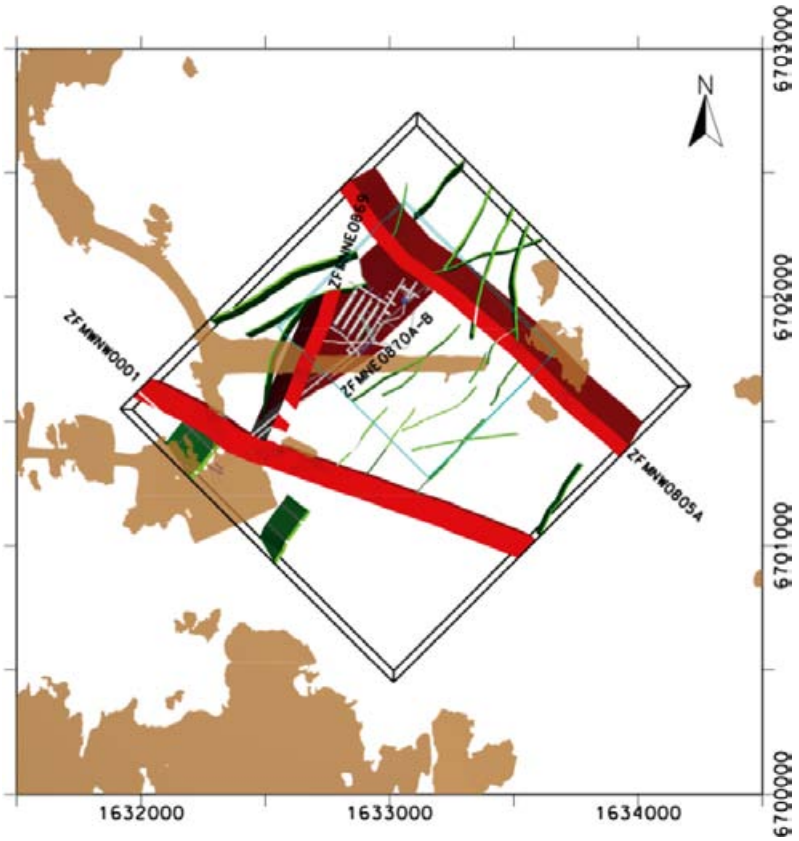

Figure 2-6. *Three dimensional model (version 0.1) of the steeply dipping deformation zones that strike NNE-SSW, NE-SW and ENE-WSW (NNE to ENE set) inside the local and regional model volumes. ZFMWNW0001 (Singö deformation zone) and ZFMNW0805A are included as reference. The colours of the zones refer to the degree of confidence where red = high and green = medium. /Curtis et al. 2009/. Light brown=Land, White=Sea.*

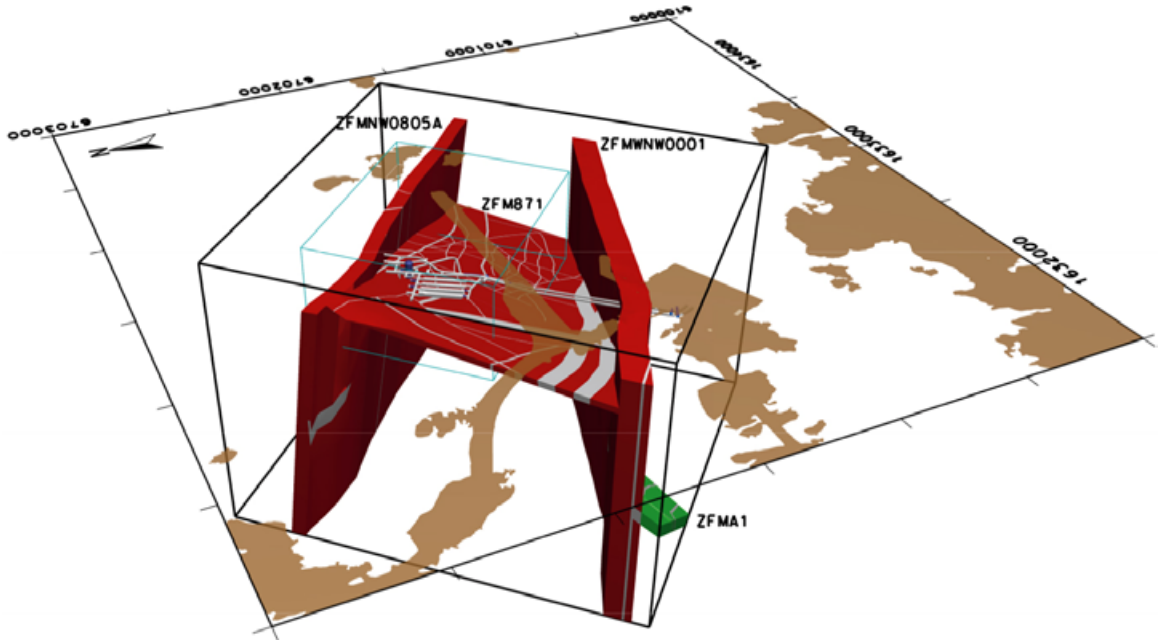

Figure 2-7. *Three dimensional model (version 0.1) of the gently dipping deformation zones (ZFMA1 and ZFM871) inside the local and regional model volumes. ZFMWNW0001 (Singö deformation zone) and ZFMNW0805A are included as reference. The colours of the zones refer to the degree of confidence where red = high and green = medium. /Curtis et al. 2009/. Light brown=Land, White=Sea.*

2.2 Hydrogeological setting

2.2.1 Regional surface and near-surface bedrock features

The SFR local and regional model areas lie within the Baltic Sea area, including only as landmass the surface locality of the SFR radioactive waste facility, the topographic feature of Asphällskulten, and the shallow banks of Grisselgrundet to the north-east (regional model), and the most northeastern extension part of Asphällskulten (local model) (Figure 1-2 *regional and local version 0.1 model areas*). Here, the Baltic Sea is shallow with a current depth of about 2–6 metres in the area where the SFR deposition tunnels are located, and the deposition tunnels are about 600 metres off the shoreline.

Both regionally and locally the general trend of the topography is a smooth lowering of the topographic elevation towards the north-east. This is shown in Figure 2-8 which presents the topography both above and below the present shoreline.

Investigations of the sea bed at the SFR /Sigurdsson 1987/ reveal that the fractured bedrock is mainly covered by a glacial till (moraine) of varying thickness containing large amounts of boulders and small amounts of fine-grained material. At present, there is no continuous layer of fine-grained sediments (e.g. clay) covering the sea bed above the SFR. According to /Sigurdsson 1987, Follin et al. 2008a/ the hydraulic conductivity of the glacial till is estimated to be within a range of 10^{-8} to 10^{-5} m/s, although for the PLU modelling somewhat lower hydraulic conductivities were used based on a considerable simplification of the detailed geometrical description of the near-surface system

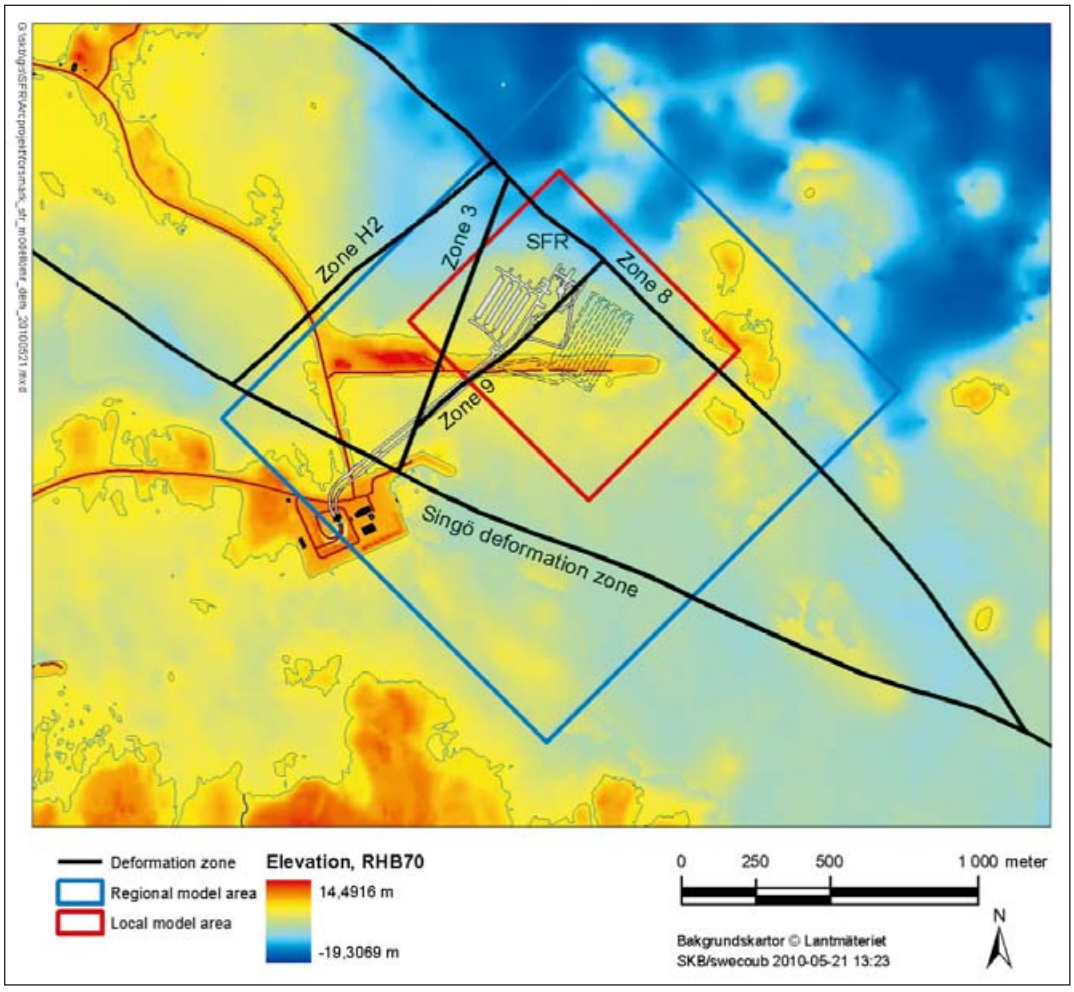

Figure 2-8. *The regional topography denoting the regional model area (blue rectangle) and the local model area (red rectangle) as well as showing the central location of the SFR waste facility, and the major fracture zones (black).*

/Follin et al. 2008a, Hedenström et al. 2008/. Based on the earlier data, /Sigurdsson 1987/ pointed out that on average the quaternary deposits have a hydraulic conductivity that is larger than the average hydraulic conductivity of the underlying rock mass (presented below).

During the Forsmark site investigations a shallow, highly transmissive bedrock aquifer was shown to play an important role in the rapid flushing of groundwater in the upper approximately 150 m of bedrock towards the north-east (i.e. towards the SFR site) /Follin et al. 2008a/. However, this shallow bedrock aquifer was considered to be truncated by the large-scale NW-SE trending regional Singö deformation zone, with no strong evidence of its extension into the SFR local model area (Figure 2-9). This conclusion is now being questioned based on observations of a shallow zone at about 120–140 m depth comprising horizontal/near horizontal transmissive fractures which appear to extend east from the Singö deformation zone, possibly linking up with the subhorizontal deformation zone H2. This is supported by the stress situation on the SFR-side of Singö which is similar to that west of Singö, and therefore it is likely that similar hydraulic structures can exist within the SFR-domain (even if not equally conductive, and even if not connected across Singö) /J. Öhman, pers. comm. April 2010/.

2.2.2 Local model bedrock features

Figure 2-3 of the local structural model shows the relationship between the most important deformation zones and their intersection of the deposition tunnel systems /Curtis et al. 2009/. Tables 2-1 and 2-2 list the results of the single hole packer tests and interference tests between selected boreholes, respectively /Öhman and Follin 2010/.

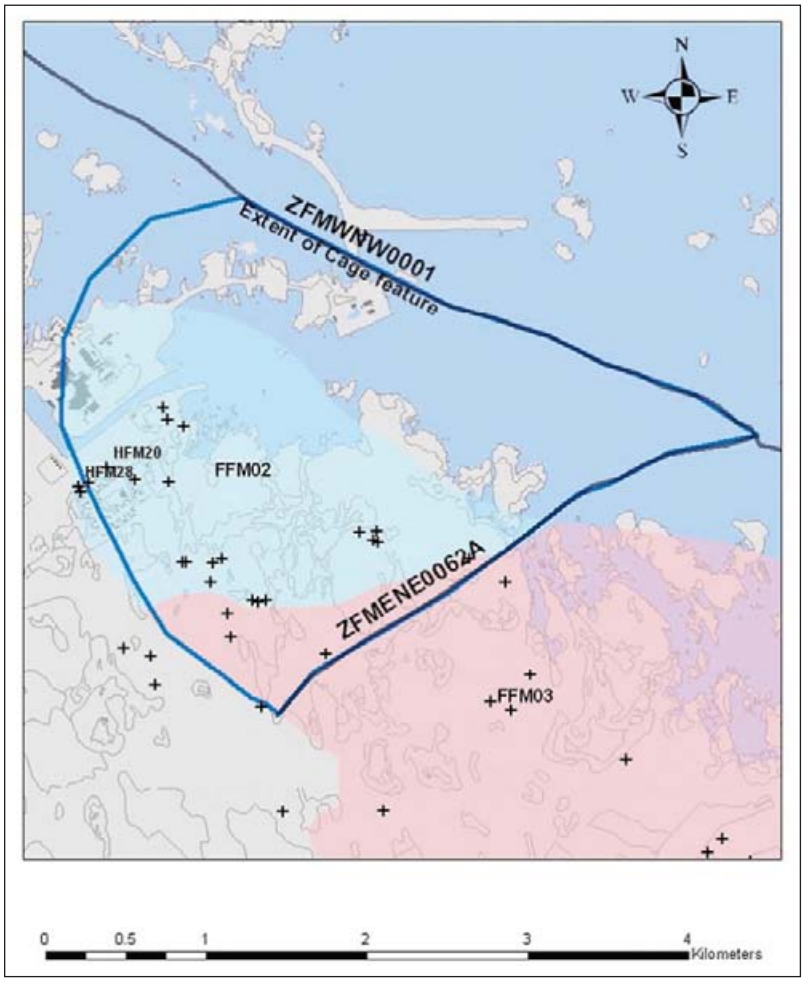

Figure 2-9. *The estimated lateral extent of the shallow bedrock aquifer (referred to in the figure as the now obsolete 'cage feature') covering the Forsmark target area /Follin et al. 2007a, b/*

Table 2-1. Individual effective ground level HCD transmissivity (Hydraulic Conductor Domain) from single hole packer tests /Öhman and Follin 2010/.

HCD	Alias	Retained intercepts	Rejected intercepts	$\mu_{log\ To}$	$\sigma_{log\ To}$
ZFM871	H2	15	3	–4.5	0.7
ZFMnw0805	Zone8	8	3	–4.9	1.1
ZFMne0870	Zone9	5	4	–5.6	0.9
ZFMnne0869	Zone3	5	1	–4	0.5
ZFMwnw0001	Singö	2	2	–3.6	0.5
ZFMnw1035	–	3	0	–3.3	0.5
ZFMwnw0804	–	2	1	–3.8	1.2
ZFMnnw0999	–	2	0	–6	1.3
ZFMnnw1209	Zone6	2	0	–5.1	0.5
ZFMwnw0813	–	2	1	–4.4	2.1
ZFMwnw3262	–	1	1	–4.6	–
ZFMwnw2496	–	1	1	–4.2	–
ZFMwnw3259	–	1	1	–4.2	–
ZFMnne2308	–	1	0	–5.4	–
Total		50	18	–4.6	1.0

$\mu_{log\ T0}$ =logarithmic T0 (T0 = ground level transmissivity (m^2/s))

$\sigma_{log\ T0}$ =standard deviation in logaritmic T0

Table 2-2: Ground level transmissivities (T0) from crosshole interference tests /Öhman and Follin 2010/.

Number of data	Observed section					
Pumped section	Zfm871 (zone H2)	Zfmne0870b (zone 9b)	Zfmnne0869 (zone 3)	Zfmnnw0999	Zfmnw0805a (zone 8a)	Zfmnw0805b (zone 8b)
Zfm871	12	6	4	3	4	0
Zfmne0870b		4				
Zfmnnw0999	2				2	1
Zfmnw0805a	2				2	1
T0 (Geometric mean)	**Observed section**					
Pumped section	Zfm871 (zone H2)	Zfmne0870b (zone 9b)	Zfmnne0869 (zone 3)	Zfmnnw0999	Zfmnw0805a (zone 8a)	Zfmnw0805b (zone 8b)
Zfm871	2.1E-05	8.4E-06	2.2E-04	1.8E-05	1.9E-05	
Zfmne0870b		2.8E-07				
Zfmnnw0999	2.5E-05				1.9E-05	6.9E-06
Zfmnw0805a	2.5E-05				1.9E-05	6.9E-06
T0 (Arithmetic mean)	**Observed section**					
Pumped section	Zfm871 (zone H2)	Zfmne0870b (zone 9b)	Zfmnne0869 (zone 3)	Zfmnnw0999	Zfmnw0805a (zone 8a)	Zfmnw0805b (zone 8b)
Zfm871	3.8E-05	9.1E-06	2.5E-04	1.9E-05	2.0E-05	
Zfmne0870b		3.0E-07				
Zfmnnw0999	5.0E-05				2.9E-05	6.9E-06
Zfmnw0805a	5.0E-05				2.9E-05	6.9E-06

T0 = the hydraulic transmissivity at the ground surface (m^2/s). The depth dependency in HCD transmissivity is assumed to follow an exponential model and T at the elevation z is calculated according to:

$$T(z) = T(0)10^{z/k}$$

where T(z) is transmissivity at elevation z (RHB70), T(0) is the expected transmissivity at zero elevation (=10 μlog To), and k is the depth interval over which transmissivity decreases one order of magnitude (=232 m).

These data underline the moderately high hydraulic conductivities of especially deformation zones H2 and 3, and less so for zones 6 and 8, and the low hydraulic conductivity which characterises zone 9. Zone 3 is the most permeable zone giving a geometric mean value of the ground level hydraulic transmissivity of $2.2 \cdot 10^{-4}$ m^2/s. These observations, together with the strong hydraulic connection between zones H2 and 3, are of importance when evaluating the hydrochemical data.

For the rock mass around the tunnels and between the interpreted fracture zones, /Holmén 2005/ gives a hydraulic conductivity value between about $2 \cdot 10^{-9}$ m/s and about $7 \cdot 10^{-9}$ m/s. For the rock mass nearer the sea floor (from the sea floor to a depth of about 25 m beneath the sea floor), the conductivity is estimated to be an order of magnitude greater. On-going revision of these data and the use of new modelling approaches may result in modifications to these conclusions /J. Öhman, pers. comm. April 2010/.

2.2.3 Evidence of time-related changes

Crucial to the hydrogeochemical evaluation is to understand the hydraulic changes that may or may not have taken place at the SFR since the initial drilling and site investigation stage, the subsequent excavation and construction stage, the present day operational stage, and predictions of post-closure conditions.

Initial drilling and site investigation phase (1980–1983)

Hydraulic test data are available from the initial drilling stage from 1980–1981 and from the second phase in 1983. Different tests have been carried out but in principal have involved conventional water pressure tests, falling head tests, transient injection tests, and pressure build-up tests /Carlsson et al. 1985/.

The hydrology of the initial 'undisturbed' bedrock prior to the excavation/construction phase has been revisited recently by /Svensson and Follin 2009/. Using post-construction data comprising a total measured inflow rate of 4.8–6.0 L/s and groundwater levels measured at 11 boreholes, simulations were carried out on the pre-construction situation. The simulations agreed with the measured field data suggesting that a discharge area once characterised the SFR locality /Holmén and Stigsson 2001a/.

With respect to hydrochemical data, none exist from these two drilling campaigns.

Excavation/construction phase (1984–1988)

In this phase hydrogeological studies have included measurement of groundwater inflow into boreholes drilled horizontally from the front of the two parallel access tunnels during their construction. These data were used to establish average inflow values per metre of borehole versus tunnel section, and further to calculate the hydraulic conductivity values for each of the tunnel sections /Carlsson et al. 1985/.

With respect to hydrochemical data during the construction stage, the first hydrochemical investigation was performed by IMAB (analytical laboratory) from 1984 to October 1986, and the second investigation by SKB from November 1986–1987.

Operational phase (1988 onwards)

Measured groundwater inflow

The important zones where groundwater inflow was measured are indicated in Figure 2-10 and have the following properties /Holmén 2005/.

- Zone H2 is a subhorizontal fracture zone that strikes to the NE and dips about 15–20° to the SE. It is a complex, heterogeneous zone with varying geological and hydraulic properties and is present in both the local and regional scale model areas. The transmissivity has been estimated to be 1.6×10^{-7} to 1.6×10^{-5} m^2/s and the hydraulic conductivity to be 1.5×10^{-8} to 1.5×10^{-6} m/s.
- Zone 3 strikes to the NNE and has an almost vertical dip. It is a composite zone, consisting of several narrower zones and fractures which diverge and converge forming complex patterns. The transmissivity has been estimated to be 2.06×10^{-6} to 2.06×10^{-4} m^2/s and the hydraulic conductivity to be 3.2×10^{-7} to 3.2×10^{-5} m/s.

- Zone 6 strikes to the NNW and has an almost vertical dip. It represents for most of its length a slightly water-bearing gouge-filled joint, occasionally with increased fracturing on one or both sides. The transmissivity has been estimated to be 3.3×10^{-7} to 3.3×10^{-5} m^2/s and the hydraulic conductivity is 2.0×10^{-7} to 2.0×10^{-5} m/s.
- Zone 8 strikes towards the NW and has an almost vertical dip. It is characterised by increased jointing and a gneissic foliation of the host rock. The transmissivity has been estimated to be 3.7×10^{-7} to 3.7×10^{-5} m2/s and the hydraulic conductivity is 1.1×10^{-9} to 1.1×10^{-7} m/s.
- Zone 9 strikes to the ENE and has an almost vertical dip. It is for most of its length a water-bearing gouge-filled joint, occasionally with increased fracturing on one or both sides. The transmissivity has been estimated to be 3.5×10^{-8} to 3.5×10^{-6} m^2/s and the hydraulic conductivity is 1.1×10^{-9} to 1.1×10^{-7} m/s.

Zones H2 and 6 are important zones for the groundwater flow in the close vicinity of the deposition tunnels. Zone H2 is a sub-horizontal zone which intersects the access tunnels below the SILO; however, the zone does not intersect the access tunnels close to the BMA storage tunnels. Zone 6 is a vertical zone that intersects the deposition tunnels BTF1, BTF2, BLA and BMA, but not the Silo.

During the construction and operational phases groundwater has drained into the excavated tunnel system and a lowering of the groundwater head has occurred in the rock mass surrounding the SFR tunnels, compared to 'undisturbed' conditions (without the tunnels). During the construction stage from 1986/87 about 50% of the total inflow of ~ 650 $Lmin^{-1}$ originated from the major Singö deformation zone and the subhorizontal zone H2 /Christiansson and Bolvede 1987/. A compilation of the measured groundwater inflow to the tunnels at SFR since 1992 is given in /Axelsson 1997/ and summarised below from /Holmén and Stigsson 2001a, b/.

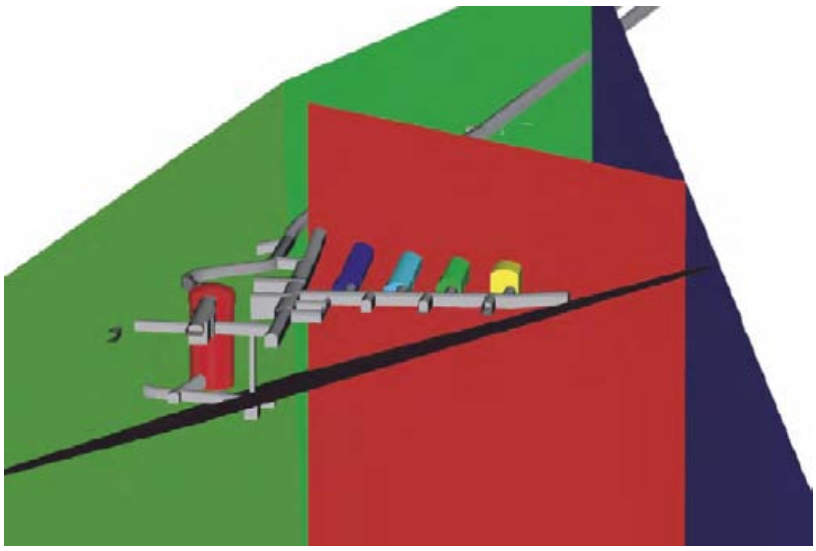

Figure 2-10. *Close-up view of the important deformation zones in relation to the layout of the SFR deposition tunnels. The deformation zone colour codings refer to Black = H2, Dark Red = 6, Green = 9 and Dark Blue = 3, and the tunnel codings to Grey = Access, Red = Silo, Dark Blue = BTF1, Light Blue = BTF2, Green = BLA and Yellow = BMA /from Holmén 2005/.*

Since the regular measurements (four times per year) started in 1992, there has been a decreasing trend in the measured inflow. Between 1992 and 1997 the following changes were recorded:

- The inflow to the entrance tunnels decreased from 419 to 375 L min^{-1} (an –11% change in inflow).
- The inflow to the loading buildings and minor tunnels decreased from 10.6 to 6.0 L min^{-1} (–43%).
- The inflow to the **Silo** decreased from 2.1 to 1.6 L min^{-1} (–25%).
- The inflow to the **BMA** decreased from 11.8 to 9.3 L min^{-1} (–21%).
- The total inflow to **BLA** and **BTF** tunnels as well as to surrounding tunnels decreased from 98.2 to 83.6 L min^{-1} (–15%).

The changes therefore were very small and the values of inflow with respect to 1997 can be assumed as representing close to a steady state situation. However, it was stressed by /Holmén and Stigsson 2001a, b/ that there were uncertainties in connection to the measurements of the inflow.

Subsequent inflow measurements up to 2006 indicated that the previously noted declining trend in total pumped-out volumes of water appeared to have levelled off. The total flow, which was 44 m^3/h in 1988, had declined to a stable value of about 20 m^3/h in 2006 /Bodén and Lundin 2007/. The increased inflow in BMA during 2006 was attributed to the installation of a new water meter that year.

During the operational phase from 1989 onwards a hydrochemical monitoring control programme was initiated /Nilsson A-C 2009/.

Modelled groundwater inflow

Figure 2-11 from /Svensson and Follin 2009/ based on particle trajectories in a west to east vertical cross-section shows the extent of the area influenced by groundwater inflow to the SFR during the excavation/operation phase. As expected, most of the inflow occurs around the excavation site, but some inflow originates at some distance towards the west at shallow depths, possibly corresponding to the shallow horizontal/subhorizontal zone mentioned above (cf. Section 221).

Post-closure

Forward, predictive modelling following closure and resaturation of the SFR may provide some insight into the expected hydraulic conditions; has been carried out by /e.g. Holmén and Stigsson 2001a, b, Odén 2009/. In such a scenario, as long as the sea covers the repository area, the regional flow in the surroundings of the SFR as well as the flow in the deposition tunnels will be small. Any flow present will be nearly vertical and directed from great depths towards the sea bed, i.e. a return to pre-excavation/construction conditions. In the event of a retreating shoreline, the general direction of the groundwater flow will change to a more horizontal flow and the magnitude of the groundwater flow will increase.

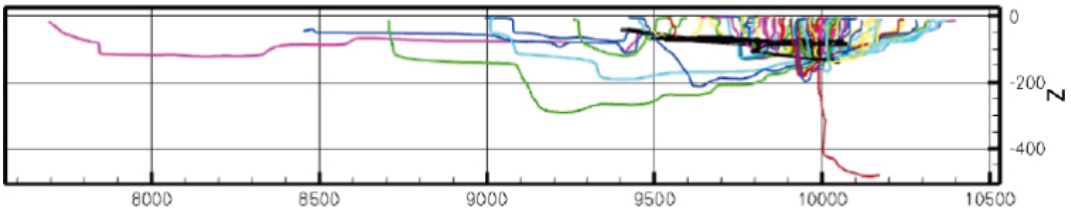

Figure 2-11. *Vertical visualisation along a left to right, W-E cross-section showing backward-tracking particle trajectories with inflow rates > 0.1 L/min. (y-axis points North and represents vertical depth in metres; x-axis represents horizontal distance in metres.) /Svensson and Follin 2009/*

3 Evolutionary effects

Past climatic changes, which in the Forsmark region has involved both glaciations/deglaciations and marine transgressions/regressions, are the major driving forces for long term hydrogeochemical changes and are therefore of fundamental importance for understanding the palaeohydrogeological, palaeohydrogeochemical and present evolution of the groundwater in the region. This section is devoted to a description of the Quaternary evolution in the area in order to provide the required background to interpret the present groundwater system.

3.1 Quaternary evidence

3.1.1 After the last deglaciation

Quaternary studies have underlined the importance of major crustal movements that have affected and continue to affect northern Europe following the melting of the latest continental ice mass, i.e. the Weichselian glaciation. These show the interplay between isostatic recovery on the one hand and eustatic sea level variations on the other. The net effect of these two processes in terms of elevation is called shore level displacement /Påsse 1997/. Detailed descriptions of the development at Forsmark after the last deglaciation, including shore level displacement and the development of the Baltic Sea, is given in /Söderbäck 2008, Follin et al. 2008a, b, Smellie et al. 2008/ and is summarised below.

In northern Sweden, during the Weichselian glaciation, the heavy continental ice at its maximum depressed the Scandinavian Shield by as much as 800 m below its present altitude. Shortly after this glacial maximum, a marked climatic change occurred about 18,000 years ago, and the ice started to retreat, a process that was completed after some 10,000 years. This was followed by a major standstill and, in some areas, a readvance of the ice front during a cold period ca. 13,000 to 11,500 years ago. The end of this cold period at approximately 10,000 years ago marked the onset of the present interglacial, the Holocene, whereupon the ice retreated more or less continuously during the early part.

As soon as the vertical stress decreased after the ice recession, the basement and crustal rocks started to slowly rise (isostatic rebound). This uplift started before the final deglaciation and, importantly, is still an active process in most of Sweden where the current rate of uplift is around 6 to 7 mm per year in the Forsmark region.

Figure 3-1 and table 3-1 show the aquatic evolution in the Baltic basin since the last deglaciation characterised by a series of brackish and fresh water stages which are related to changes in sea level. This evolution has been divided into four main stages: the Baltic Ice Lake, the Yoldia Sea, the Ancylus Lake and the Littorina Sea /Björck 1995, Fredén 2002/. The most saline period during the Holocene occurred approximately 4500 to 3000 BC, when the surface water salinity in the Littorina Sea was 10 to 15‰ compared with approximately 5‰ today in the Baltic Sea /Westman et al. 1999/.

Table 3-1 Evolution of the Baltic Sea basin since the last deglaciation /Follin et al. 2008b/.

Baltic stage	Calender year BC	Salinity	Environment in Forsmark
Baltic Ice Lake (not applicable in Forsmark)	13,000 to 9500	Glacio-lacustrine	Covered by inland ice.
Yoldia Sea (perhaps not applicable in Forsmark)	9500 to 8800	Lacustrine/Brackish /Lacustrine	At the rim of the retreating inland ice.
Ancylus Lake	8800 to 7500	Lacustrine	Regressive shoreline from about 140 to 75 m elevation RHB 70 (elevation reference system, see section 1.4).
Littorina Sea (® Baltic Sea)	7500-present	Brackish	Regressive shoreline from about 75 to 0 m at SFR. Most saline period 4500 to 3000 BC. Present-day Baltic Sea conditions have prevailed during the last ca. 2,000 years.

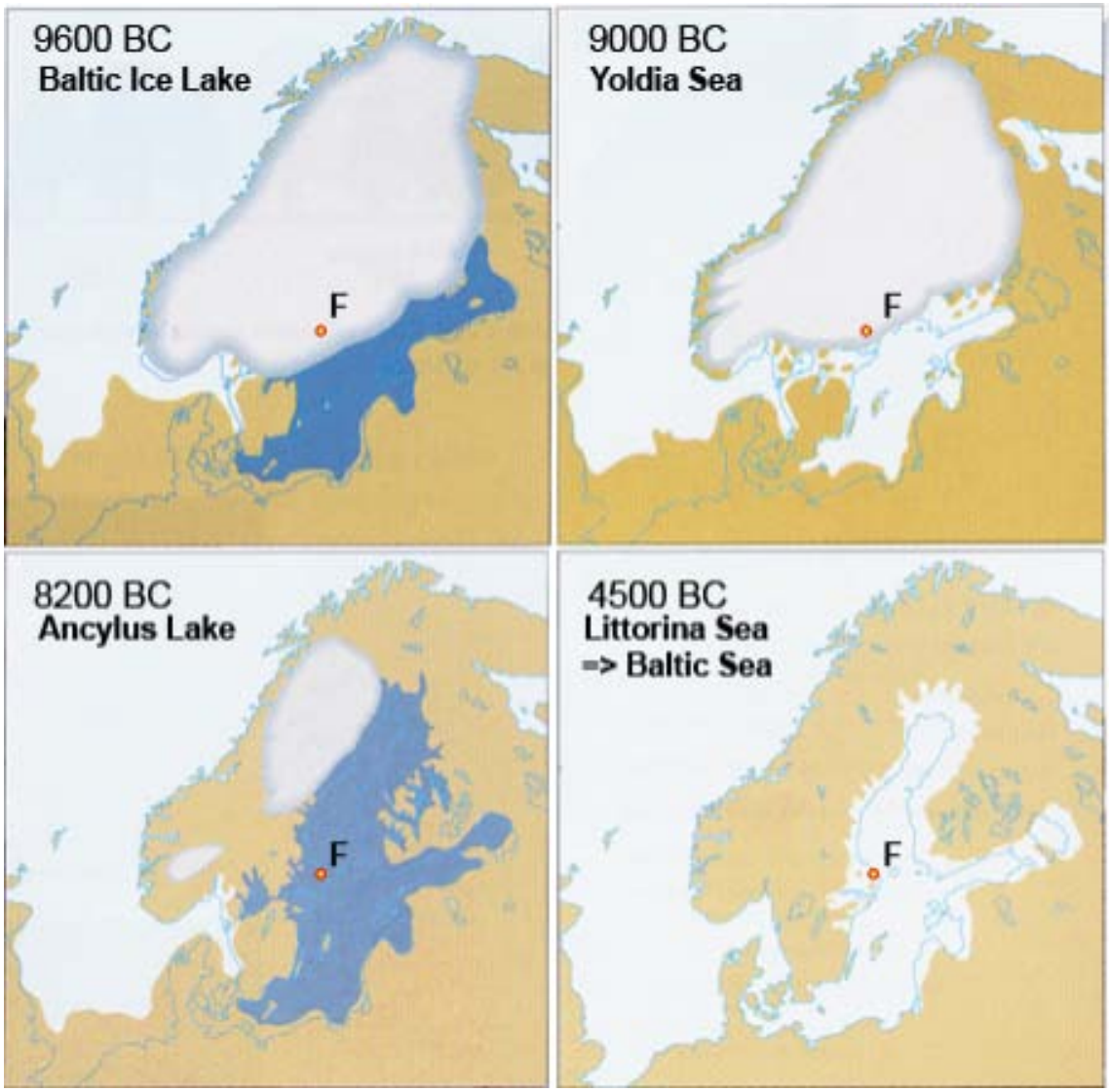

Figure 3-1. *Map of Fennoscandia illustrating some of the important stages during the Holocene period. Four main stages characterise the development of the aquatic systems in the Baltic basin since the last deglaciation: the Baltic Ice Lake (13,000 to 9500 BC), the Yoldia Sea (9500–8800 BC), the Ancylus Lake (8800 to 7500 BC) and the Littorina Sea (7500 BC to present). Fresh water is symbolised with dark blue and marine/brackish water with light blue. The Forsmark region including SFR (notated 'F') was probably at or close to the rim of the retreating ice sheet during the Yoldia Sea stage. (from /Follin et al. 2008b/).*

3.1.2 Permafrost

In general, but not always, the glaciation is preceded by tundra and then permafrost. Permafrost formation is governed by cold and dry climates where an annual ground temperature of between –5 and –2°C is defined as the boundary for extensive discontinuous permafrost (50–90% of landscape covered by permafrost) and –5°C and colder as the boundary for continuous permafrost (90–100%) /Heginbottom et al. 1995/. However, it is also stated that a large part of the area with continuous permafrost has a ground temperature warmer than –5°C. Sporadic permafrost (less than 50% of landscape covered), may exist when the annual mean temperature is between 0 and –2°C.

In parts of northern Canada permafrost presently exists to between 400–600 m depth /Ruskeeniemi et al. 2002, 2004, Holden et al. 2009/, and most is thought to date back to the Pleistocene period /Tarasov and Peltier 2007/. In Siberia permafrost extends to 1,500 m depth and more (e.g. /Alexeev and Alexeeva 2003/), but this represents a very old accumulative effect incorporating input from several glacial periods far back in time. In northern Fennoscandia some discontinuous remnants of permafrost from the Weichselian and the Holocene are believed to exist /Kukkonen and Šafanda 2001/.

Prior to the Weichselian glacial maximum at approximately 18,000 years ago, the ice margin is thought to have been more permanently located across southern Fennoscandia some 30,000 to 50,000 years ago, and to have been subject to fluctuation. There is the possibility, therefore, that the Forsmark site has been subject to variable permafrost conditions for a long period of time until eventually overrun by the advancing continental ice sheet.

The impact of permafrost on groundwaters is largely unknown as most evidence has been removed/modified either during permafrost decay coeval with the advancement of the ice cover, and/or subsequently flushed out during deglaciation (see /Smellie et al. 2008/ for discussion). However, the possibility of preservation of such evidence in the matrix porewaters cannot be ruled out (see /Waber et al. 2009/).

3.2 The scenario for groundwater evolution from before the last deglaciation to the present day

As shown above, the given Quatermary evidence for Holocene evolution is relatively detailed compared with that of glacial and older periods and therefore there is the likelihood that evidence of groundwater evolution can be recognised in the bedrock aquifer in the Forsmark region. (cf. Figure 3-2 and Figure 3-1 above)

When the continental ice melted and retreated (i.e. deglaciation stage approximately 18,000 BC to 8000 BC), glacial meltwater was hydraulically injected under considerable head pressure into the bedrock close to the ice margin. The exact penetration depth is still unknown, but depths exceeding several hundred metres are possible according to hydrodynamic modelling /e.g. Svensson 1996/. Any permafrost decay groundwater signatures may have been disturbed or destroyed during this stage.

Several different non-saline and brackish lake/sea stages then transgressed the Baltic Sea basin during the period ca. 9000 BC to 1500 AD. Of these, two periods with brackish water can be recognised; Yoldia Sea (9500 to 8800 BC) and Littorina Sea (from 7500 BC continuing to the present), with the Baltic Sea from 2,000 years ago to the present. The Yoldia period has probably resulted in only minor contributions to the subsurface groundwater since the water was very dilute to brackish in type from the large volumes of glacial meltwater it contained. Furthermore, this period lasted only for 700 years. The Littorina Sea period in contrast had a salinity maximum of about twice the present Baltic Sea and this maximum prevailed at least from 4500 to 3000 BC; during the last 2,000 years the salinity has remained almost equal to the present Baltic Sea values (/Westman et al. 1999/ and references therein). Dense brackish sea water such as the Littorina Sea water was able to penetrate the bedrock resulting in a density intrusion which affected the groundwater in the more conductive parts of the bedrock. The density of the intruding sea water in relation to the density of the groundwater determined the final penetration depth. As the Littorina Sea stage contained the most saline groundwater, it is assumed to have had the deepest penetration depth eventually mixing with preglacial groundwater mixtures already present in the bedrock.

These different stages have influenced the Forsmark region apart from the Yoldia Sea transgression which was of less importance and may even be not applicable because of its relatively short period of duration and the very dilute nature of the brackish water.

When the Forsmark region was sufficiently raised above sea level 1,000 to 500 years ago to initiate recharge of fresh meteoric water, this formed a lens on the surface of the saline water because of its low density. As the present topography of the Forsmark area is flat and the time elapsed since the area was raised above sea level is short, the flushing out of saline water has been limited and the freshwater lens remains at shallow depths (from the surface down to 25 to 100 m depending on hydraulic conditions). The entire SFR local model volume is situated below the present Baltic Sea with the exception of some small islands and shallow banks and therefore fresh modern water is not to be expected.

As a result of the described sequence of events, saline (non-marine), glacial and marine waters at the SFR are expected to have been mixed in a complex manner at various levels in the bedrock, depending not only on the hydraulic character of the fracture zones and groundwater density variations, but also on anthropogenic activities including hydraulic testing, groundwater sampling and the change in hydrogeological conditions caused by the existing SFR repository.

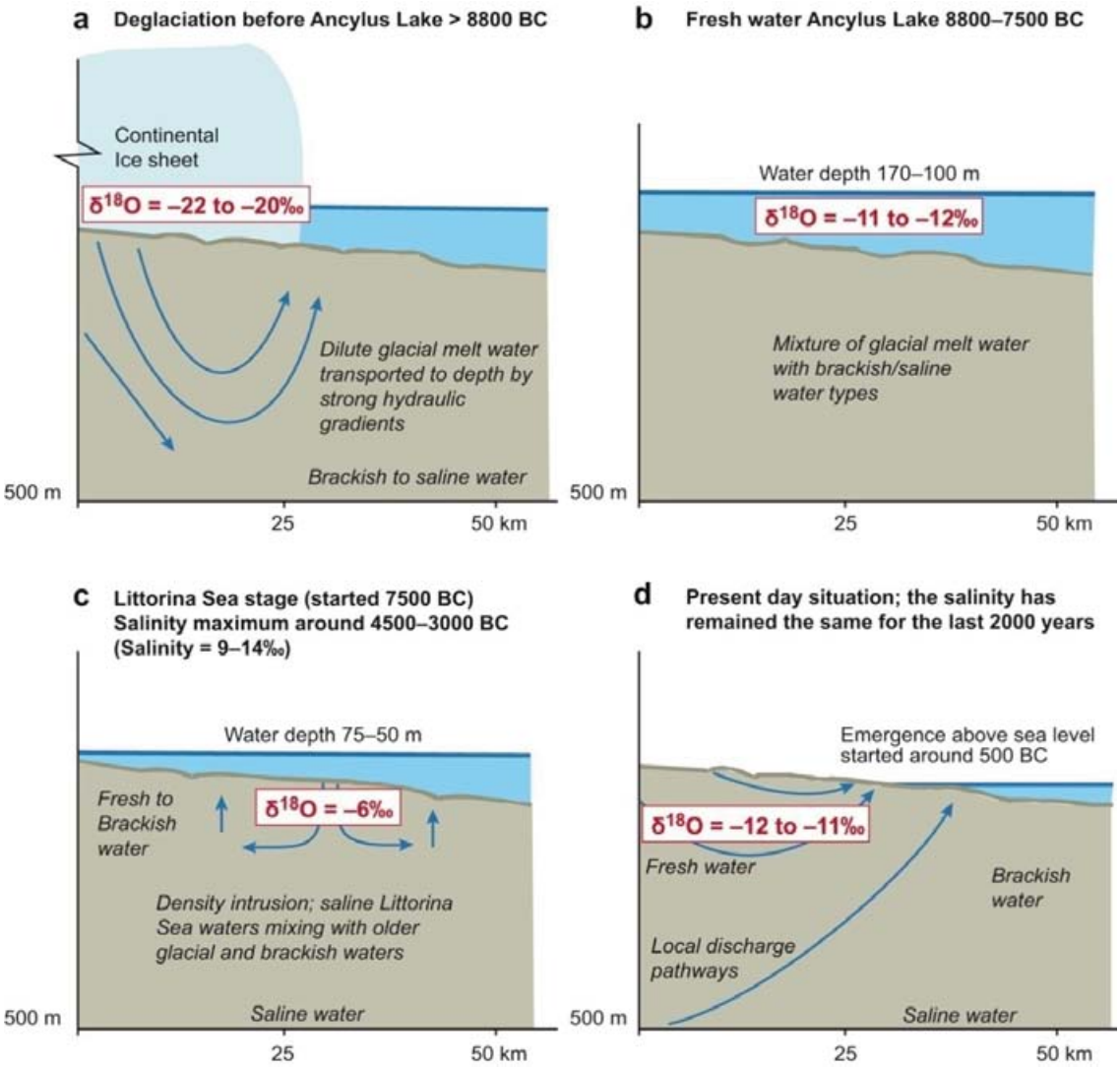

Figur 3-2 a-d. *The conceptual model for the Forsmark region following the last deglaciation. The different stages are: a) deglaciation before the Ancylus Lake (>8800 BC), b) freshwater Ancylus Lake between 8800 to 7500 BC, c) density intrusion of Littorina Sea water between 7500 BC to 0 AD, and d) the present day situation where the SFR is situated below sea-level just outside the coast line. Blue arrows indicate possible groundwater flow patterns (after /Laaksoharju et al. 2008/).*

3.2.1 The possible influence of older waters

The climate changes discussed above and in /Söderbäck 2008/ and /Follin et al. 2008b/ affect not only the precipitation and hence the amount of water, but also the type of water infiltrating the bedrock.

The infiltrating water can be glacial meltwater, precipitation, or sea water dependent of the prevailing climatic conditions. The hydraulic driving forces or the density of these water types, together with the hydrogeological properties of the bedrock, determine where and how deep the waters can penetrate. However, climatic change is a cyclic process and tends to flush out earlier water types, but the driving forces and conditions can vary and residuals of earlier climate input can be preserved often in less transmissive fractures and/or rock volumes. Extreme conditions, such as the maximum melting of the inland ice, the most saline sea water, or the longest wet period, provide the best possibility to leave an imprint on the bedrock groundwater. These palaeohydrogeochemical events therefore provide an important framework to understand the hydrogeochemical evolution of the bedrock groundwaters. However, to only consider scenarios occurring after the last deglaciation can be seriously misleading, especially considering hydrochemical input data to establish boundary conditions for hydrodynamic modelling of the Forsmark region. For example, analyses of some of the groundwaters from the

relatively tight and isolated bedrock outside the deformation zones show compositions significantly influenced by glacial meltwater (probably from the last glaciation but may also be older) and brackish non-marine water of unknown age. In other words, there may be an important groundwater component from before the last deglaciation that has influenced to varying degrees the present-day hydrochemistry of the SFR local model volume. This is also supported by evidence of pre-Holocene porewater analysed within the Forsmark site investigations /Waber et al. 2009/. Based collectively on the above described observations, the present groundwaters are a result of complex mixing and reactions over a long period of geological time. Mixing will be more important in those parts of the bedrock with dynamic hydrogeological properties, for example the more conducting fractures and fracture zones in the SFR model volume. In other less dynamic parts, the groundwater chemistry will be more influenced by water/rock interaction processes and diffusion processes. In common with the Foresmark site, diffusion processes also may have preserved an older groundwater type, however no porewater analyses have been carried out within the SFR site investigations.

3.2.2 Working hypothesis

The five key water types recognised in the Forsmark Site investigations were in chronological order: *Saline Water > Brackish Non-marine Water > Last Deglaciation Meltwater > Brackish Marine (Littorina/Baltic) Water > Fresh Water* /Laaksoharju et al. 2008, Smellie et al. 2008 (Note that Last Deglaciation refers to the period 18,000 to 8000 BC). These waters are also basically similar to the ones characterising the SFR site but in rather different portions. For example, fresh groundwater of present meteoric origin is almost absent because the SFR is located under the Baltic Sea. In addition, saline water (Cl >6,000 mgL-1) is not found, probably due to the relatively shallow depth of the groundwaters sampled (i.e. < –400 masl).

3.2.3 Present conceptual model

In the context of geological time scales, fluid inclusions in calcite of Palaeozoic origin show the presence of very saline (around 20 wt %) mainly Ca-Cl fluids /Sandström et al. 2008/. It can be assumed, therefore, that during the Late Palaeozoic when several kilometres of marine and terrestrial sediments covered the Precambrian Shield area of south-east Sweden, brine solutions were formed saturating both the fractures and eventually the interconnected pore spaces in the underlying crystalline bedrock. The present non-marine saline water may still contain components of this original brine water.

Of greater importance for the present groundwater chemistry at the SFR is the evolution during the Weichselian and Holocene times. Figure 3-3a shows a tentative distribution of groundwater types and salinity gradients in the SFR area before the intrusion of the last deglaciation meltwater just prior to the Holocene. Based on an understanding of the climatic changes that have occurred since the last deglaciation, it is logical to presume that there must have been at this time old meteoric waters comprising components derived from both temperate and cold climate events. These waters would have intruded the bedrock and have had long periods of time to interact with the minerals. Assuming there were favourable gradients, old meteoric waters could have been partially mixed with deeper, more saline groundwaters, but the high density contrast would have prevented further mixing. What can be said with confidence is that the residual old brackish waters in the Forsmark region do not have a marine signature. In the SFR model volume the old non-marine water has been mixed with glacial water from the last deglaciation (Figure 3-3b); the largest components of glacial waters are found between –100 and –250 masl.

During the subsequent Littorina Sea stage (Figure 3-3 c) the SFR area was covered by brackish marine water assumed to be at around 6,500 mgL-1 Cl /Pitkänen et al. 1999, 2004/. This maximum salinity (twice the present salinity of the Baltic Sea) lasted at least between 4500 and 3000 BC. Due to the unstable density situation generated by the higher density Littorina Sea water located over previously infiltrated last deglaciation meltwater of lower density, the Littorina Sea water entered the deformation zones and fractures and mixed/displaced the previously resident fresh water of glacial and old meteoric character.

The present situation is shown in Figure 3-3d, which illustrates the intrusion of present Baltic Sea water in some fractures down to about –100 masl. This intrusion is probably to a large extent driven by the hydraulic gradient created by the existing SFR storage facility.

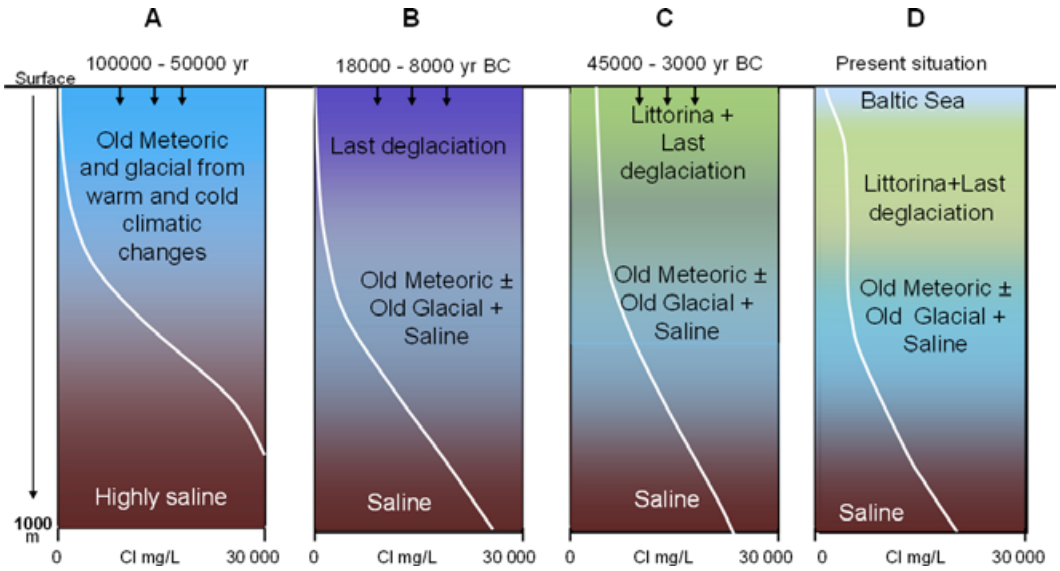

Figure 3-3. *Sketch showing tentative salinities and groundwater-type distributions versus depth for the transmissive deformation zones at SFR. From left to right: a) situation prior to the last deglaciation, b) last deglaciation and intrusion of Late Weichselian meltwater, c) the Littorina Sea water penetration caused by density intrusion, and d) the present situation with possible penetration of local Baltic Sea water.*

The above description is valid generally for most areas in the Forsmark bedrock where first the last deglaciation meltwater, then later the brackish marine (Littorina Sea) water, and finally present Baltic Sea water have been introduced. Further conceptual development of the Forsmark area, for example, future land uplift processes, are described in /Söderbäck 2008, Tröjbom et al. 2007/.

3.3 Groundwater types used in the SFR modelling

Based on these palaeoclimatic considerations, and in order to facilitate the description and interpretation of figures and diagrams presented in Chapter 6, a subdivision into different water types, similar to the approach used within the site modelling /e.g. Smellie et al. 2008/, is used here. From a compilation of all available data from the SFR local model volume, and the earlier gained data set from the Forsmark site investigation (PLU), it can be concluded that (cf. Figure 3-4 a-d):

1) The range in chloride concentration of the SFR groundwaters is small (1,500 to 5,500 mgL-1 Cl) compared with the Forsmark site investigation area (50–16,000 mgL-1 Cl), but the $d^{18}O$ values showed a similar variation (–15.5 to –7.5‰ V-SMOW) when compared with Forsmark (–16 to –8‰ V-SMOW).
2) The SFR data set only covers depths down to about –400 masl.
3) Fresh meteoric water components of present precipitation type are very minor (negligible).
4) Marine indicators, such as Mg/Cl, K/Cl and Br/Cl ratios, show relatively large variations especially considering the limited salinity range and the shallow depth of sampling.

Based on these observations, coupled to the need to separate groundwaters of different origins and residence times in the bedrock, a subdivision of the groundwaters has been adopted which is somewhat different to the one used during the Forsmark site investigations (PLU). The subdivision described below has been established to construct a hydrogeochemical model and facilitate interaction with the hydrogeological models.

Whilst the present method to subdivide the SFR groundwaters into different types to achieve better understanding has been broadly successful, the complexity of the hydrogeochemical system has given rise to some anomalies. In Chapter 6 some samples/data points seem to deviate from the other samples representing the same groundwater group. The most common explanations for these anomalies include erroneous analytical concentrations (e.g. especially early on in the sampling during 1986) and sudden isolated increases/decreases in components in an otherwise long-term stable groundwater environment.

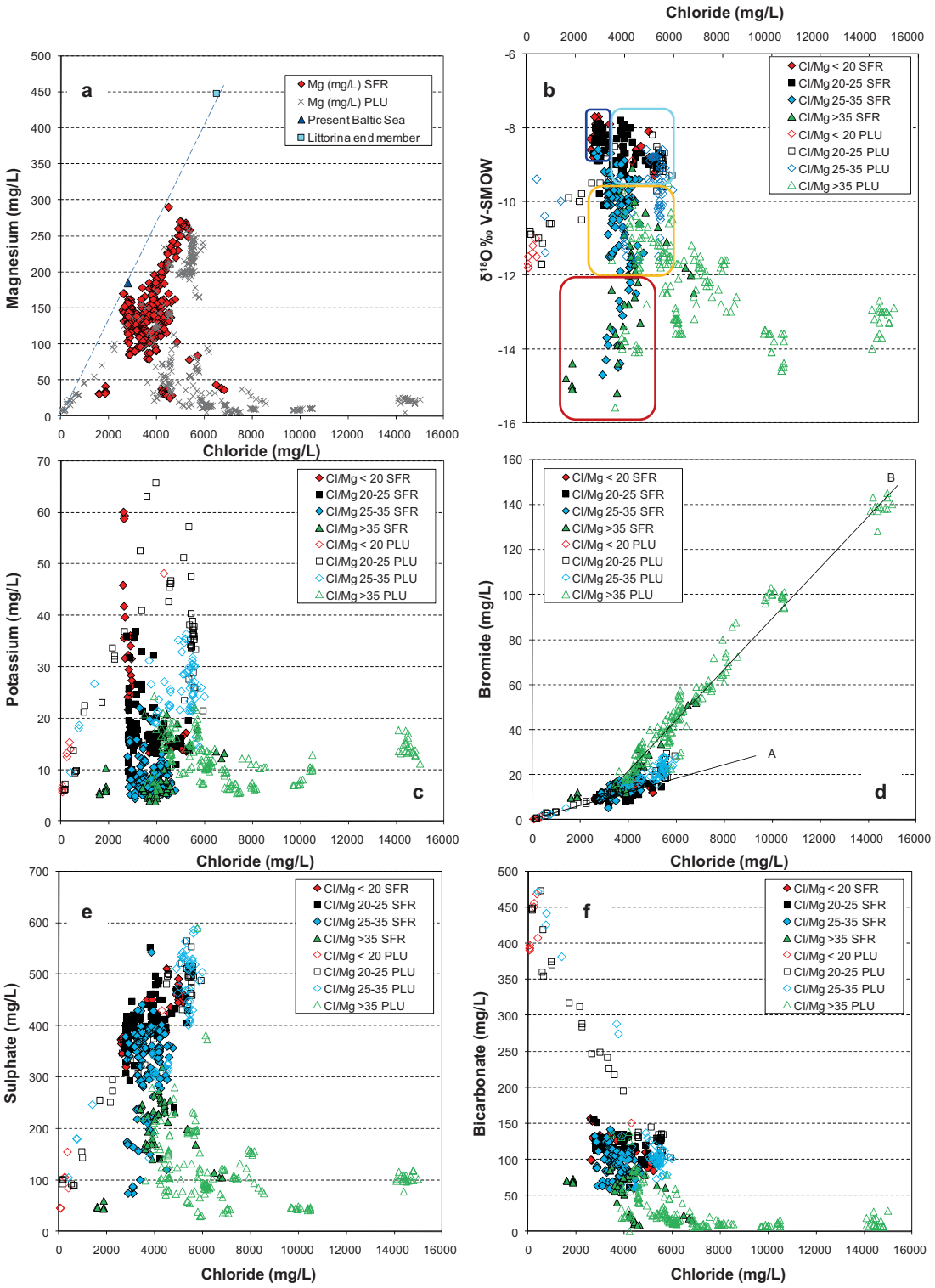

Figure 3-4a–f. *Plots of magnesium and $\delta^{18}O$ versus chloride concentration with boxed areas signifying groundwater types, and potassium, bromide, sulphate and bicarbonate versus chloride concentration. PLU data includes data from the Forsmark site only. Figure 3-4a also shows the mixing line between the Littorina end member, Baltic Sea water and meteoric water. Most of the SFR samples are depleted in magnesium compared to this mixing line /Smellie et al. 2008/. Figures 3-4b-f show the groundwater samples categorised according to the Cl/Mg weight ratio. Furthermore, in Figure 3-4b, the areas occupied by the different groundwater types, see below for definitions and colour code, are displayed as coloured boxes. Figure 3-4d shows also dashed lines corresponding to typical mixing lines for groundwaters of marine (A) and non-marine origin (B),respectively.*

Local Baltic Sea

Water type; Brackish marine water with a Cl content of 2,500 to 3,500 mg/L and $d^{18}O$ at –9 to –7.5‰ VSMOW; Na-(Ca)-(Mg)-Cl-SO_4 in type. This is a brackish water with a Cl/Mg weight ratio <27 (with a few exceptions) indicating a marine origin which is further supported by the contents of sulphate and potassium and the Br/Cl ratio. Only minor modification of this water has occurred caused by ion exchange and microbial reactions. The Cl and $d^{18}O$ ranges correspond to that of Baltic Sea water sampled off the coast at the SFR, but some samples also contain components of Littorina and glacial water types. The Local Baltic Sea waters are the youngest waters present at the SFR.

Littorina type water with a glacial component

Water type: Brackish marine water with a Cl content of 3,500 to 6,000 mg/L and $d^{18}O$ at –9.5 to –7.5‰ V-SMOW; Na-Ca-(Mg)-Cl-SO_4 in type. This water type has a higher salinity than the present Baltic Sea and is commonly found in the Forsmark area to the west. The Cl/Mg ratio is generally < 27, but exceptions do occur. The sulphate concentration and Br/Cl ratio support a marine origin for the saline component. The potassium concentration is increased but not as high as in the Local Baltic Sea type of groundwater. This is probably due to dilution from the contributing glacial melt-water. The Littorina type of groundwater previously observed during PLU was often more saline and showed similar potassium concentrations as the Baltic Sea water. The slightly depleted $d^{18}O$ values compared to the Littorina end member (–5‰ V-SMOW), indicate a significant component of glacial water probably from the last deglaciation. Some samples may also contain portions of Baltic Sea water.

Brackish Glacial

Water type: Brackish glacial: Na-Ca-Cl groundwater with a Cl content of 1,500 to 5,000 mg/L and $d^{18}O$ < –12.0‰ V-SMOW: Na-Ca-Cl in type. This water type has low Mg (Cl/Mg ratio > 32) and K, has higher Br/Cl ratios than marine waters, and is usually relatively low in SO_4 and HCO_3. It is a mixture of glacial (last deglaciation or older) + brackish non-marine water ± Littorina. The marine signature is generally weak and the Br/Cl ratio deviates from that of marine waters. The brackish glacial waters are the oldest present at the SFR and the amounts of post-glacial components are small.

Mixed brackish water (transition type)

Water type: Brackish groundwater with a Cl content of 2,500 to 6,000 mg/L and $d^{18}O$ at –12.0 to –9.5‰ V-SMOW: Na-Ca-(Mg)-Cl-(SO_4) in type. The waters in this group result from the mixing of the above three groundwater types (the mixing may either be natural or artificially created by the drawdown caused by the SFR repository or during the drilling and sampling procedures). Most of these waters contain components of brackish marine waters (maybe of different ages but mostly Littorina in type) + glacial waters (from the last deglaciation or older) ± weakly brackish waters.

4 Hydrogeochemical data

4.1 Databases

The dataset forming the basis for the modelling stage version 0.2 in the SFR extension project contains quality assured data from the recent investigation phase in the target area south-west of the repository /Jönsson et al. 2008, Thur and Nilsson 2009a, b, Thur et al. 2009, Lindquist and Nilsson 2010/ as well as from earlier studied boreholes in the present SFR facility /Nilsson A-C 2009/ and from two PLU boreholes /Gustavsson et al. 2006/. The main part of the data consists of basic groundwater analyses including isotopes, although a few gas, microbe and redox data are also available. Quality checked data were extracted from the Sicada database (Sicada-09-182 (0:1) and Sicada-09-189 (0:1), complemented with late data (quality checked) from borehole KFR106) and compiled to produce the Hydrogeochemistry Data Table version 0.2. This data table, in Excel format, is used for all the interpretation and modelling work and is stored in the SKB model database SKBDoc for traceability.

The data (values) from Sicada were not changed, only the data structure, during the procedure to compile the table, unless errors or questionable data were discovered. If so, the same changes or comments on data were also introduced in Sicada. Furthermore, complementary information on deformation zones, flow anomalies and hydraulic transmissivities (approved geological deformation zone model and quality checked data from Sicada) were included in the table and some groundwater samples were commented upon or explained. The samples/records were categorised and divided into two sheets; Dataset I (suitable for modelling) and Dataset II (unsuitable for modelling). The criteria for this categorisation are described in Section 4.3.4.

4.2 Available data

The groundwater data obtained from the hydrogeochemical investigation programme in the SFR extension project comprise a total of 14 borehole sections in four core drilled and three percussion boreholes. The sampling was performed in cored boreholes with installed fixed packer equipment and in percussion boreholes using equipment for hydraulic tests (HTHB). Gas data (N_2, H_2, CO_2, O_2, Ar, CH_4, He, CO, C_2H_2, C_2H_4, C_2H_6, C_3H_8 and total gas volume) and microbe data (total number of cells, concentration of ATP, number of cultivable, heterotrophic aerobic bacteria (CHAB) and most probable number of cultivable metabolic groups, i.e. iron, manganese, sulphate and nitrate reducing bacteria as well as acetogens and methanogens) are available from two sections in the borehole drilled from the SFR tunnel system, KFR105, but no colloid determinations were performed. Redox potential measurements were also performed in these two borehole sections but reliable data were obtained only from the bottom section /Lindquist and Nilsson 2010/. The sampling locations, i.e. the SFR extension boreholes together with three PLU boreholes located within the SFR extension regional model volume, are presented in Figure 4-1. NOTE: In this report, data from one of the three PLU-boreholes, KFM11A, were omitted from the interpretation and modelling work (cf. Section 4.3.4).

Besides the recent SFR extension project, further useful groundwater data were extracted from the SKB database Sicada related to the period 1984 to October 2008; altogether a total of 45 borehole sections in 18 early boreholes drilled from the SFR tunnel system. This dataset includes, therefore, samples from investigations prior to the operational phase of the SFR repository (1984–1988) as well as from the routine SFR groundwater control or monitoring programme that has been ongoing since 1989. On-line measurements of pH, Eh and electrical conductivity (EC) are available from three borehole sections (KFR01:1, KFR10 and KFR7A:1) and from two different sampling campaigns in each borehole (1986–87 and 2000 respectively); however, the redox potential data are of doubtful quality. Gas data (N_2, H_2, CO_2, O_2, Ar, CH_4, He, CO, C_2H_2, C_2H_4, C_2H_6, C_3H_8 and total gas volume) and microbe data (restricted to total number of cells) have been obtained from the same three boreholes during the sampling campaign in 2000. The SFR boreholes and the sampled borehole sections are displayed in Figure 4-2.

The number of approved samples, cf. Section 4.3, from each borehole section (Early SFR boreholes, SFR extension project and PLU) is listed in Table 4-1 and the sample distribution versus depth for the entire time period 1986 to 2009 is given in Figure 4-3.

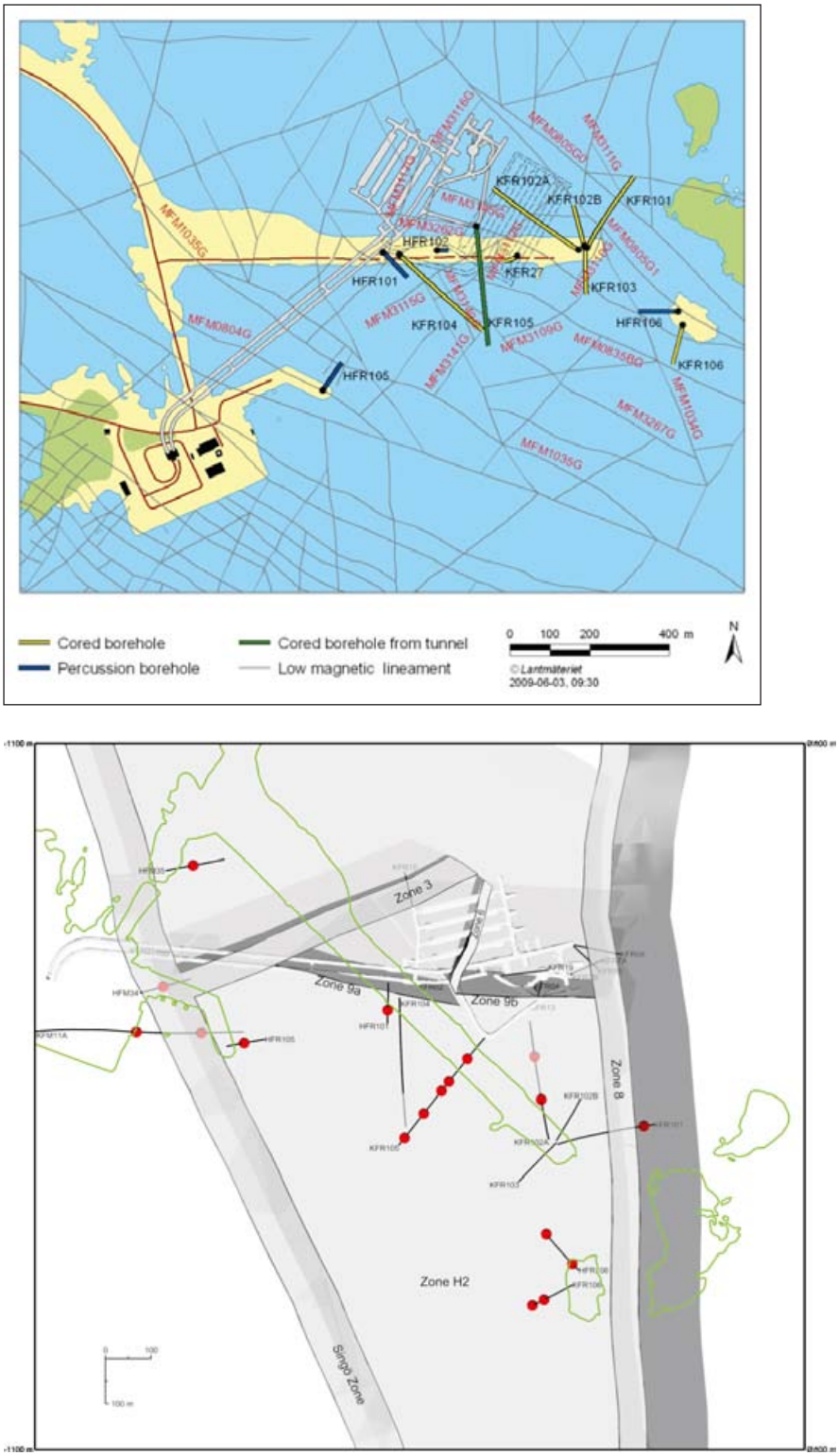

Figure 4-1a, b. *Location of sampled boreholes/borehole sections in the SFR extension project.* ***a)*** *Location of the boreholes.* ***b)*** *Location of the sampled borehole sections in relation to major deformation zones. Three PLU boreholes (HFM34, HFM35 and KFM11A) are added to the figure. The centre of each section is given as a red ball and the zones are labelled according to SFR terminology. Note the decrease in colour intensity along the boreholes when viewed through a penetrated rock/deformation zone volume.*

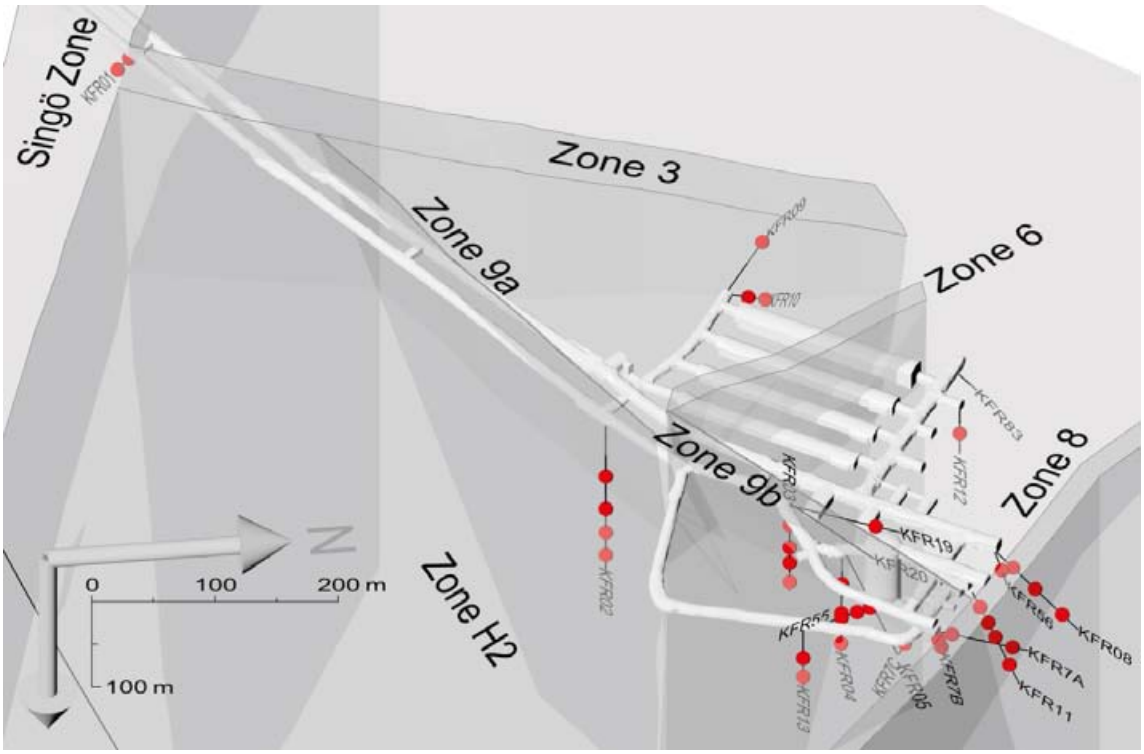

Figure 4-2. *3D presentation of today's tunnel system in the SFR showing the location of the deformation zones and the sampled boreholes/borehole sections. The red balls indicate the centre of the sampled sections and the zones are labelled according to SFR terminology. Note the decrease in colour intensity along the boreholes when viewed through a penetrated rock/deformation zone volume.*

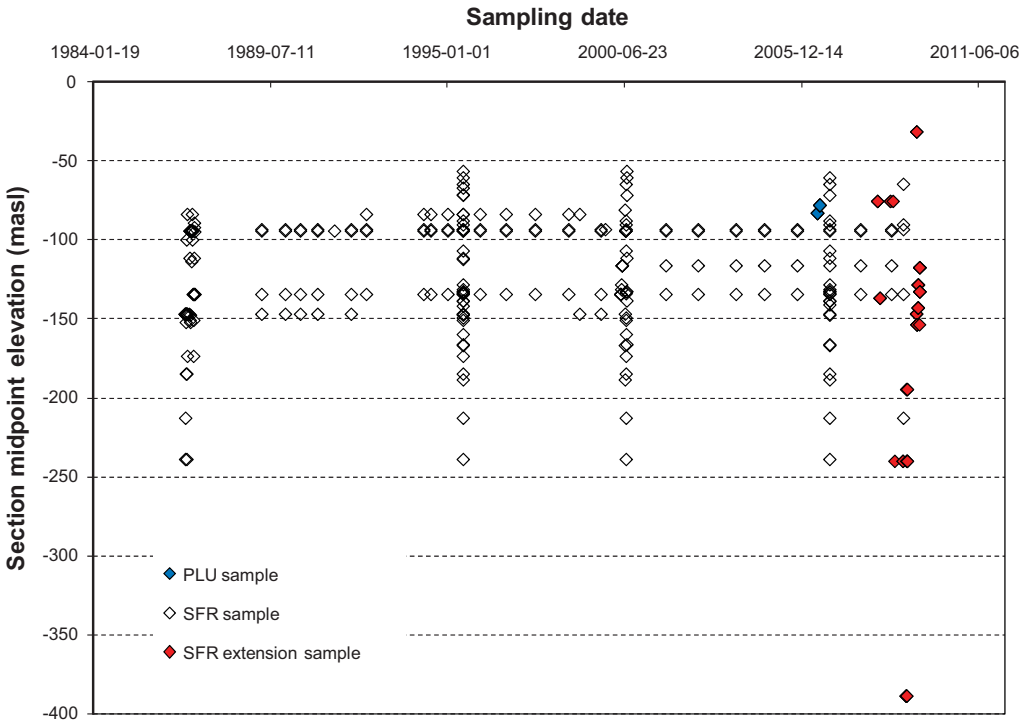

Figure 4-3. *Sample distribution versus depth, 1986 to 2009. Samples from boreholes HFR34 and HFR35 and the site investigation in Forsmark (PLU), early SFR boreholes (SFR) and within the SFR extension project (SFR Ext.).*

As can be seen, the number of samples from each borehole section in the early SFR boreholes varies considerably and the sporadic occurrence complicates evaluation of changes and trends. Furthermore, these data are obtained over a long period of more than twenty years and therefore relate to different development stages of the SFR. For example:

1. There are no groundwater chemistry data from the first drilling stage (1980–1981) prior to the commencement of the excavation phase, only hydrogeological measurements. These boreholes were drilled mainly from off-shore platforms and a few from shore and harbour locations.
2. Early approved data from the before the operational stage of the repository (November 1986 to December 1987). These data are used to represent 'undisturbed conditions', i.e. not affected by the SFR operational phase starting in 1988 but possibly affected by the preceding excavation phase.
3. Data from 2006 (i.e. the last extensive sampling occasion) which includes all boreholes/ borehole sections where it was still possible to collect samples. These data are used together with the recent data from PLU and from the SFR extension project to present and describe the present day groundwater situation in the investigation area.
4. Data obtained between 1987 and 2006 as well as after 2006. These data are used to support the interpreted groundwater conditions and to verify changes and trends.

Table 4-1. Available and approved data in the Hydrogeochemistry data table version 0.2 for modelling purposes. Indicated are the sampled boreholes/borehole sections, the number of samples (Dataset I) and the available redox measurements, gas analyses and microbe determinations.

Idcode	Secup (mbl*)	Seclow (mbl*)	Elevation Secmid (masl)	No. of samples**	Eh, pH_F (years)	Gas (years)	Microbes (years)
Early SFR boreholes							
KFR01	11.0	43.5	–71,58	3			
KFR01:1	44.5	62.3	–94,23	40	1987**, 2000**	2000	2000
KFR02	43.0	80.0	–146,93	4			
KFR02	81.0	118.0	–184,93	5			
KFR02	119.0	136.0	–212,93	5			
KFR02	137.0	170.3	–239,08	5			
KFR03	5.0	44.0	–106,87	3			
KFR03	45.0	56.0	–132,87	3			
KFR03	57.0	80.0	–150,87	4			
KFR03	81.0	101.6	–173,67	4			
KFR04	28.0	43.0	–111,48	5			
KFR04	44.0	83.0	–138,52	3			
KFR04	84.0	100.5	–166,29	3			
KFR05	57.0	79.0	–141,06	1			
KFR05	80.0	96.0	–159,86	2			
KFR08	6.0	35.0	–87,81	3			
KFR08	36.0	62.0	–90,29	4			
KFR08	63.0	104.0	–93,31	27			
KFR09	0.0	80.2	–80,94	1			
KFR09	63.0	80.2	–83,68	13			
KFR10	0.0	107.3	–116,23	12	1986***, 2000***	2000	2000
KFR10	87.0	107.3	–146,99	19			
KFR11	7.0	24.0	–89,19	1			
KFR11	25.0	39.0	–92,06	1			
KFR11	40.0	55.0	–94,75	1			
KFR11	56.0	98.1	–99,88	2			
KFR12	0.0	50.25	–112,25	1			
KFR12	20.0	33.0	–113,62	1			
KFR13	4.0	33.0	–141,84	1			
KFR13	34.0	53.0	–166,84	3			
KFR13	54.0	76.6	–188,64	3			
KFR19	51.0	65.0	–66,99	1			

Idcode	Secup (mbl*)	Seclow (mbl*)	Elevation Secmid (masl)	No. of samples**	Eh, pH_F (years)	Gas (years)	Microbes (years)
Early SFR boreholes							
KFR19	77.0	94.0	–60,43	3			
KFR19	95.0	110.0	–56,35	2			
KFR20	0.0	109.7	–71,24	1			
KFR55	8.0	21.0	–128,34	3			
KFR55	22.0	39.0	–131,39	3			
KFR55	40.0	48.0	–133,97	3			
KFR56	9.0	81.7	–64,66	4			
KFR7A	2.0	19.0	–132,65	3			
KFR7A	20.0	47.0	–133,46	1			
KFR7A:1	48.0	74.7	–134,43	33	1987***, 2000***	2000	2000
KFR7B	4.0	7.0	–138,85	2			
KFR7B	8.6	21.1	–147,59	4			
KFR7C	0.0	34.0	–149,37	4			
SFR extension project							
HFR101	107.3	197.0	**–136,80**	3			
HFR105	55.6	120.0	**–75,40**	6			
HFR106	36.0	41.0	–31,36	3			
HFR106	175.0	190.4	–146,90	3			
KFR101	279.5	341.8	–240,15	7			
KFR102A	214.0	219.0	–194,64	5			
KFR102A	423.0	443.0	–388,97	5			
KFR105	4.0	119.0	–117,42	4			
KFR105	120.0	134.0	–128,38	5	_	2009	2009
KFR105	138.0	169.0	–132,73	4			
KFR105	170.0	264.0	–142,94	4			
KFR105	265.0	306.8	–153,59	5	2010	2009	2009
KFR106****	143.0	259.0	–187.20	3			
KFR106****	260.0	300.0	–261.02	3			
PLU data							
HFM34	0.0	200.8	–82,92	3			
HFM35	0.0	200.8	–78,24	3			
KFM11A	447.5	454.6	–389,68	7	Excluded from evaluations and interpretations.	20	
KFM11A	446.0	456.0	–389,62	4			
KFM11A	690.0	710.0	–593,76	7			

*mbl = metre borehole length

** Including laboratory measurements of pH and EC, and field measurements of pH and EC for samples in the SFR extension project and in PLU.

***Indicative Eh values were obtained; however they do not meet present quality demands

**** Late data extracted after the official data delivery from the Sicada database

4.3 Quality assured and categorised data

4.3.1 Analytical uncertainty

The groundwater analyses treated in the present report have been carried out during more than twenty years and the analytical methods as well as the performing laboratories have changed several times during this time period. For a general evaluation of hydrogeochemical data from the early SFR boreholes and information on detection limits and measurement uncertainties, see /Nilsson A-C 2009/. Some consistency checks, in order to establish a reliable set of major constituent concentrations for each of the samples included in the version 0.2 modelling (Dataset I) and also to justify rejection of some of the samples (Dataset II), are presented in Figures 4-4 to 4-7.

The chloride concentrations and the electrical conductivity (EC) values are compared in an x-y scatter diagram see Figure 4-4. The data from November 1986 and thereafter follow the trend line quite well, indicating that the EC and chloride data sets are consistent. The chloride to EC correlation combined with the relative charge balance (acceptable limit of ±5%) are useful tools in order to verify that the concentrations of the most dominating ions are consistent. Only very few samples collected after November 1986 fall outside the charge balance limits. Most of the already rejected earlier samples (1984–Oct 1986) showed large charge imbalances /Nilsson A-C 2009/.

Furthermore, the dataset offers some possibilities to compare results from different methods and/or laboratories. Analyses after year 2000 include both sulphate and elemental sulphur determinations by Ion Chromatography (IC) and ICP-AES, respectively. The agreement between the two methods is reasonably good as indicated by deviations from the theoretical correlation line shown in Figure 4-5. The ICP results generally show somewhat higher values which may be due to effects from the presence of sulphide. This effect is not proportional to the sulphide-sulphur concentration since sulphide-sulphur enters the plasma as hydrogen sulphide gas.

Bromide analyses have been included in the analytical programmes since November 1986. Bromide concentrations are plotted versus the corresponding chloride concentrations in Figure 4-6 as a rough consistency check. The data points form two rather scattered trends corresponding to: 1) a marine origin (Br/Cl slope close to 0.0035), and 2) a trend more typical of water/rock interaction (Br/Cl slope approx. 0.01). The bromide analyses are probably impaired by larger uncertainty than most other major constituents; however, the broad trend lines may partly be caused by complex mixing patterns of the marine waters with groundwaters of other origins and possibly released from organics during diagenetic reactions /Upstill-Goddard and Elderfield 1988/.

A limited number of samples include values for both total/ferrous iron by spectrophotometry and elemental iron by ICP-AES. The agreement between the spectrophotometric and the ICP results is very good with one exception, see Figure 4-7. This is an indication that the presence of iron species in a colloidal phase is insignificant in all cases except one. The spectrophotometric method does not include, or only partly includes, iron possibly associated with particles and colloids that passes a 0.40 µm filter, but the ICP method makes no distinction between different iron containing species.

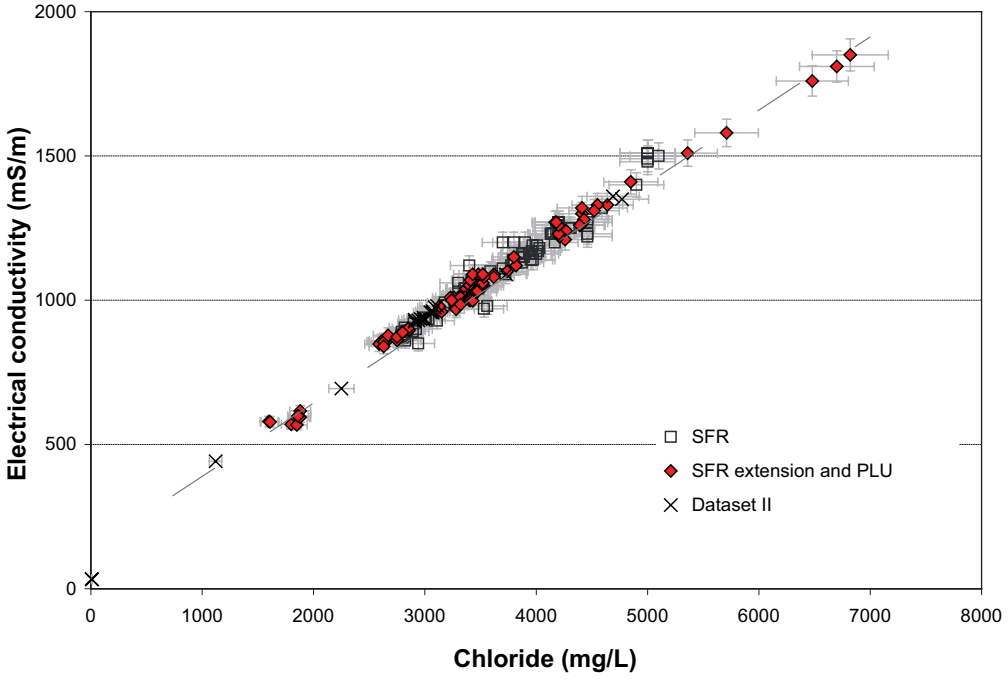

Figure 4-4. *Chloride concentrations plotted versus EC values. The samples are from Nov. 1986 to Oct. 2008.*

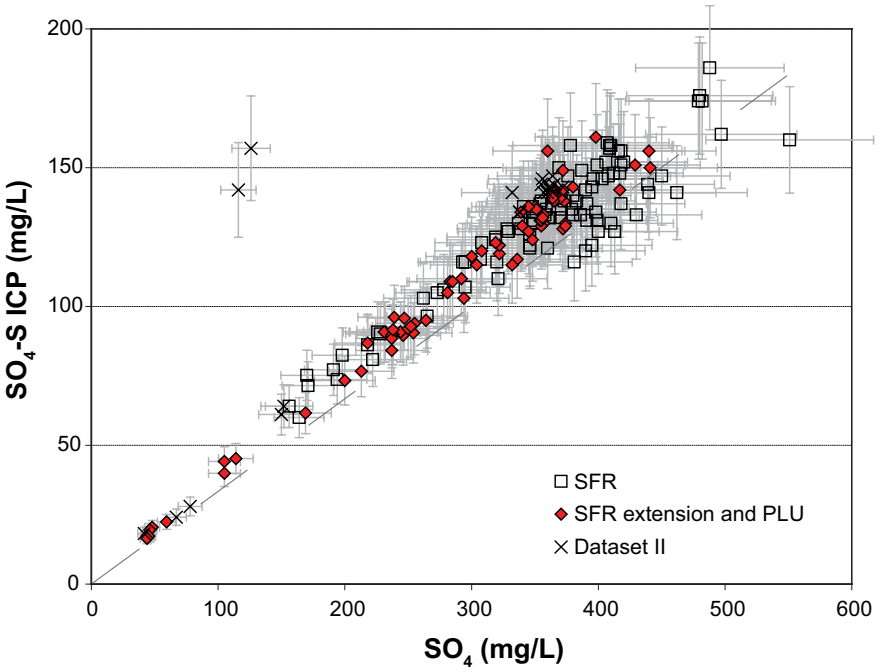

Figure 4-5. *Comparison of sulphur by ICP-AES and sulphate by IC (91 samples). The samples are from 2000 to Oct 2008. Without significant contribution of other sulphur species, 3×SO_4-S by ICP should correspond to SO_4 by IC. The lower SFR data plotting below the line represent less precise early samples (e.g. 1987).*

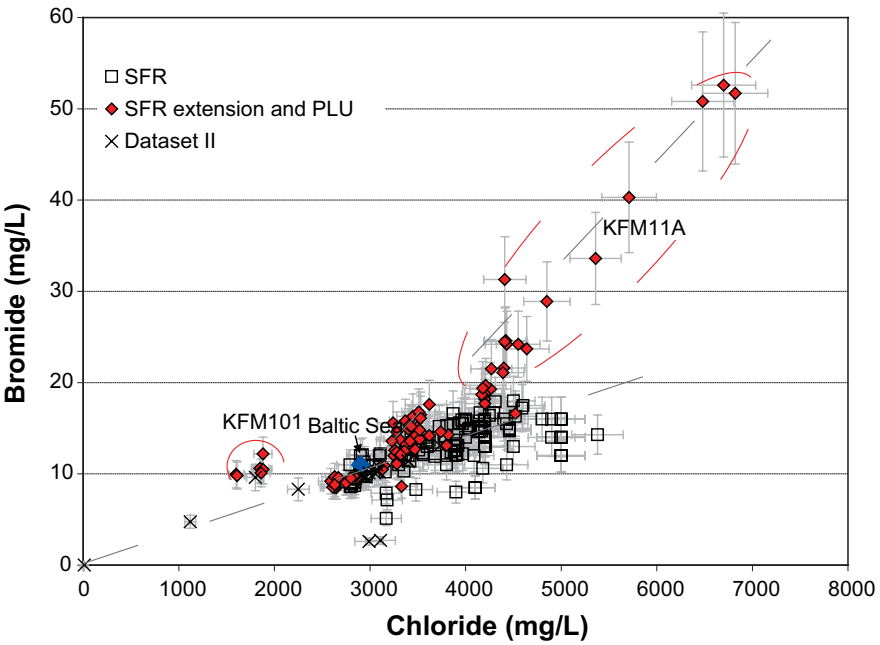

Figure 4-6. *Plot of bromide concentrations versus chloride concentrations. The samples are from Nov. 1986 to Oct. 2008. The dashed lines correspond to typical mixing lines for groundwaters of marine and non-marine origin, respectively.*

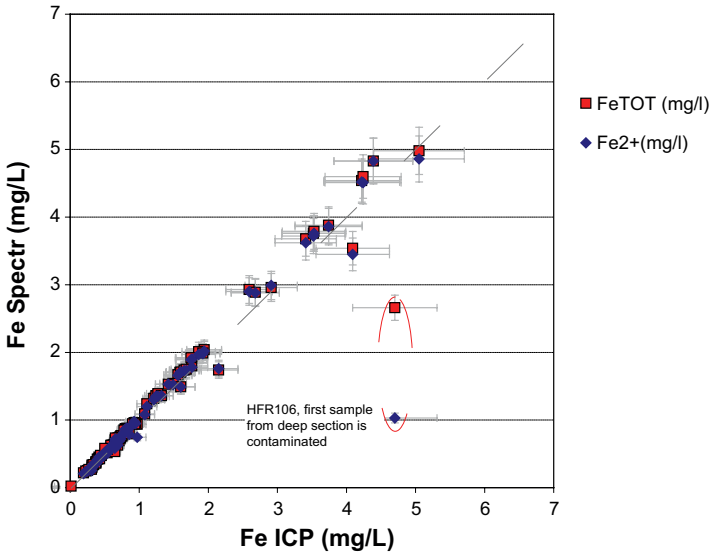

Figure 4-7. Comparison of iron concentrations. Total and ferrous iron by spectrophotometry is plotted versus iron determined by the ICP-AES technique.

4.3.2 Impacts from sampling and sampling conditions

Factors and conditions that are known to, or may have an impact on the sample quality are:

- Insufficient exchange of water from the borehole section prior to sampling may result in samples consisting partly of section water and partly of formation groundwater. The water initially present in the section may differ considerably in composition from that of the desired formation groundwater in the bedrock. It may represent a water mixture from the entire borehole or a different part(s) of the borehole. Furthermore, processes, for example microbial production of sulphide, may be more pronounced in the borehole section compared to the surrounding water-conducting fracture system in the bedrock. Plug flow calculations have been used to estimate the percentage of section water in samples from the SFR extension project, see below.
- For the same reason the drilling water content in the samples may remain unacceptably high. During drilling uranine dye was added to the drilling water as a tracer (0.2 mgL^{-1}) to allow calculation of the drilling water content. Tap water was used as drilling water for boreholes KFR101 and KFR102A in order to avoid any change in the groundwater marine signature that might impact on the evaluation of groundwater origin. Borehole KFR106 was not initially planned for hydrogeochemical investigations and was unfortunately drilled using sea water. Borehole KFR105 was drilled from the construction tunnel in the SFR repository where the water flow is directed towards the tunnel. Therefore, there was little risk of contamination from drilling, drilling water or other borehole activities. Remaining drilling water was not expected to be a problem and the lower drainage basin in the SFR repository was accepted as a source of drilling water. The drilling water budget calculations for KFR105 verified that all the drilling water was recovered /Nilsson G 2009, Lindquist and Nilsson 2010/. The same pressure conditions are of course valid also for the early SFR boreholes drilled from the tunnel system. Furthermore, it is more than 20 years since they were drilled and possible traces of drilling water should have disappeared a long time ago.
- During sampling, fracture networks intersecting the boreholes may lead to short circuiting of the groundwater flow in the surrounding bedrock and also to bypassing the packer system used to isolate the borehole section being sampled. This means that the section sampled may have been supplied by mixed groundwaters from higher or lower levels in the bedrock, and/or mixed borehole waters above or below the packers. In both cases the sampled groundwaters when interpreted in isolation may be evaluated erroneously as being of suitable quality.

- Pressure gradients (possibly resulting from an impact from the adjacent SFR tunnel system) between borehole sections may cause an initial downward transport of large volumes of water in the borehole before installation of the fixed packers to isolate borehole sections. This will affect subsequent sampling and sample quality. Two examples of boreholes having pressure gradients are borehole HFR106 and KFM11A. Samples from borehole KFM11A are excluded from the approved dataset for modelling due to interpretation problems.
- The presence of the tunnel system has an impact on the hydrogeological conditions in terms of changed flow paths and groundwater drawdown effects. These effects are observed from long term hydrochemical trends as very slow but systematic changes in the groundwater composition, i.e. dilution with modern marine water from the Baltic Sea and more mixing of groundwaters with different origin. However, this has not disqualified any samples since they are presently representative for the groundwater development close to the repository. The slow dilution is mainly observed in boreholes intersecting major vertical deformation zones.
- Air-lift pumping was used for sampling in boreholes KFR101and KFR106. These boreholes do not have installed circulation sections with wide stand pipes that otherwise allows the lowering of a pump for groundwater sampling /Thur and Nilsson 2009a, Berg 2010/. In borehole sections routinely used for pressure measurements, the only possible sampling method is by air-lift pumping using nitrogen gas to lift the water volume in the borehole section to the ground surface. It is possible that this pumping method affects the sample quality differently compared to conventional pumping, and therefore the following effects might be expected: 1) Depending on the borehole section geometry and volume it may be difficult to obtain sufficient exchange of initial section water due to both low pumping efficiency and gas consumption. 2) The groundwater in the section will probably experience a vigorous turbulence effect compared with the slow mechanical groundwater extraction normally encountered when pumping in the stand pipe. This may affect parameters such as sulphide (i.e. through increased microbe activity, addition of precipitation to the waters etc.), trace metals and TOC/DOC. 3) The groundwater reaches the surface as a series of pulses. This may affect parameters related to gas phases, for example causing loss of radon and other dissolved gases, and moreover it is more difficult to avoid air intrusion when collecting samples for sulphide analyses since the water volume from one pulse may be insufficient to fill a Winkler sample bottle.

The listed possible impacts on the quality of the approved groundwater data (and also the quality of the chemical analyses) may to some extent be excluded or verified by other samples from the same borehole sections. Most of the early SFR borehole section samples represent time series, i.e. they have been sampled at several occasions during a time period of more than twenty years and, generally, they show either a quite stable water composition or a clear trend due to the changed hydraulic conditions from the impact of the SFR repository. Besides long time series, data exist also as sample series, i.e. regular and frequent samples collected during a period of days or weeks during continuous discharge from the borehole section being sampled. Sample series were collected from the recent SFR extension project boreholes as normal routine practice. Sample series have also been collected from the early SFR boreholes on several occasions but from a limited number of borehole sections. Consistent results from sample time series and sample series increases the confidence in the data.

4.3.3 Estimations of initial section water contribution to the samples

Water samples should ideally consist of 100% formation groundwater from the water bearing fractures in the bedrock close to the borehole section in order to be fully representative. Generally, at least three but preferably five section volumes of groundwater are discharged prior to sampling in order to obtain high quality samples. However, to which extent the desired condition is attained depends on the distribution and hydraulic transmissivity of the flow anomalies that characterise the borehole section. Two examples are presented in Figure 4-6. The sketch on the left-hand side of the figure shows a single water bearing fracture (**A** and **B**), with high hydraulic transmissivity, located in the upper/nearest part of the borehole section, close to the outlet from the section. This situation is favourable since the water volume in the part of the borehole section beneath the fracture will remain trapped regardless of the discharge from the section (i.e. it is a dead volume). If, on the other hand, there are several fractures in the section (**C** and **D**; right-hand side of the figure), borehole water between the fractures will continue to contribute to the sample being extracted until formation water from the last fracture reaches the outlet.

Simple plug flow calculations, as described in /Nilsson et al. 2010/, have been used to make rough estimations of the contribution of initial section water to the final SFR extension samples collected. The results are presented in Table 4-2 below. The travel times are calculated assuming that the flow is plug flow. In reality, the flow velocity has a distribution across the borehole which is dependent on the roughness or irregularity of surfaces and geometrical conditions in the borehole section. Since the borehole sections are filled with dummies and tubing, it has been assumed reasonable to multiply the calculated travel times by a factor of 1.5 to 2. From Table 4-2 it can be concluded that reasonably representative samples were obtained from boreholes HFR106, KFR101and KFR102A, the bottom section in KFR106 and sections 120–137 and 265–303 m borehole length in KFR105. On the other hand, the estimations indicate that the groundwater in the shallow section in KFR106 and in KFR105 (sections 4–119, 138–169 and 170–264 m borehole length) were not sufficiently exchanged.

In spite of the removal of large volumes of water, the water composition in the samples from the bottom section of HFR106 was not stable and the first sample showed a similarly dilute composition as the stable sample series collected from the upper section. It is likely that this trend arises due to the pressure conditions. There is a pressure gradient between the two sampled borehole sections which are approximately 0.5 m apart and both are characterised by high hydraulic transmissivity which will facilitate water exchange. Therefore, a significant water volume may have been transported downwards prior to the packer installation and sampling. This can be traced by the gradual decrease of shallow groundwater contribution to the samples reflected in the water composition trend.

The reason for the fairly low content of formation water in the final samples from KFR105 (sections 4–119 m and 170–264 m borehole length) is that the total flow is obtained from a large number (about 50 in both cases) of water bearing fractures and the contribution from each one of them is small. In section 138–169 m, with fewer water bearing fractures, removal of twice the discharged volume would have been needed in order to reach 98% formation water. The situation in section 265–303 m is similar to section 138–169 m; however, twice the volume was pumped from this

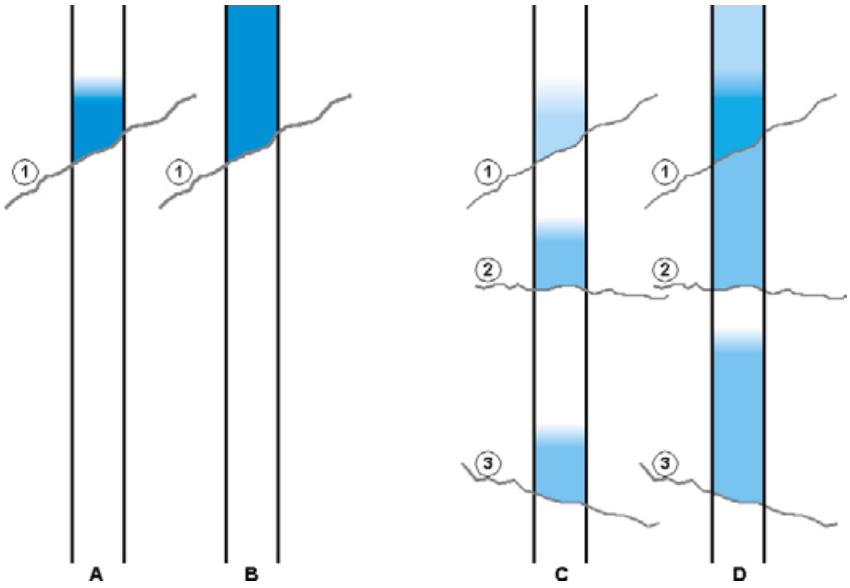

Figure 4-8. *Estimation of initial section water contribution to the samples. The colour strength illustrates the amount of new formation groundwater in a borehole section during pumping. A and B show a situation with one water yielding fracture. Shortly after pump start (A) the water from the fracture has not reached the outlet from the section. After a certain time (B), all the water being extracted from the section is formation groundwater. C and D show a situation with three fractures yielding a similar contribution of section water to the total flow. Shortly after pump start (C), no formation groundwater has reached the outlet from the section. After a certain time (D), corresponding to situation B, formation groundwater from fracture 1) has reached the outlet and formation groundwater from fracture 2 has passed fracture 1. Formation groundwater from fracture 3 has not yet reached fracture 2) and the water at the outlet from the borehole still represents a mixture between formation groundwater and initial section water since fractures 2) and 3) are not yet contributing.*

borehole section before the final sample was collected. In section 120–137 m borehole length the conditions were favourable since there was only one dominating flow anomaly and an absence of small contributions from fractures behind this anomaly. When interpreting the results from the plug flow calculations, it is necessary to consider also the uncertainty and resolution of the transmissivity values used in the calculations. If the largest flow anomalies are close to the detection limit, small fractures below the limit may contribute to a relatively large part of the total flow. In all the above cases, the detection limits were about 2 orders of magnitude below the largest single anomalies and in some cases more than 3 orders of magnitude below the total transmissivity for the entire section. Small, non-detected anomalies are therefore not likely to contribute with more than one or two percent to the total flow.

4.3.4 Data selection

In /Nilsson A-C 2009/ the data from the early SFR boreholes (1984 to 2007) were evaluated with respect to quality and an assignment with respect to their value for further hydrogeochemical interpretation work was made using the same general approach as in /Smellie et al. 2008/. However, some modification was necessary to accommodate: a) data that were collected over a long time period with gaps in analyses and improvements in analytical procedures, b) absence of drilling fluid data, and c) because the system has been transient since the SFR construction, it was difficult to select undisturbed samples. In this 0.2 version, including also groundwater data from the recent SFR extension project, the categorisation is simplified and the samples are judged either as useful for modelling (Dataset I) or not useful (Dataset II). The criteria for the judgement are listed below.

Samples omitted from Dataset I and included in Dataset II are the following:

1. Samples collected during the first investigation in SFR from 1984 to October 1986. It is clear from the scattered concentration values and the often unacceptably large charge imbalances that analytical data from this first investigation are less reliable /Nilsson A-C 2009/.
2. Samples having a charge imbalance exceeding ±5%.
3. Drilling water samples and samples with a high drilling water content (> 10%).
4. Samples collected for process control purposes as, for example, return water from drilling.
5. Early samples with high pH values which probably reflect concrete grouting in galleries and tunnels.
6. Samples with a very incomplete dataset
7. Sample series from the two investigated sections in borehole KFM11A (PLU) due to very unstable water composition (cf. Section 4.3.2).

Some of the data in Dataset II may be useful in some special contexts (e.g. assessing hydraulic properties or evaluation of drilling impacts) but need to be used with caution.

Table 4-2. Removed water volumes and estimation of formation water contribution to each sample (SFR extension boreholes).

Borehole: section no.	Section (mbl)	Sample no	Removed volume (L)	Formation water (%)	
				Plug flow	2 x plug flow
KFR105:1	265-303	16333	25.20	40	<1
		16334	411	78	68
		16335	805	99	78
		16336	1185	99	98
		16337	1618	99	99
		16365	-		
KFR105:2	170-264	16357	16.8	<1	<1
		16359	870	93	90
		16358	945	93	91
		16360	1148	93	92
KFR105:3	138-169	16367	11.4	3	<1
		16370	556	95	92
		16369	591	95	92
		16368	752	96	92
KFR105:4	120-137	16361	5.3	<1	<1
		16362	527	100	100
		16363	1107	100	100
		16364	1777	100	100
		16366	2266	100	100
KFR105:5	4-119	16371	1.33	<1	<1
		16374	470	76	72
		16373	510	76	72
		16372	864	88	76
KFR101:1	279.5-341.76	16209	24	2	<1
		16210	62	90	72
		16208	120	99	90
		16239	163	99	99
		16145	230	99	99
		16240	589	99	99
		16241	1055	100	99
		16242	2109	100	100
KFR102A:2	423-443	16226	221	99	98
		16227	824	100	100
		16228	1726	100	100
		16232	2333	100	100
		16233	2865	100	100
KFR102A:5	214-219	16234	256	100	100
		16235	794	100	100
		16236	1713	100	100
		13237	2354	100	100
		13238	2953	100	100
KFR106:1	260-300.13	16602	568	100	100
		16603	606	100	100
		16604	685	100	100
KFR106:2	143-259	16599	614	90	89
		16600	655	90	89
		16601	739	90	89
HFR106:1	175-190.4	16327	237000	100	100
		16328	711000	100	100
		16329	1185000	100	100
HFR106:2	47-174	16330	770000	100	100
		16331	231000	100	100
		16332	385000	100	100

* Proportion of formation water estimated from plug flow
** Proportion of formation water based on the assumption that 2 × plug flow is required to reach the corresponding proportion of formation water.

5 Data from other disciplines or investigations

Data and information from other disciplines, that have been used to understand different water sampling aspects, or to construct the hydrogeochemical conceptual model presented in this report, are summarised in Table 5-1.

The hydrogeochemical model and the description presented in Chapter 7 are based on the deformation zones (their positions and extensions) as defined in the Geological Site Descriptive Model (SDM) version 0.1 and summarised in Chapter 2 of this report. This initial model version is based on information from the early boreholes drilled from the surface and subsequently from the SFR facility itself, but does not consider the new boreholes drilled within the SFR extension project. Information from the new boreholes will be included in the final geological model version 1.0 scheduled for April–May 2010. This, in turn, will provide the geological basis for the final Hydrogeological Site Descriptive Model version 1.0. There is a risk that the final geological model may require some modification to the final Hydrogeochemical Site Descriptive Model version 1.0.

Hydrogeological information is especially useful in various contexts, for example;

- To help evaluate the quality of the hydrochemical samples (i.e. identification of mixing processes, influence of short circuiting, demarcation of potential contamination sources etc.).
- To help construction of the conceptual hydrogeochemical model.
- To help understand the development of the groundwater system over time. Knowledge of the hydraulic properties of the SFR site over time has two important applications: a) present-day hydraulic conditions have produced groundwater patterns which replicate to a large extent what will result during the next glaciation (long-term perspective), and b) the future impact of extended excavations and underground construction on groundwater chemistry can be predicted from past to present-day observations at the SFR site (short-term perspective).

This means that integration between the hydrogeological and hydrogeochemical models will be even more important during the version 1.0 phase.

Table 5-1. Data from other disciplines or investigations and area of use.

Type of data	Area of use
Transmissivity of specific flow anomalies (T_d)	Estimations of initial section water contribution to each sample (Plug flow calculations).
Flow anomaly position (l_i= borehole length from top of casing to inferred flow anomaly from PFL log).	
Geometric information on borehole and borehole equipment (i.e. borehole diameter and volumes or packers, tubing and dummies).	
Removed water volume before collection of sample.	
EC for discrete fractures (from PFL log)	3D visualisation of EC/salinity distribution.
Geology SDM version 0.1 (Deformation zone model) /Curtis et al. 2009/.	3D visualisations and interpretations, connections between groundwater composition/residence times and geol. entities.

6 Explorative analyses

Explorative analysis was performed in order to describe the data and construct a conceptual model for the area, see sections 3.3.3 and 6.1 and Chapter 7. In this context, explorative analysis implies a general examination of the groundwater data using traditional geochemical approaches such as:

1. use of ion-ion/isotope cross plots to provide a first insight to the origin and evolution of the groundwaters and make a subdivision into water types,
2. use of x-y scatter plots to describe depth variations,
3. use of ion-ion/isotope cross plots to check correlations related to groundwater types,
4. 3D presentations of electrical conductivity (EC) as well as of water type distribution in order to demonstrate variations in the model volume and possible association with deformation zones.

Since the approved dataset comprises a long time period (November 1986 –December 2010), the data in this chapter are used somewhat differently. The 3D presentations include new data from the SFR extension boreholes together with data from 2006 from the early SFR boreholes. The selection of the most recent complete dataset from 2006 to represent present conditions seems justified since most of the changes in the groundwater composition occurred prior to 2000 (see /Nilsson A-C 2009/ for time series of data) and the conditions have been more or less stable since then. The x-y scatter plots, on the other hand, present all approved data from the entire time period and often PLU data from Forsmark are included for comparison. Changes in groundwater composition with time are treated in Section 6.6.

The spatial distribution of the salinity was examined to provide an initial basic understanding of the hydrogeochemical conditions in the model volume. The electrical conductivity (EC) is a direct measure of the salinity in the groundwaters in the different boreholes/borehole sections. A three-dimensional visualisation of the boreholes is presented in Figures 6-1 (a, b), showing the distribution of EC in groundwaters in the regional (a) as well as the local volume (b) in relation to major deformation zones. The displayed EC data were measured at two different occasions using two different methods; 1) borehole measurements during PFL logging and pumping from a specific fracture, and 2) measurements in groundwater samples from investigated borehole sections. The EC data from the PFL logging were included to obtain a better data coverage of the model volume and a more complete picture. Some caution is needed in the interpretation since the values do not represent exactly the same conditions. However, in those cases where both measurements are available for the same part of the borehole, the values agree fairly well.

Some observations from the salinity distribution in the 3D Figure 6-1 (a, b) are listed below.

- The overall EC range at the SFR site (600–1,600 mSm^{-1}) corresponds to a chloride concentration of 1,500–5,500 mgL^{-1} down to a depth of about –400 masl. In four bore-holes, KFR101, KFR102A, KFR106 and KFR02 groundwaters with lower EC/Cl concentration are found at greater depth than groundwaters with higher EC/Cl concentration; this contrasts with the more common increase in salinity with depth normally recorded in bedrock groundwater environments.
- The highest EC values are found in early samples from boreholes KFR7A and KFR10 intersecting deformation zones 8 and 3, respectively. These boreholes and the two zones also connect to zone H2. At present the EC reaches a maximum of about 1,300 mSm^{-1}, although early samples from the two mentioned boreholes recorded EC values up to about 1,600 mSm^{-1} corresponding to about 5,500 mgL^{-1} Cl.
- The lowest EC value of 600 mSm^{-1},corresponding to about 1,600 mgL^{-1} Cl (i.e. lower than the present Baltic Sea), is found in borehole KFR101 at a depth of –240 to –262 masl. Chemical and isotope analyses confirmed a significant glacial meltwater contribution in this groundwater and contamination from meteoric water can be excluded.

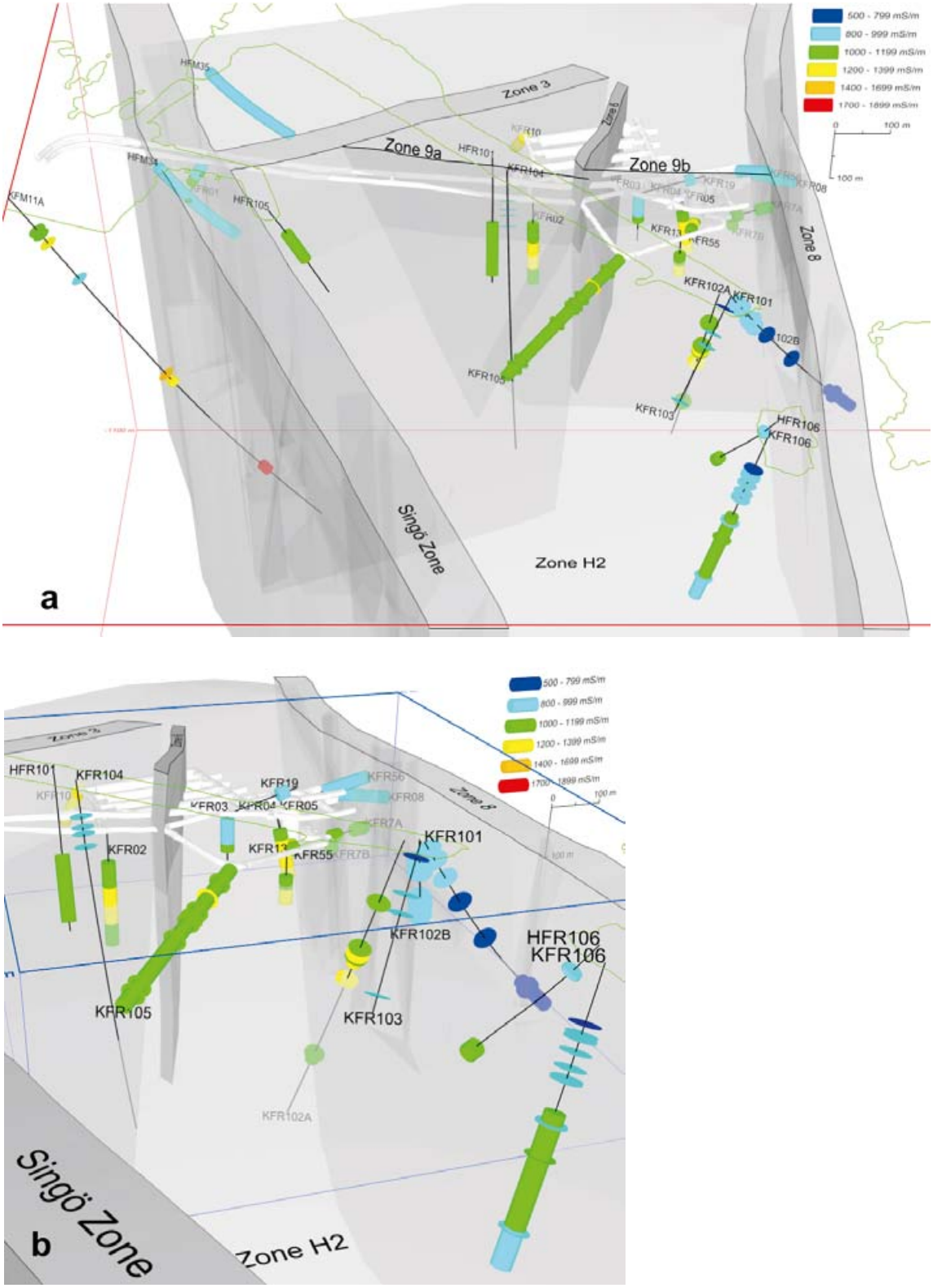

Figure 6-1 a and b. *3D presentation of the distribution of Electrical Conductivity (EC) in relation to major deformation zones in the: a) regional, and b) local model volumes. Fracture EC values measured during PFL flow logging are represented by disks and EC measured in samples from investigated sections are represented as cylinders. The early SFR boreholes are represented by EC data from 2006 (cf. Table 4.1). a) Overview showing all the boreholes included in the SFR model version 0.2. b) Detail concentrated to the local model volume. Zones 9a and 9b are omitted to improve clarity. Note the decrease in colour intensity along the boreholes when viewed through a penetrated rock/deformation zone volume.*

6.1 Depth trends

6.1.1 Selected major ions

Three important hydrochemical indicators (Cl, Mg and $\delta^{18}O$) were used for the subdivision of the groundwaters into different groundwater types (section 3.4). Plots against elevation (two elevation ranges), showing also the water types (colour coded), are given in Figure 6-2 (a–f).

Chloride (6-2 a, b) is one of the main components in these groundwaters and it is directly correlated with their salinity, see also Figure 6-1. The main hydrogeochemical data included in the SFR 0.2 version represent the depth range 20–400 m where the chloride concentration varies between 1,600 and 5,500 mgL^{-1}. However, only a few data points are below 2,800 mgL^{-1} Cl (equal to the concentration of the present Baltic Sea) or exceeding 4,500 mgL^{-1} Cl, (the typical Littorina type composition identified from the PLU investigation). All of the latter were observed prior to 1995 since impacts from the SFR facility have caused dilution with time. The chloride concentrations do not show any clear depth trend, but rather reflect consequences of groundwater type and association to different deformation zones. The groundwater type coding reveals that more dilute brackish groundwater of the local Baltic type is found at shallow depths down to 100 m while the groundwater with the lowest salinity (1,600 mgL^{-1} Cl) is of the brackish glacial type and found at approximately 240 m depth. The most saline groundwater is generally found at intermediate depths (100–200 m) and represents the brackish marine Littorina type.

The magnesium concentration (6-2 c, d) emphasises the marine influence in most groundwaters within the SFR model volume. The magnesium concentration varies between approximately 30 to 300 mgL^{-1} and the lowest concentrations (< 10 mgL^{-1}) observed from PLU were absent in samples from the SFR site. This implies that even the mainly non-marine groundwaters contain a minor marine component. The younger marine groundwaters of the local Baltic type generally show magnesium concentrations between 90 and 150 mgL^{-1} and are found down to depths of about 100 m while the older marine groundwaters of the Littorina groundwater type show magnesium concentrations between 150 and 280 mgL^{-1} and are found at depths between 100 and 200 m. Both these groundwater types are preferably encountered in, or adjacent to, deformation zones, see Figure 7-1. The magnesium concentrations in groundwaters of the two mainly non-marine water types are still relatively high, although the Mg/Cl ratio decreases and the marine component is less conspicuous.

With respect to oxygen-18 (6-2 e, f), three ranges are distinguished: a) enriched values ranging from $\delta^{18}O = –9.5$ to –7.5‰ V-SMOW representing groundwaters of marine origin (local Baltic and Littorina type), b) values in the intermediate range between $\delta^{18}O = –12$ and –9.5‰ V-SMOW representing mixed brackish groundwater of the transition type, and finally c) depleted values of $\delta^{18}O = –16$ to –12‰ V-SMOW with a significant glacial component giving a low $\delta^{18}O$ signature. The enriched values are found at shallow (local Baltic type) and intermediate depths (Littorina type) and in connection to deformation zones, see Figure 7-1, while the most depleted values are found above and below zone H2 and also relatively deep in zone 8 (KFR101).

Figure 6-3 (a-e) shows the variation of the potassium, sulphate and bromide with depth. In most cases, in common with chloride, magnesium and $\delta^{18}O$, the subdivision of the of the groundwater types is reflected in the other major elements. By comparing the brackish marine and the brackish non-marine groundwaters at similar depths, the marine groundwaters generally show higher potassium and sulphate concentrations as well as Na/Ca weight ratios (Figure 6-4 b, c) than the non-marine groundwaters. This is more or less true also for bicarbonate (Figure 6-4 a) due to the residence times reflected in the groundwater types. Bromide (Figure 6-3 e, f) shows a somewhat increasing trend with depth but, except for the comparatively low concentrations in the local Baltic groundwater type, the correlation with groundwater types is somewhat weak.

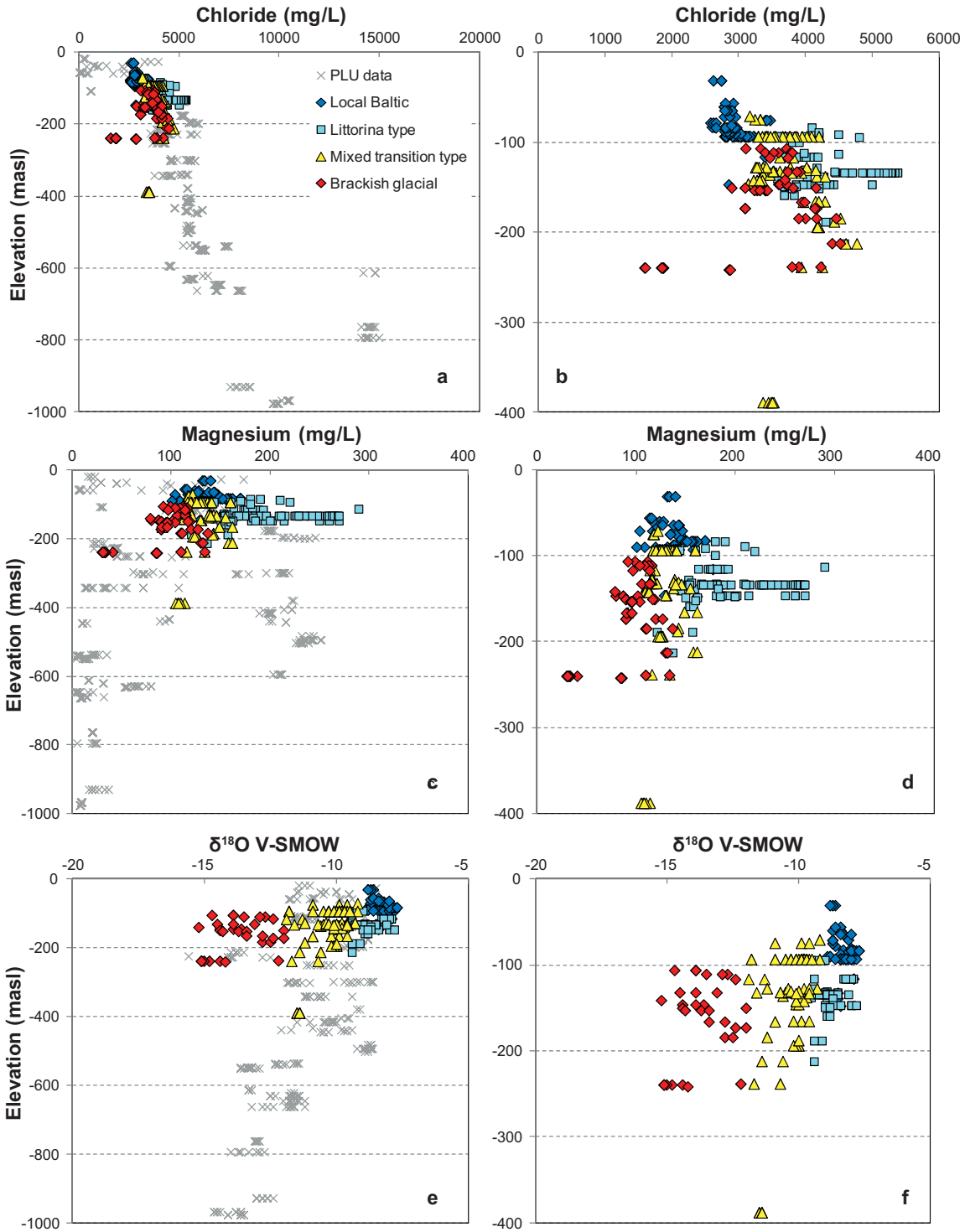

Figure 6-2 a-f. *Distribution of chloride, magnesium and $\delta^{18}O$ with depth related to the different groundwater types defined for the SFR Site in section 3.4. The diagrams to the left include PLU data (Forsmark) down to 1,000 m while the diagrams to the right are restricted to 400 metres depth which is more relevant to the SFR extension data.*

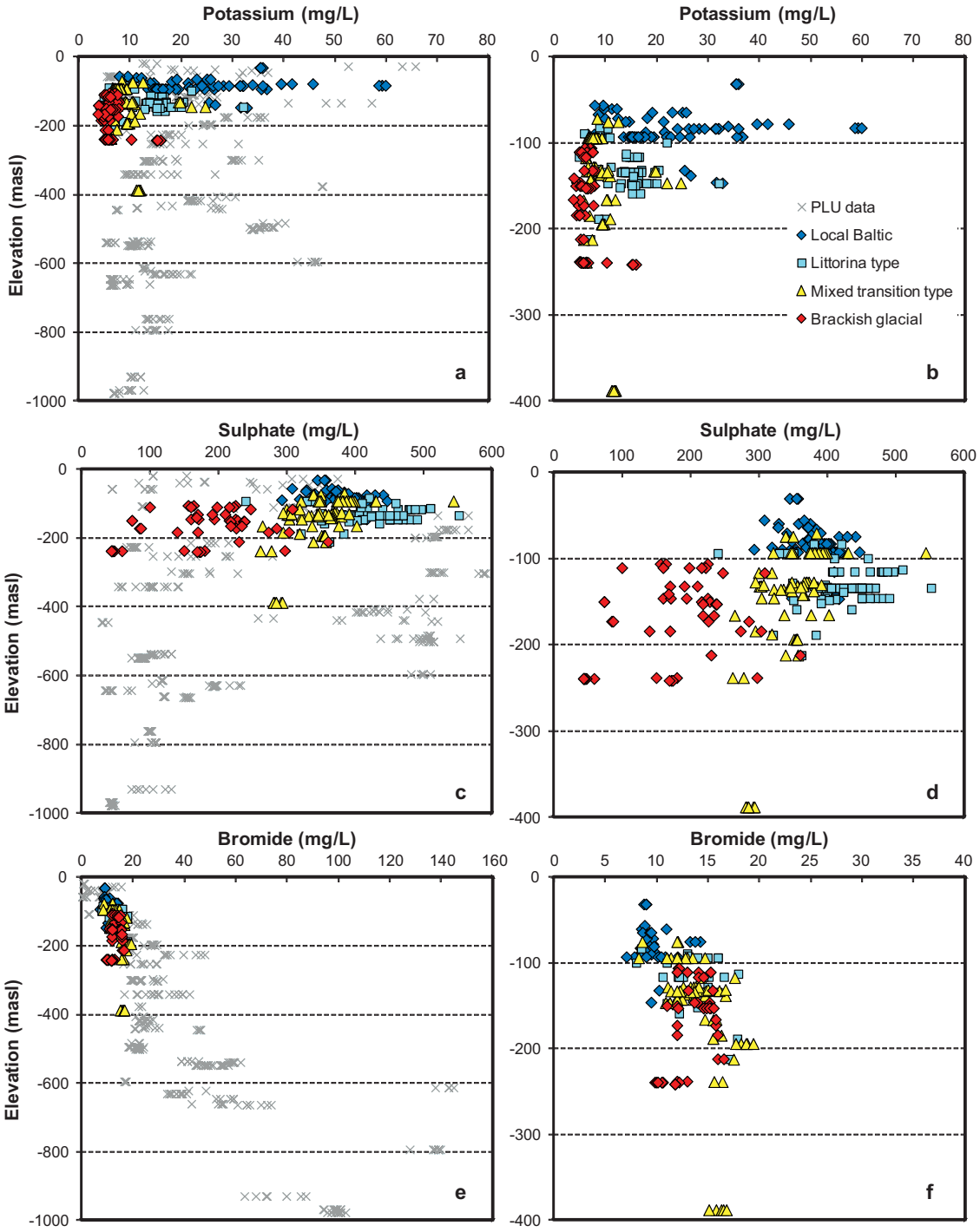

Figure 6-3 a-f. *Distribution of potassium, sulphate and bromide with depth related to the different groundwater types defined for the SFR Site in section 3-4. The diagrams to the left include PLU data (Forsmark) down to 1,000 m while the diagrams to the right are restricted to 400 metres depth which is more relevant to the SFR extension data.*

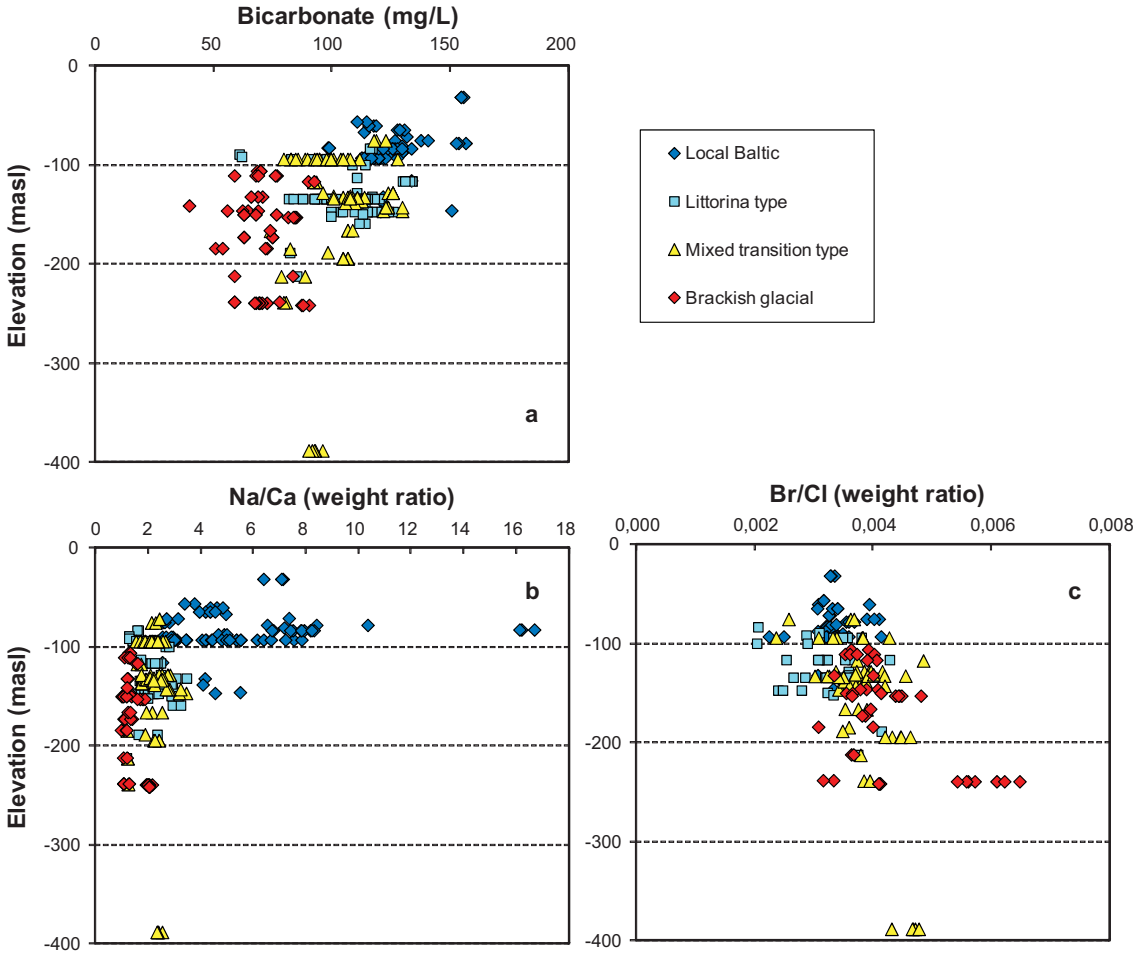

Figure 6-4a-c. *Distribution of bicarbonate concentration and Na/Ca and Br/Cl weight ratios with depth related to the different groundwater types defined for the SFR Site in section 3.4.*

Some observations of special interest from the plotted depth distributions are listed below:

- The highest chloride and magnesium concentrations, and also some of the most enriched $\delta^{18}O$ values, are observed in early samples from the SFR boreholes, i.e. KFR7A and KFR10 at depths of –134.43 and –116.23 masl, respectively. None of the groundwaters sampled in the recent boreholes, representing the SFR extension phase, show these high salinities. Both sampled borehole sections are located at depth in two different vertical deformation zones, zone 8 and zone 3 where they also connect to zone H2, see Figure 7-1. Furthermore, the salinity has decreased with time at both locations following the first sampling in 1986 due to the drawdown of Baltic Sea water resulting from the presence of the SFR repository. However, samples from both boreholes still retain the Littorina type signature today.
- The lowest chloride and magnesium concentrations and also the most depleted $\delta^{18}O$ values are observed in the recently drilled borehole KFR101 at –240.15 masl. The chloride concentration is significantly lower than Baltic Sea and varies between 1,600 and 1,800 mgL^{-1}. None of the other boreholes show concentrations in this low range.
- Four boreholes KFR101, KFR102A, KFR106 and KFR02, see Figure 6-1, show a decreasing salinity trend with depth in boreholes. This salinity difference is most striking in KFR101. These conditions are due to the presence of Littorina or mixed transition type groundwaters located above the brackish glacial type groundwater of lower salinity.
- The local Baltic type water is typically found at relatively shallow depths close to zones 3 and 8 and the Singö zone. Borehole KFR08 penetrating zone 8 has been frequently sampled and is considered typically representative for marine water of local Baltic type. It is unclear if the Baltic Sea water was present in this bedrock fracture system before the excavations of the SFR facility. The boreholes were drilled from the tunnels and the drawdown effect in the meantime may have caused the intrusion of this water between the excavation and the first sampling.

- A few samples of local Baltic type groundwater have been collected at a deeper level than the other data representing this groundwater type (at 130–150 m depth). These data points represent single samples from boreholes HFR106, KFR7A, KFR7B and KFR10. These samples represent outliers in the time series measurements from these boreholes where the dominant groundwater is of Littorina type in all cases except for the bottom section of HFR106. The series of samples collected from this section show a trend from a more diluted Baltic type to a more saline brackish glacial type groundwater. This is most likely due to a decreasing contribution of shallower groundwater to the samples. A pressure gradient between the two sections may have caused a downward water flow and supplied the lower section with groundwater of a more shallow type prior to sampling, cf. Section 4.3.3.

6.1.2 Selected minor ions

Trace metals and rare-earth (REE) components generally occur in groundwaters at concentrations of less than 1 mgL^{-1} /Drever 1997/. The following elements have been regularly analysed within the present SFR site investigation programme: Al, B, Ba, U, Th, Fe, Mn, Li, Sr, Sc, Rb, Y, Zr, In, Sb, Cs, La, Ce, Pr, Nd, Sm, Eu, Gd, Tb, Dy, Ho, Er, Tm, Yb and Lu. Also included are commonly occurring heavy trace metals such as Cu, Ni, Cr, Zn, Pb and Mo even though these may be influenced by contamination related to borehole activities. The risk of contamination is large also for aluminium and the usefulness of the analytical results can be questioned. However, the trace metals and REE data from previous investigations in the early SFR boreholes are few and patchy for the model volume which limits interpretation. This report is restricted to short discussions about the redox sensitive elements iron, manganese, hydrogen sulphide and uranium as well as TOC/DOC in Section 6.3.

6.2 Major ion-ion/isotope plots

Figures 6-5 to 6-7 show a collection of ion-ion/isotope cross plots which can provide additional insight to the origin and evolution of the groundwaters, such as revealing whether the ground-water composition is affected by processes other than mixing (e.g. precipitation/

dissolution of mineral phases or ion exchange). Two chloride ranges are given covering the entire PLU range to the left, and the more narrow range relevant for the SFR site to the right. In Figure 6-5, magnesium, $\delta^{18}O$ and potassium are plotted versus chloride. Figures 6-6 and 6-7 displays bicarbonate, bromide and sulphate as well as Na/Ca weight ratio versus chloride.

Magnesium and $\delta^{18}O$ are the determining indicators used for the subdivision into groundwater types together with chloride and, therefore, they show a clear contrast between the pre-Littorina brackish non-marine groundwaters and the more recent marine groundwaters (local Baltic and Littorina types). Magnesium (Figure 6-5 a and b) is susceptible to ion-exchange reactions and consequently the brackish marine groundwaters do not follow strictly the mixing line between Littorina, Baltic Sea and fresh meteoric water (cf. Figure 3-4a). It can be concluded, therefore, that despite the effect of reactions, the Mg content in the brackish marine groundwaters is still sufficient to serve as a distinct marine indicator. Data on $\delta^{18}O$ ratios are sparsely available before 1995; Figure 6-5 c and d display the narrow chloride concentration range and at the same time the large variation in $\delta^{18}O$.

Potassium (6-5 e, f) and also bicarbonate, bromide, sulphate and Na/Ca weight ratio (6-6 a-f and 6-7 a and b) show a more or less clear distinction between the different groundwater types. As expected, most of the overlap is by the mixed transition type with the other groundwater types. The potassium concentration is high in both types of brackish marine groundwaters as demonstrated by the two peaks (Figure 6-5 e) at chloride concentrations close to 3,000 mgL^{-1} and at above 5,500 mgL^{-1} for the local Baltic and the Littorina type of groundwater, respectively. The fact that none of the samples in the SFR dataset reflects the strongest Littorina signatures from PLU is very obvious from this plot. The Littorina – glacial meltwater mixture found at the SFR site plots more towards the glacial meltwater side than the typical Littorina type groundwater sample from PLU.

The bicarbonate concentrations (Figure 6-6 a, b) are related to the microbial breakdown of organic material and are, as expected, highest in the shallow brackish marine groundwaters of the local Baltic type (usually higher than the original 70–90 mgL^{-1} found in the Baltic Sea water at the surface). Also, the transition type groundwaters and the brackish glacial groundwaters have concen-

trations well above 50 mgL^{-1} and the extremely low values encountered in the PLU dataset do not occur in the SFR groundwaters. Furthermore, if the depth distribution is taken into account the SFR samples are generally higher in bicarbonate compared with PLU data from the same depth. Finally, the bicarbonate concentrations were high enough (> 30 mgL^{-1}) to allow ^{14}C dating of all the recent SFR samples.

The bromide versus chloride plots (Figure 6-6 c,d) indicate two somewhat diffuse mixing trends for the brackish non-marine and brackish marine groundwaters, respectively (cf. Figure 4-6). Marine waters should have a bromide/chloride ratio of approximately 0.0035 whereas higher ratios (around 0.01) are more typical of water/rock interaction. The bromide/chloride ratio is usually a reliable marine indicator, but since the overall differences are not large enough, together with the associated analytical uncertainties which tend to obscure the details, the magnesium signature is still more informative when differentiating between a marine and non-marine origin.

From Figure 6-6 e and f it is clear that the major source of sulphate in the SFR groundwaters is of marine origin and correspondingly high sulphate contents are associated with both the local Baltic and the Littorina type groundwaters. The sulphate-sulphide system is presented in more detail in Section 6.3.

The Na/Ca weight ratio (6-7 a, b) shows a clear correlation to groundwater types with the highest values for the two marine groundwater types. However, the Littorina type values are significantly lower than the Baltic type which is probably the result of more intense water/rock reactions (ion exchange) and mixing with a non-marine saline component. The brackish glacial type shows a ratio close to one and is clearly affected by a deeper non-marine saline component.

6.3 Eh and redox sensitive elements

The results from actual measurements of Eh and redox sensitive elements (Mn, Fe, S and U) are discussed in this section. No redox pair calculations or speciation-solubility calculations have been performed to date due to scarcity of data and time constraints. Also, the few microbial analyses conducted and the role of microbes in the redox context will be treated in more detail in the final SDM report version 1.0.

6.3.1 Measured Eh

Redox measurements can be subjected to both technical and interpretative problems. Over the last 25 years, SKB has developed methodologies for measurement of this parameter /Auqué et al. 2008/ which can provide informative and reproducible results. Potentiometric Eh measurements have been performed in a few borehole sections at the SFR site in 1987, 2000 and 2009–2010 but none of the measurements were conducted *in situ* as was the case for PLU. Instead, the outlet in the tunnel from each borehole section was connected directly to a measurement cell where pumping was not required since the water discharged by natural over-pressure.

Redox measurements were conducted in three of the early SFR boreholes in 1987 and repeated in the same three borehole sections in 2000 /Nilsson A-C 2009/. The borehole sections were KFR01 (44.5–62.3 m), KFR7A (48.0–74.7 m) and KFR10 (87.0–107.28 m during 1987, and the entire borehole in 2000). The results from these measurements are uncertain and do not meet stipulated quality criteria. However, the measured potentials during 1987 in KFR7A –180 mV and in KFR01 –140 mV were in line with measured Eh values from the PLU investigation of brackish marine waters of Littorina type /Gimeno et al. 2008/. The measurements in 2000 were less successful and also that from KFR10 in 1987. Oxygen diffusion into tubing connecting the borehole outlet and the measurement cell is a likely explanation to some of the anomalously high potentials measured. However, an increase in Eh with time due to introduced shallow waters due to drawdown caused by the repository and the altered hydraulic conditions cannot be entirely excluded. However, the major problem is that the Eh measurements are very few, and this together with the large uncertainty in the measured values makes interpretation uncertain.

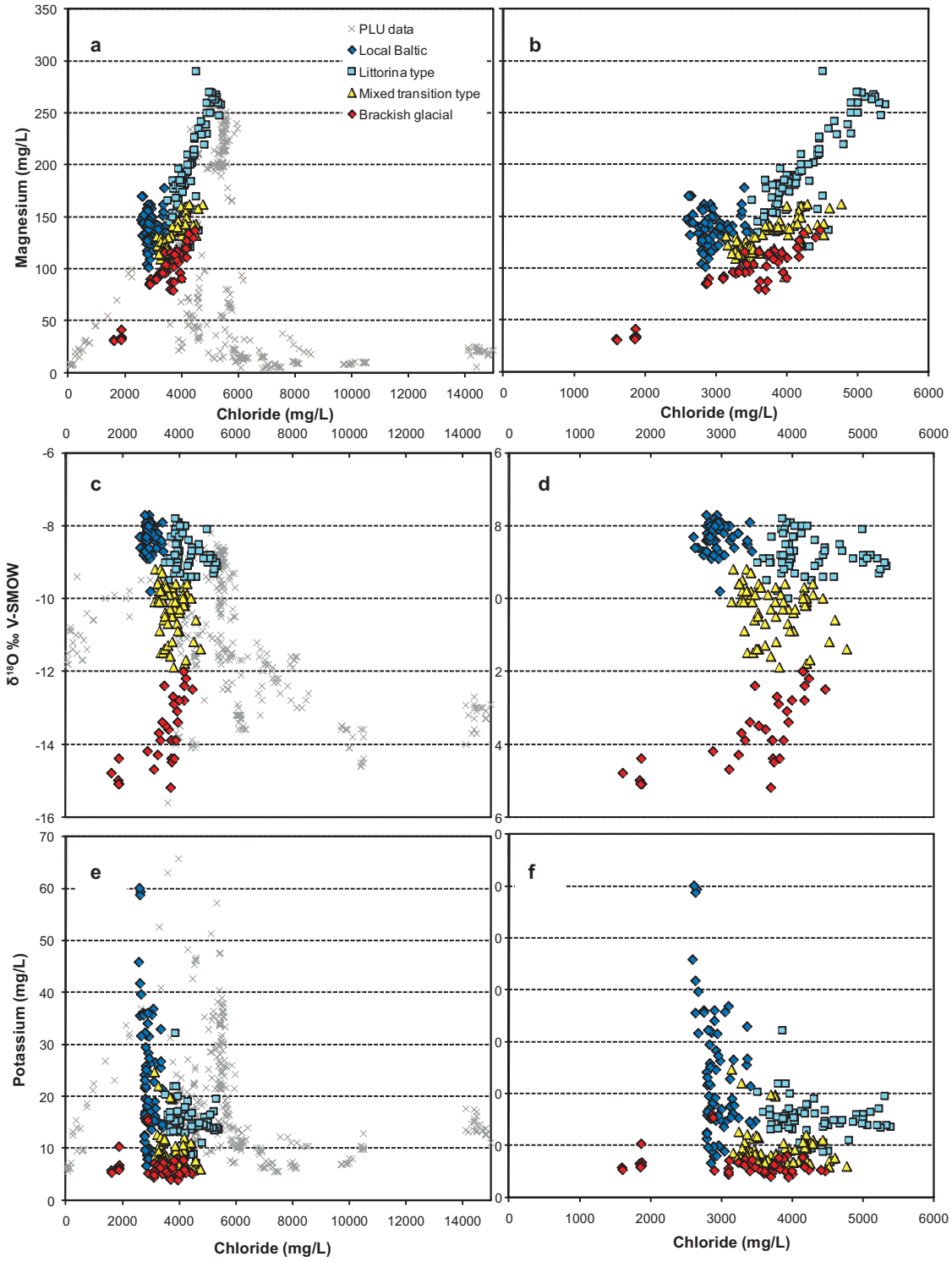

Figure 6-5 a-f. *Plots of magnesium, $\delta^{18}O$ and potassium versus chloride concentration at two different chloride scales referring to the PLU data (Forsmark) and SFR data, respectively. The groundwater samples are colour coded according to the different groundwater types defined for the SFR Site in Section 3-4.*

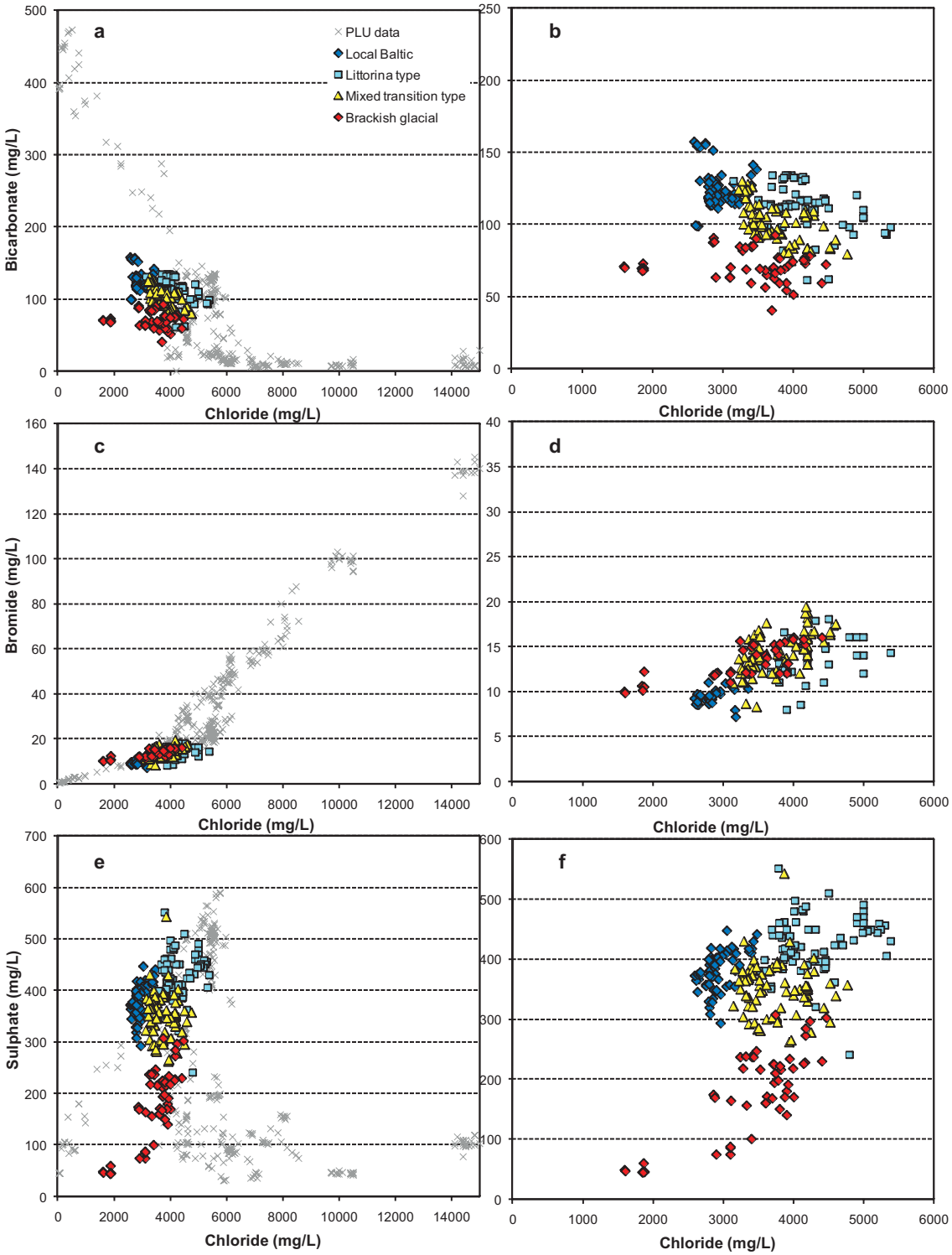

Figure 6-6a-f. *Plots of bicarbonate, bromide and sulphate versus chloride concentration. The plots use two different chloride scales referring to the PLU-data (Forsmark) and SFR data, respectively. The groundwater samples are colour coded according to the different groundwater types defined for the SFR Site in Section 3.4.*

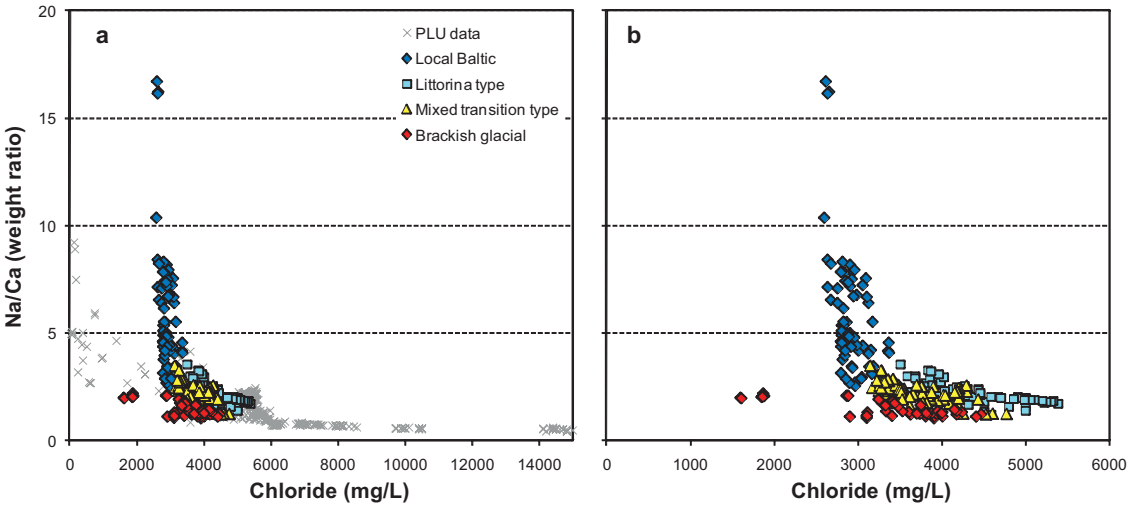

Figure 6-7a,b. *Plots of Na/Ca weight ratio versus chloride concentration. The plots use two different chloride scales referring to the PLU-data (Forsmark) and SFR data, respectively. The groundwater samples are colour coded according to the different groundwater types defined for the SFR Site in Section 3.4.*

Recent potentiometric Eh measurements within the SFR extension project demonstrate the difficulties to obtain reliable results. Measurements were conducted in two borehole sections in borehole KFR105 drilled from the SFR construction tunnel /Lindquist et al. 2010/. The first measurements were rejected due to possible oxygen intrusion but results from repeated measurements in the inner section provided relevant results verified by two different types of electrodes (Eh = –190 ± 15 mV).

6.3.2 Iron and manganese

The distribution of iron and manganese with depth are presented in Figure 6-8 a and b. Ferrous iron values from the SFR site range from 0.1 to 8 mgL^{-1} and for manganese between 0.1 to 4 mgL^{-1}. Only a few relatively shallow borehole sections between 90 m and 150 m depth show concentrations above 2 mgL^{-1} (Fe) and above 1.5 mgL^{-1} (Mn). However, no significant trend with depth can be observed. Instead, the highest values (over one order of magnitude for both Fe and Mn) are associated with the brackish marine Littorina type groundwaters mainly found in or adjacent to major deformation zones. Relatively high iron concentrations are found also in groundwaters of the local Baltic type, which is not reflected in the Mn contents. In contrast, manganese is more abundant in the brackish glacial groundwater than in the Baltic groundwater type. There is no clear correlation between Mn^{2+} and Fe^{2+} but the transition type groundwaters show generally low contents of both elements and the brackish glacial type show low iron concentrations, although some increased manganese concentrations are observed.

The presence of significant concentrations of ferrous iron provides additional support to the observed reducing conditions suggested from the measured Eh.

6.3.3 Sulphate and sulphide

Sulphide analyses have not been performed regularly in the early SFR boreholes but there are data from a few selected borehole sections dating from 1986, 2000 and 2006. The recent sampling programme in the SFR extension boreholes, however, has included sulphide analyses.

In common with the PLU investigation /Laaksoharju et al. 2008/, the sulphide data are difficult to evaluate due to uncertainties involving possible artefacts related to sampling conditions. Generally, the sulphide concentrations are very low and most of the initial samples from early, as well as recent boreholes, show concentrations below the detection limit. The increase in sulphide concentration with time observed in PLU is also observed in the only new SFR borehole (KFR101) that has been resampled after a few months. In this case, the sulphide concentrations amounted initially to 0.022 mgL^{-1} in November 2008 (first sampling) and then showed higher values, but with a decreasing trend in the

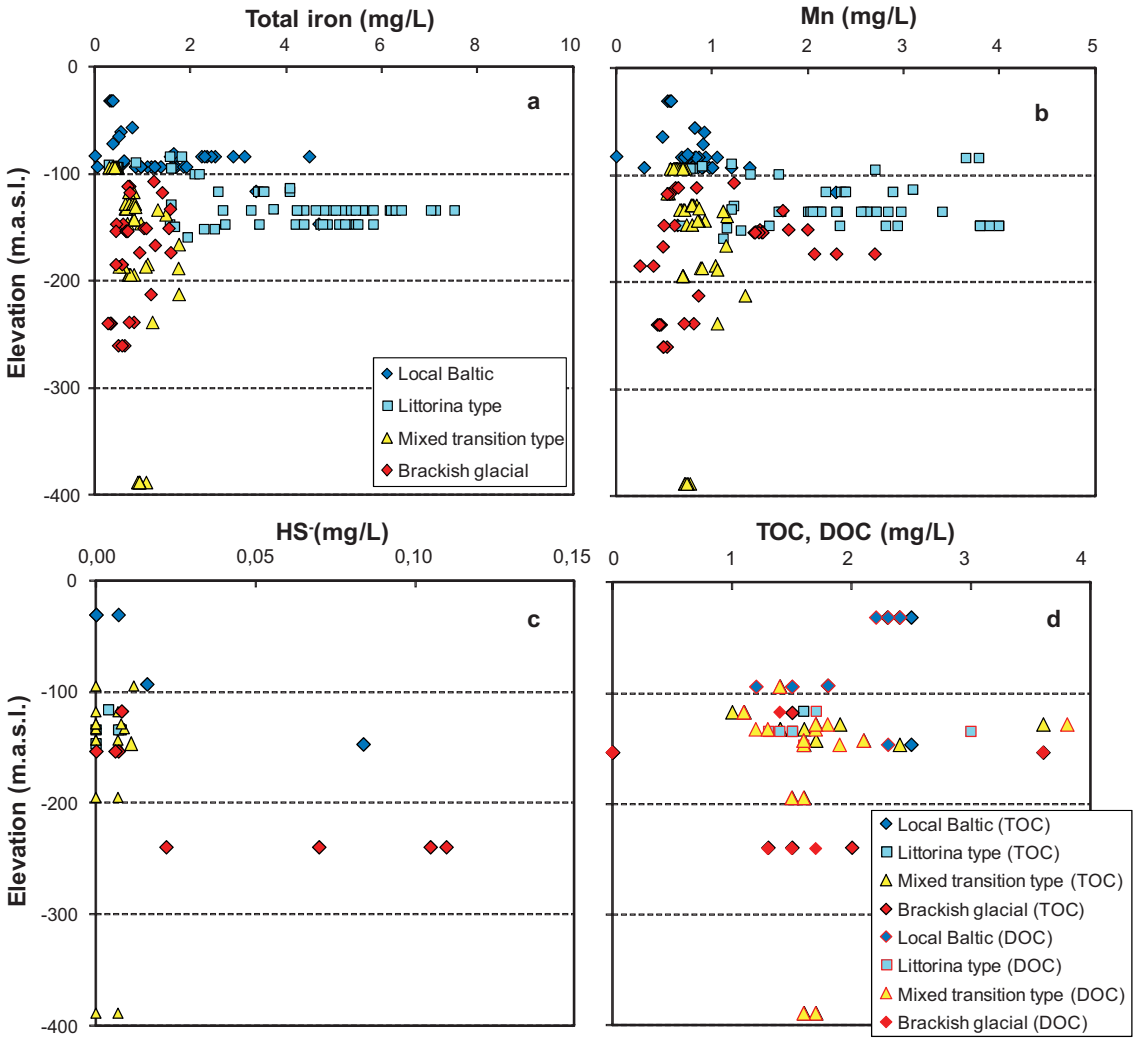

Figure 6-8 a-d. *Distribution of iron, manganese, hydrogen sulphide and TOC/DOC with depth related to the different groundwater types defined for the SFR Site in section 6.1.*

time series from March 2009 (0.110, 0.105 and 0.077 mgL^{-1}). The estimations in Table 4-2 based on plug flow indicate that the November 2008 sample, as well as the 2009 samples in March, contained almost entirely formation water (>90%). At the first sampling occasion, it is most probable that the sulphide concentrations were similar in the section water and in the formation groundwater. After four months, the sulphide concentration in the borehole section water may have increased enough to contribute significantly to the measured sulphide values observed despite the high percentage of formation water in the groundwater samples.

Groundwaters from a few early SFR borehole sections (1986–1987) show high initial concentrations of sulphide and clearly lower values in samples collected in 2000, but generally most concentrations are low and even below the detection limit. The exact sampling procedure is not documented for the very early samples, i.e. what was the time delay after drilling?, what were the exchanged water volumes before sampling?, which preceding investigations were carried out in the borehole section?, or other possible causes that might have impacted on the sulphide concentrations. Because of this, and the inadequate sulphide time series data, it is difficult to use with confidence the sulphide data from early SFR boreholes. Consequently, in Figure 6-8c which plots HS^- against elevation (masl), not very much can be said about any trends.

Sulphide in the groundwater is produced by sulphate-reducing bacteria which creates isotope fractionation of ^{32}S and ^{34}S resulting in a larger portion of the heavy isotope remaining in the sulphate because the sulphide is enriched in ^{32}S. Figure 6-9 a-c shows $d^{34}S$ versus elevation (masl), sulphate and chloride content for both the SFR and PLU data. It can be concluded that most of the SFR data show the same trends as the PLU data. The main source of the sulphate in the groundwater system

is marine (also supported by other marine indicators see Figures 6-6 and 6-7) and values around +21 to +24‰ CDT are common, supporting that many of the groundwaters have been subjected to some sulphate reduction. This is also supported by the fact that many of the groundwaters with a clear marine origin have undergone a reduction of their original SO_4/Cl ratio (cf. Figure 6-6 f), i.e. sulphate has been consumed. This may have happened in the bedrock or in the sediments before entering the fracture system. Four samples show significantly lower $d^{34}S$ values which are not readily understood and it is planned to reanalyse the samples.

6.3.4 Organic carbon (TOC and DOC)

Organic carbon is not a redox sensitive element *sensu stricto* but the amounts of available reduced carbon species influence the microbial processes.

Organic material in the groundwaters has been analysed and is presented either as TOC (Total Organic Carbon) or as DOC (Dissolved Organic Carbon) if filtered through a 0.4 um filter before being analysed. In a number of samples, both TOC and DOC have been analysed. Figure 6-8d compares TOC and DOC versus elevation (masl) which shows a generally good agreement implying that almost all organic carbon is present as molecules less than 0.4 µm in size.

The DOC values in deep groundwaters are expected to be close to the detection limit (1 mgL^{-1}) but at the SFR generally higher values can be expected due to past and present input of brackish Sea water. This is also seen in Figure 6-8 d which displays DOC and TOC in the range of 1 to 4 mgL^{-1}. There is no specific trend versus depth but the highest DOC values are present at depths of about –100 to –150 masl.

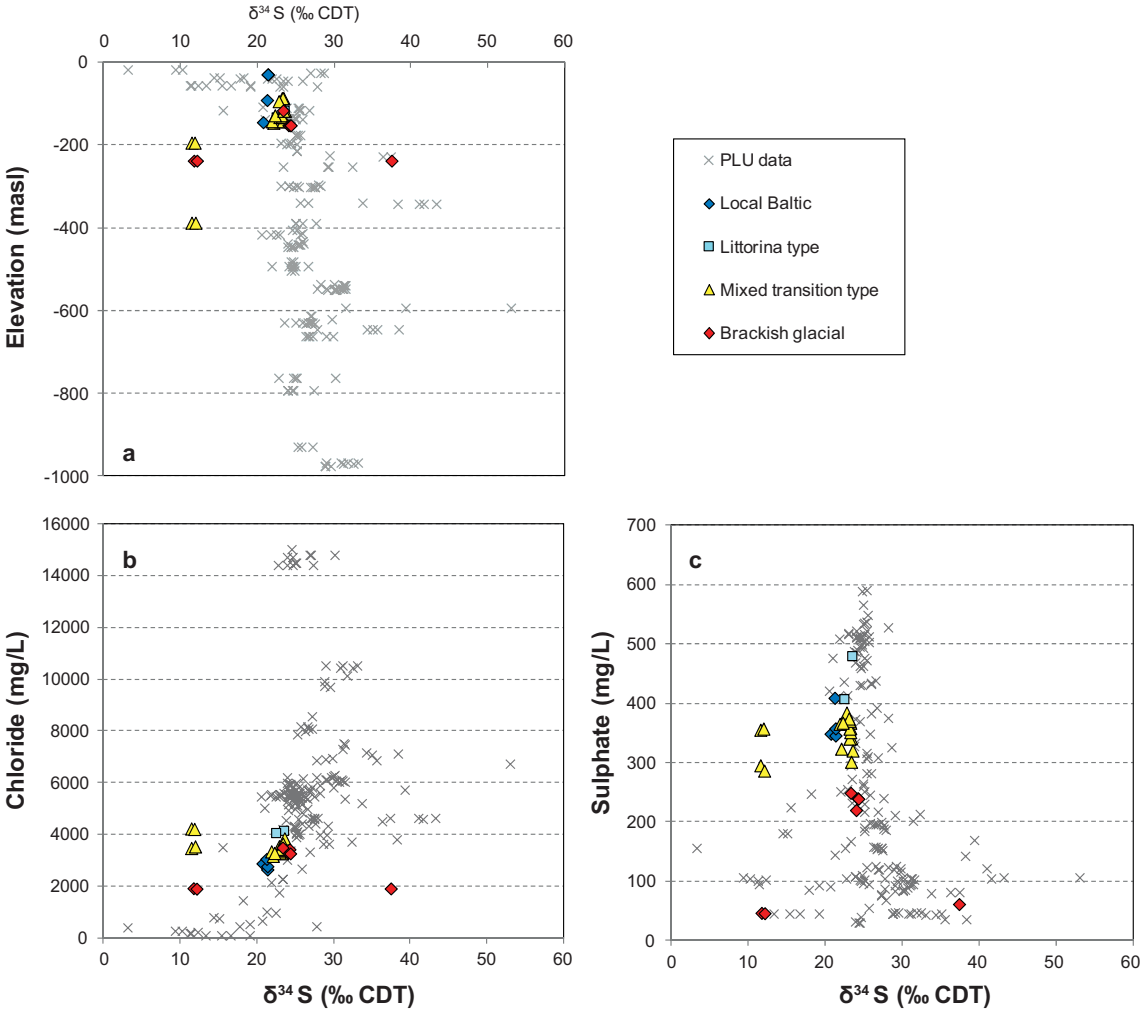

Figure 6-9. *Stable sulphur isotopes in sulphate versus elevation (masl) (a), sulphate content (b), and chloride content (c).PLU data includes Forsmark only.*

6.3.5 Uranium

Uranium in groundwaters commonly shows a trend of decreasing concentration with depth because U-VI is much more soluble than U-IV and is generally reduced with depth to the more insoluble U-IV form as the redox potential drops. This mobility is also dependent on available bicarbonate for complexation. In the PLU investigation, elevated uranium concentrations (>10 μgL^{-1}) were found in several borehole sections and also at depth down to 600 metres. These were generally associated with Littorina type groundwaters which were not oxidising but had Eh values > –190 mV and bicarbonate > 30 mgL^{-1}. The uranium concentrations in the groundwaters in the early SFR boreholes as well as in the new SFR extension boreholes show large variations from a few μgL^{-1} up to 140 μgL^{-1}, but generally most concentrations are higher than 10 mgL^{-1}, see Figure 6-10 a,b. These elevated concentrations, however, seem to have no connection to any specific groundwater type at SFR. Furthermore, the plot does not indicate any clear depth dependence. However, the sampling locations below about 200 m depth in the SFR extension project are very few and the really high concentrations among the PLU data are characteristic of deeper sampling locations.

As an integral part of the hydrogeochemical studies, but also from a safety assessment viewpoint in PLU as well as in the SFR extension project, it has become important to explain these elevated uranium concentrations. Several different hypotheses have been proposed which have been individually addressed in /Smellie et al. 2008/.

The conclusion from the PLU site investigation at Forsmark was that the most probable explanation to the elevated dissolved uranium contents was the presence of an easily dissolvable uranium phase heterogeneously distributed in the fracture system. When coming in contact with groundwaters characterised by Eh higher than –200 mV and HCO_3 concentrations more than 30, mgL^{-1} this uranium phase may become mobile. Solubility calculations showed that a stable U(VI)-carbonato complex is probably responsible for the higher concentrations observed in these groundwaters /Gimeno et al. 2008/.

There are strong indications that most groundwaters at the SFR site, independent of groundwater type, have Eh in the relevant range to support the above explanation. Furthermore, from Figure 6-10b, it is obvious that most samples show bicarbonate concentrations well above 60 mgL^{-1}. Ongoing work which includes fracture mineral sampling together with groundwater sampling in the SFR extension borehole KFR106, is focussed on the uranium issue with special emphasis to locate the solid uranium phase.

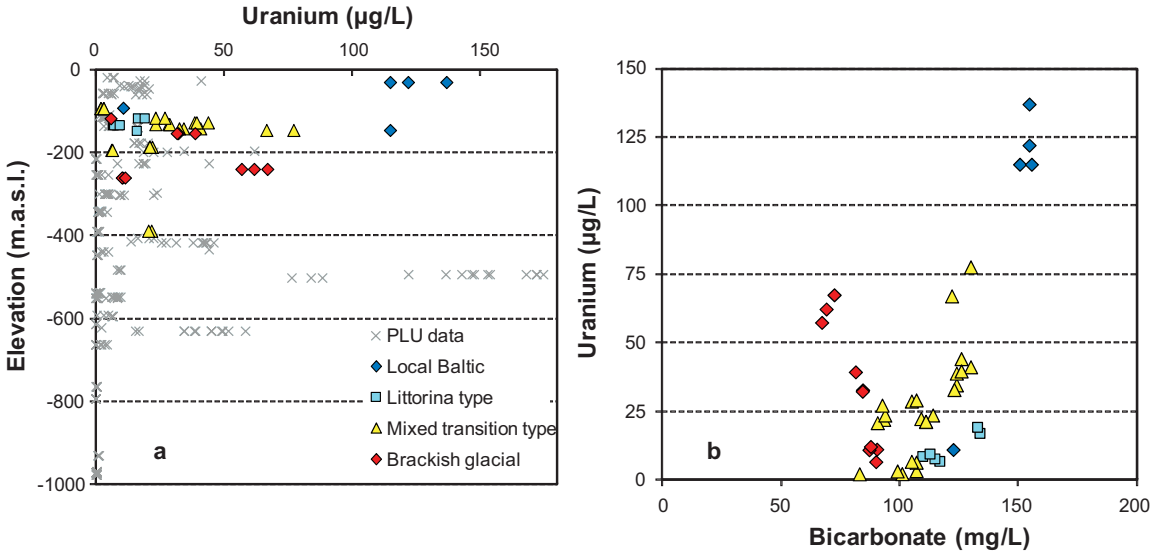

Figure 6-10 a, b. *Plots of uranium concentration versus depth (a) and bicarbonate concentration (b). PLU data includes Forsmark only.*

6.3.6 Concluding remarks on redox

Despite the scarcity of Eh information *sensu stricto* and the relatively low number of sulphide measurements (and the questionable representativeness of these data), the presence of Fe(II) and Mn(II) in the groundwaters supports reducing conditions in line with present understanding of the groundwater system at SFR. The relatively high U content also detected in the PLU data was at Forsmark ascribed to groundwaters with Eh values higher than –190 mV but still reducing and bicarbonate contents larger than 30 mgL^{-1}. This seems to be valid also for the SFR samples. In conclusion, mildly reducing conditions are supported by the groundwater chemistry and also by the few successful Eh measurements.

6.4 Residence times

A key factor in validating the suggested past and present groundwater evolution in the SFR model volume is to constrain the average residence time for each of the defined groundwater types. This can, at least theoretically, be approached qualitatively in terms of groundwater composition, i.e. based on aspects of water/rock reaction kinetics, or on a more quantitative level by using radioactive isotopes /Smellie et al. 2008/. In the present investigation the data are restricted to tritium (^{3}H) and carbon–14 (as pmC) which can only suggest different times of isolation from the atmosphere. However, in defining the different groundwater types the ratio of the stable oxygen isotopes (expressed as $d^{18}O$) has been used also to distinguish groundwaters with cold climate components (glacial meltwater), which in turn provide relative information on residence time.

A serious drawback with the SFR investigations is the absence of ^{36}Cl data which would have been very helpful for the identification of an old non–marine saline component similar to that described in the Forsmark and Laxemar areas.

It is important to keep in mind that the groundwater samples are usually influenced by mixing, and this is especially true for the SFR samples as the present SFR tunnels have changed the hydrogeological conditions resulting in an increased drawdown of young Baltic sea water along some fracture zones resulting in the mixing of groundwater types of different age and origin.

6.4.1 Tritium and radiocarbon

Recent recharge of either meteoric water of a young age in Forsmark (i.e. less than 50 years) or in the case of the SFR site present Baltic Sea water, can be traced by the content of atmospheric thermonuclear tritium from the early 1960s still present in the recharging precipitation and the infiltrating sea water and shallow groundwaters. Figure 6-11 shows tritium plotted versus depth and includes data obtained after year 2000 from the SFR site as well as from PLU. The plot shows a characteristic decrease in tritium to a depth of around 150–200 m which represents the limit of recharge water of a young age (<50 y). However, significant tritium content still persists within the entire depth interval which may be due to various sources of contamination /Smellie et al. 2008/. In the SFR case, the samples were collected in the vicinity of the repository and also the nuclear power facility which suggest obvious sources for contamination. For example, borehole KFR102A shows detectable tritium content only in the bottom section below the SFR Silo and borehole KFR105 shows its highest tritium values in the first section close to the tunnel orifice. The reason may be that the groundwater in KFR102A is influenced by Silo sourced tritium while the groundwater in KFR105 is seeing recent, reactor released tritium. Therefore, the general groundwater flow direction which is downwards and towards the SFR repository implies no contradiction to this hypothesis.

Radiocarbon (^{14}C), with a half-life of 5,730 years, extends the range of detection up to 30,000 years for groundwater residence time. Theoretically, this range should cover comfortably the period since the last deglaciation, in particular confirmation of the Littorina Sea transgression. However, this is more complicated in practice. The analyses of carbon isotopes from the SFR site are relatively few and have been mainly carried out during the last 10 years. All carbon analyses are on inorganic carbon (TIC) and Figure 6-12 shows $^{14}C_{TIC}$ (pmC) versus elevation (a), bicarbonate content (b), $d^{18}O$ (c), and $d^{13}C$ (d). It is obvious that the lowest ^{14}C contents are found in groundwaters below –100 masl with bicarbonate contents lower than 110 mgL^{-1}. These groundwaters also have the most depleted $\delta^{18}O$, i.e. a large component of glacial water. Generally, low ^{14}C corresponds to low $d^{13}C$.

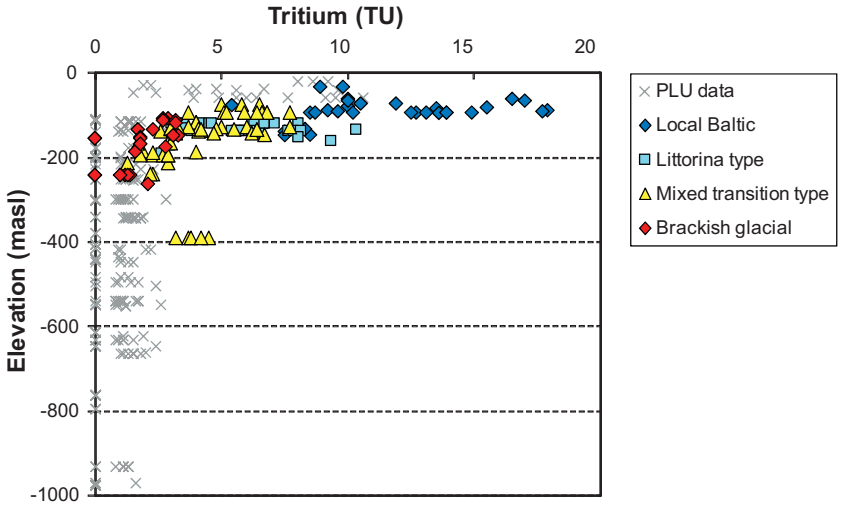

Figure 6-11. *Distribution of tritium (TU) with depth related to the different groundwater types defined for the SFR Site in section 6.1. The samples included are from 2000 and later. PLU data include Forsmark only.*

The general understanding of the relative residence times of the different groundwater types is supported by two samples representing present Baltic Sea which show the highest ^{14}C contents (45 to 60 pmC) and high tritium values thus indicating a modern origin (<50 years old). However, even though the ^{14}C contents are still lower than expected at 45–60 pmC, this supports the influence of reactions that have contributed "dead" carbon to the inorganic system in the groundwaters, either through calcite dissolution or breakdown of old organic material. The contribution from reactions is also supported by the increased bicarbonate values (Baltic Sea waters usually have values around 70–90 mgL^{-1}). During the PLU site investigation in Forsmark attempts were made to correct the ^{14}C contents for reactions, mainly based on $d^{13}C$, cf. discussions in. This was however shown to be difficult and very shaky and has not been even possible to apply on the SFR data /Smellie et al. 2008/.

The four Littorina type groundwaters show ^{14}C contents between 22 to 42 pmC in agreement with the PLU data on brackish marine waters. The brackish-glacial groundwaters, in contrast, generally show expected low values of 8 to 20 pmC. The transition type waters show as anticipated a broader range of ^{14}C (10 to 44 pmC) in line with their mixed origins.

6.4.2 Conclusions on residence times

Based on the available information from radiometric isotope analyses (tritium and ^{14}C), more quantitative information from stable isotopes (O, C and S), and the general understanding of the site, the following conclusions can be drawn.

The oldest groundwater in the SFR area contains significant portions of glacial meltwater identified by depleted $d^{18}O$. A possible scenario is that glacial meltwater (most probably from the last deglaciation) has been injected into the fracture zones and further into smaller fractures by large hydraulic heads during the melting of the continental ice sheet. The dilute glacial melt water mixed with existing brackish non-marine water of unknown origin, already present in the fracture system.

In the larger fracture zones, and especially at shallow depth, the groundwater was probably very dilute following the deglaciation and during the following period of fresh water accumulation on the sediment/bedrock surface (the Ancylus Lake, cf. Figure 3-1). When the Littorina Sea transgressed (starting some 9,500 a ago with a salinity maximum between 4500 to 3000 BC) it intruded into the bedrock driven by density differences. The combined isotope information supports the presence of marine water with higher salinity and longer residence times than the present Baltic Sea. This brackish marine water subsequently mixed with a dilute water with depleted $d^{18}O$. It is also clear that the Littorina water has not penetrated the less transmissive fractured bedrock between the more highly transmissive fracture zones to the same extent as the glacial melt water.

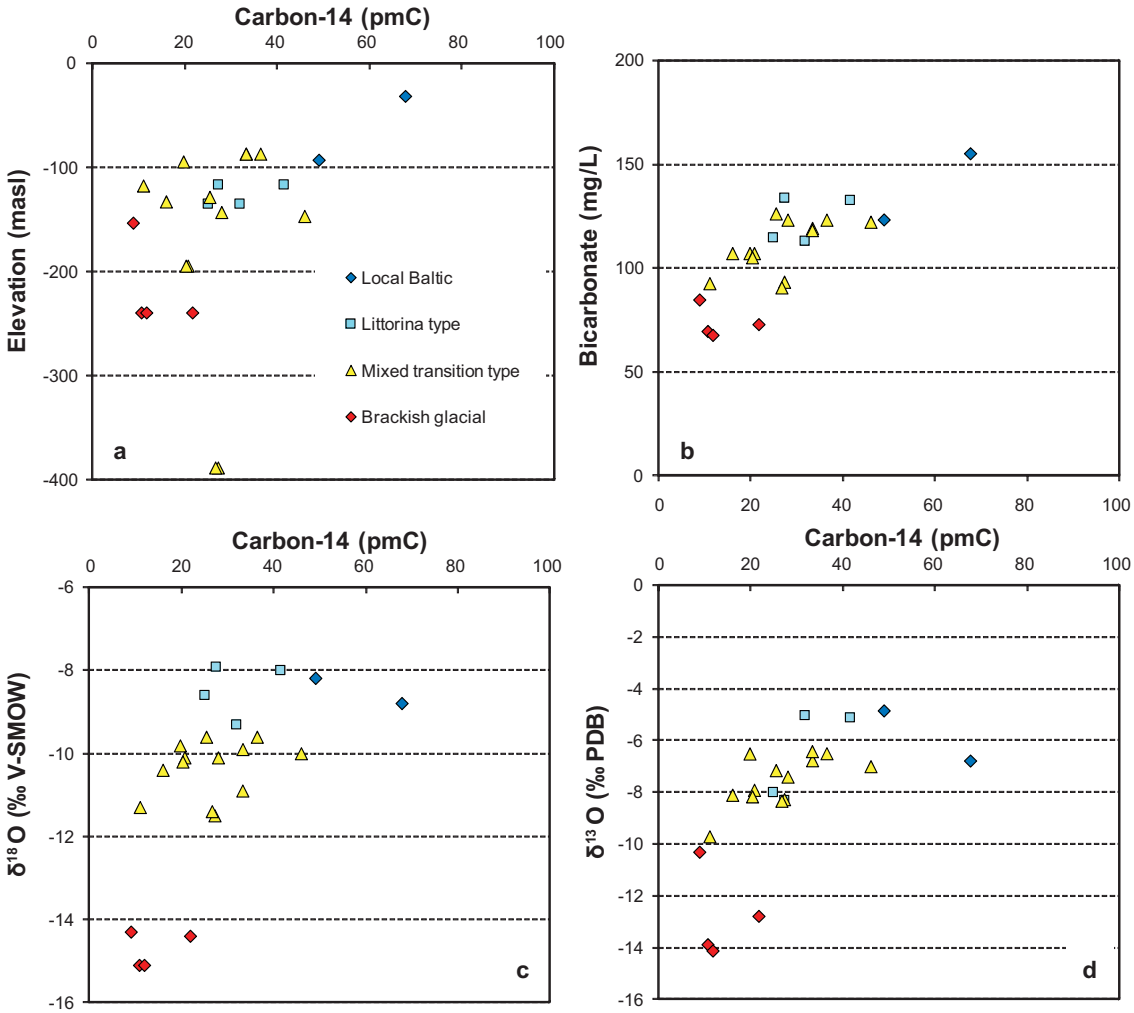

Figure 6-12a-d. *Carbon-14 content in inorganic carbon (largely equal to bicarbonate) in groundwaters from SFR plotted versus elevation (masl): (a), bicarbonate (b), $d^{18}O$ (c) and $d^{13}C$ (d).*

The fact that all samples from the SFR model volume contain groundwaters with bicarbonate contents higher than 30 mgL^{-1}, and that all carbon isotope analyses show the presence of radiocarbon (8 to 60 pmC), indicate that the major input to the carbon system has occurred after the deglaciation.

The last water type to intrude is the present Baltic Sea. Based on its tritium content, which is similar in many of the SFR sampling sections, this intrusion is relatively late and has been accelerated by the drawdown caused by the SFR facility (cf. Section 6.5 below).

6.5 Changes in groundwater composition since construction of the SFR

The impact of changes in flow paths and groundwater drawdown effects from the SFR tunnel system has affected the groundwater composition in the SFR boreholes with time. The effects are observed from long term trends in the early SFR boreholes which penetrated most of the transmissive fracture zones implying generally slow but systematic changes in the groundwater composition /Laaksoharju and Gurban 2003, Nilsson A-C 2009/.

Figures 6-13 to 6-15 present the available and approved pH, bicarbonate and chloride data as a function of time for the period 1986 to 2009. The overall changes in the minimum and maximum values are relatively small for pH and bicarbonate (weak increase) and somewhat larger for chloride (decrease in those boreholes with the, initially, most saline groundwaters). The lowest chloride con-

centrations observed are, however, not due to recent dilution with Baltic Sea water impacting from the SFR repository. These low salinity waters are old and contain a significant portion of glacial meltwater, cf. Section 6.1. The four boreholes and borehole sections included in the annual sampling programme are penetrating major deformation zones where most of the changes occur, while some of the other borehole sections, sampled less frequently, represent less transmissive bedrock with a more stable water composition. This is obvious from Figure 6-14 where the lowest bicarbonate concentrations are found in some of the less frequently sampled borehole sections.

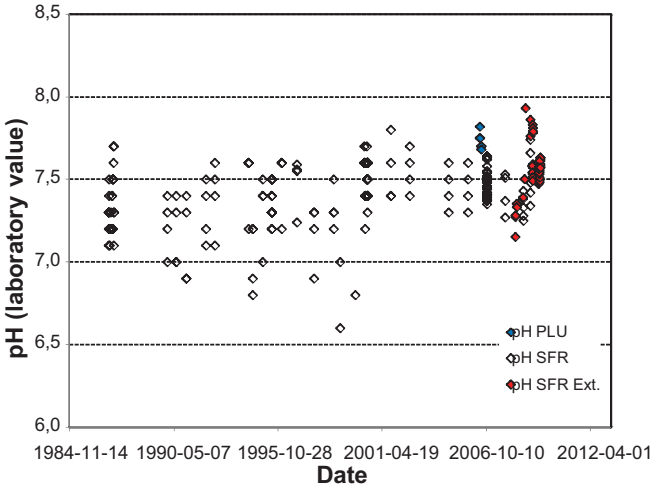

Figure 6-13. *Variation in measured pH (laboratory values) from 1986–2009. Data plotted are for boreholes HFR34 and HFR35 from the site investigation in Forsmark (PLU), for the early SFR boreholes (SFR), and also for boreholes drilled within the SFR extension project (SFR Ext.). Note; the quality of the pH data may vary over time.*

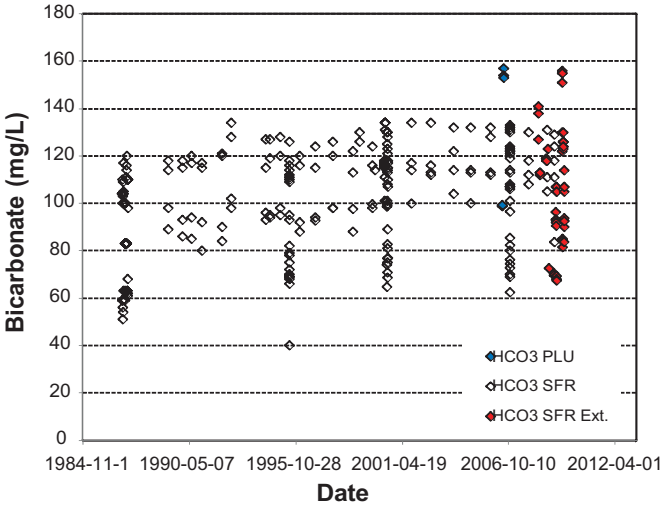

Figure 6-14. *Variation in bicarbonate concentrations from 1986–2009. Data plotted are for boreholes HFR34 and HFR35 from the site investigation in Forsmark (PLU), for the early SFR boreholes (SFR), and also for boreholes drilled within the SFR extension project (SFR Ext.).*

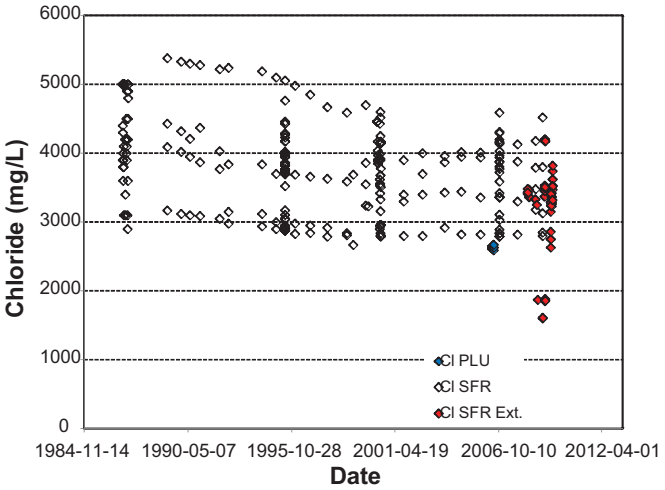

Figure 6-15. *Variation in chloride concentrations from 1986–2009. Data plotted are for boreholes HFR34 and HFR35 from the site investigation in Forsmark (PLU), for the early SFR boreholes (SFR), and also for boreholes drilled within the SFR extension project (SFR Ext.).*

Where and how the changes occur provide valuable information about the hydraulic conditions at the site and especially in the different major deformation zones. However, it is possible that some changes were sufficiently rapid and had already occurred before the first sampling occasion, which could explain, for example, the occurrence of the Baltic type of groundwater in boreholes KFR08 and KFR56 already from the first sampling occasion in 1986.

Long term trends in chloride, magnesium and oxygen-18 data from the last twenty years of groundwater sampling in the SFR repository bedrock volume were presented as x/y scatter diagrams in /Nilsson A-C 2009/. In Table 6-1 the changes in groundwater types have been listed and related to the different deformation zones as defined in the geology model version 0.1. It has to be pointed out that the geological deformation zone model used in this report is based only on the early SFR boreholes and not on recent information from the SFR extension project.

Comments to Table 6-1 and the observed changes are summarised as follows:

- The very strategic large scale vertical **Singö zone** is intersected by borehole KFR01. Groundwater samples have been collected from two sections of this borehole, both representing the Singö zone but frequent annual sampling has only been performed from the inner section. A slow transition from Littorina type groundwater towards the Baltic type is observed in both sections due to the introduction of present Baltic Sea water. However, only the upper section shows a full transition to the Baltic type. Most of the changes occurred before 2000 and since then the groundwater composition has remained quite stable. As expected, the largest changes in groundwater pressure and inflow to the boreholes and the tunnel system occurred soon after construction. Since then the pressure conditions have slowly stabilised to reach close to equilibrium around year 2000. This naturally effects also the groundwater composition.
- Two other major vertical zones are **Zone 3 and Zone 8**. Both these zones are intersected by some relatively shallow boreholes, as well as one deeper borehole which extends into zone H2. The groundwater from the shallow borehole KFR09, intersecting Zone 3, initially showed a strong Littorina signature but has developed a typical Baltic character with time. The two shallow boreholes, KFR56 and KFR08 intersecting Zone 8, initially yielded, and yield also today, groundwater of local Baltic type. The groundwaters in the two boreholes at greater depth (KFR10 and KFR7A at –116 and –134 masl, respectively) were initially of Littorina type and have maintained this signature to the present day. The highest salinity encountered at the SFR site (chloride concentration of about 5,000 mgL^{-1}) was observed in early samples from these two boreholes. Following this, the salinity has decreased with time and none of the later samples from the earlier drilled SFR boreholes (and from the recently drilled boreholes) record high salinities. However, the groundwater composition does not change significantly after 2000.

- The gently dipping **zone H2** is intersected by several boreholes, see Figures 6-16 and 7-3. The only borehole intersecting zone H2 in the vicinity of zone 8 is KFR7B. Here, the groundwater type is changed from Littorina type to local Baltic type which is analogous to the two sections in KFR7A, and indicates the further enhanced importance of zone 8 as a downward transport pathway for modern Baltic Sea water due to the presence of the SFR tunnel system. The changes of groundwater types observed in most other boreholes intersecting zone H2 (KFR02, KFR03, KFR04, KFR13) are illustrated in Figure 6-16. Corresponding data from borehole KFR05, also intersecting H2, are too few and have been omitted in the illustration. It is clear that the initial groundwater types are different in or adjacent to zone H2 in most of the boreholes (KFR03 is the exception) and that the difference is towards the Littorina type but often remaining as a mixed transition type. Furthermore, the changes observed after 2000 seem irregular but there is a common trend towards more mixed transition type groundwaters extending from zone H2 to an increasing number of sections.
- Several borehole sections in different boreholes represent the **bedrock matrix between the major zones.** The three upper sections in boreholes KFR02, KFR03 and KFR04 show an increasing glacial signature with time which may be due to mixing with groundwater from above or laterally rather than from zone H2 below, while in the section below zone H2 in KFR02 changes from the glacial to the mixed transition type occur. The groundwaters in the second section in both KFR04 and KFR55 change from Littorina type to mixed transition type.

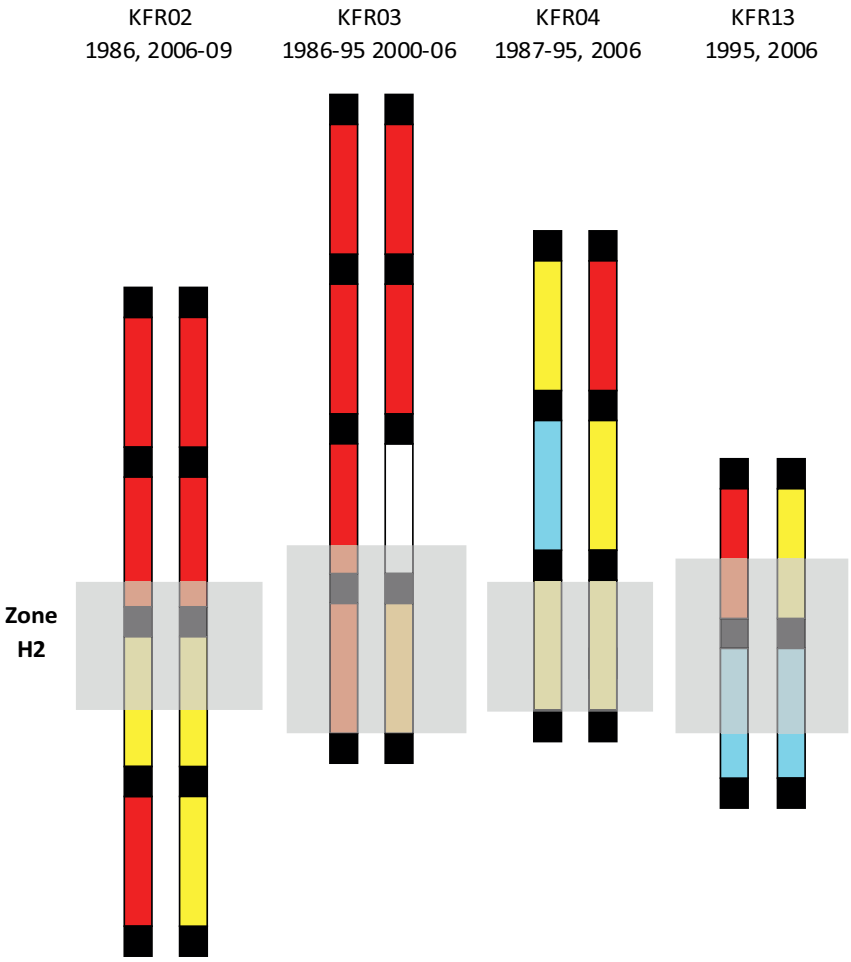

Figure 6-16. *Illustration of changes in water type in some boreholes intersecting zone H2. The borehole section lengths and the extension of zone H2 is not to scale. The transparent grey representation of zone H2 roughly covers the part of the section contained in the zone. Turquoise = Littorina type, Yellow = Mixed transition type, and Red = Brackish glacial type groundwater.*

Table 6-1. Changes in water chemistry in borehole sections and intersected major zones.

Borehole	Section (mbl)	Elevation Secmid (masl)	Year; Cl (mgL^{-1})	Year; Cl (mgL^{-1})	Change in chemistry*	Zone
KFR01	11.0–43.5	–71.58	95; 3,170	06; 2,790	T → B	Singö
KFR01	44.5–62.3	–94.23	87; 4,200	08; 3,480	T → T(B)	Singö
KFR10	0.0–127.8	–116.23	00; 3,850	08; 4,180	L → L^+	H2 and 3
KFR7A	2.0–19.0	–132.65	95; 3,950	06; 3,356	L → B	H2
KFR7A	48.0–74.7	–134.43	87; 4,900	09; 3,800	L → L(B)	H2 and 8
KFR10	87.0–107.28	–146.99	86; 5,000	99; 3,860	L → L(B)	H2 and 3
KFR7B	8.6–21.1	–147.59	86; 4,300	06; 3,860	L → B	H2
KFR03	57.0–80.0	–150.87	87; 3,100	00; 4,160	G → G(T)	H2
KFR04	84.0–100.5	–166.29	95; 4,290	06; 4,200	T → T	H2
KFR13	34.0–53.0	–166.84	95; 3,940	06; 3,970	G → T	H2
KFR03	81.0–101.6	–173.67	86; 3,100	00; 4,140	G → G(T)	H2
KFR02	81.0–118.0	–184.93	86; 4,000	06; 4,167	G → G	H2
KFR13	54.0–76.6	–188.64	95; 4,430	06; 4,310	L → L	H2
KFR02	119.0–136.0	–212.93	86; 4,400	09; 4,520	T → T	H2
KFR56	9.0–81.73	–64.66	95; 2,910	09; 2,800	B → B	8
KFR08	36.0–62.0	–90.29	95; 3,040	09; 2,850	B → B	8
KFR08	63.0–104.4	–93.31	89; 3,170	09; 3,130	B → B	8
KFR55	40.0–48.0	–133.97	95; 3,860	06; 3,880	L → T	9B
KFR03	45.0–56.0	–132.87	95; 3,740	06; 3,870	G+→ G	9B
KFR09	63.0–80.24	–83.68	86; 4,100	99; 2,670	L → B	3
KFR19	77.0–94.0	–60.43	95; 2,890	06; 2.790	B → B	–
KFR08	6.0–35.0	–87.81	95; 2,900	06; 2,840	B → B	–
KFR03	5.0–44.0	–106.87	95; 3,720	06; 3,110	G → G^+	–
KFR04	28.0–43.0	–111.48	87; 3,400	06; 3,800	T → G	–
KFR55	8.0–21.0	–128.34	95; 4,020	06; 3,770	T → T	–
KFR55	22.0–39.0	–131.39	95; 3,990	06; 4,150	L → T	–
KFR04	44.0–83.0	–138.52	95; 4,270	06; 4,290	L → T	–
KFR02	43.0–80.0	–146.93	86; 3,600	06; 3,720	G → G^+	–
KFR02	137.0–170.3	–239.08	86; 3,900	06; 3,940	G → T	–

* Explanation: mbl = metres borehole length. B = Present local Baltic, L = Littorina type, T = Mixed Transition type, G = Brackish Glacial type. Groundwater types indicated in between brackets (e.g. L(B)) means that the groundwater type is still Littorina but is changed towards the local Baltic type. G → G^+ means that the original groundwater type was glacial and the last sample showed an even lower $\delta^{18}O$ signature.

7 Hydrogeochemical site description

7.1 Introduction

The main aim of the hydrogeochemical site descriptive model is to present an understanding of the site based on the measurements, interpretations and model contributions described in the previous chapters. The main objective is to describe the chemistry and distribution of the groundwater and the hydrogeochemical processes involved in its origin and evolution and to incorporate the use of available geological and hydrogeological site descriptive models. This chapter outlines the visualisation of a preliminary SFR hydrogeochemical site descriptive model according to present understanding.

7.2 Hydrogeochemical visualisation

As described in Chapter 2 (cf. Figures 2-5, 2-6, 2-7 and 2-10), the SFR site/target area is delimited by two vertical to steeply dipping zones ZFMWNW0001 (Singö) in the southwest and ZFMNW0805A (zone 8) in the northwest. Together with the other steeply dipping zones, i.e. ZFMNE0870A and B (zone 9a and b), ZFMNNW1209 (zone 6) and ZFMNNE0869 (zone 3) inside the target area, they have served as important groundwater flow pathways over long periods of geological time. Prior to the last glaciation, the groundwater flow was considered regional, slow moving and upwards along these pathways, whilst post-glacial activity has been more dynamic and downwards along the pathways driven by density differences and increasing hydraulic gradients coeval with land rise. Presently, these structures have facilitated in particular the drawdown of near-surface waters (e.g. Baltic Sea) resulting from the excavation and construction phases of the SFR waste storage facility (cf. Section 6.5). Several of these vertical zones have contact with the gently dipping deformation zone ZFM871 (zone H2) which is located just beneath the silo at SFR and covers most of the local model area. This provides the possibility for transported groundwaters of varying age and chemistry, certainly during the last deglaciation and Holocene time, to be further distributed and mixed within the different flow paths in the plane of this zone.

Visualisation of the hydrogeochemical site understanding is based on the exploratory analysis part of the programme outlined in section 6, interfaced with relevant input from the geological site descriptive model and published hydrogeological information (cf. Chapter 2). To visualise the groundwater chemistry, two main cross sections were selected (cf. Figure 7-1) that best illustrate the SFR site/target volume (regional and local model volume) based on geology and hydrogeology. However, in contrast with the PLU investigations where such cross sections were used to construct 2D visualisations, at SFR this approach has proved to be unsuitable because of the structural complexity and the concentration and number of boreholes used to demarcate the SFR site/target area. Two dimensional visualisations are planned in the future on a more regional scale using selected boreholes. Instead, presented below are a series of 3D visualisations viewed towards the north-west (i.e. from the south-east) approximately parallel to section A in Figure 7-1.

The 3D sections were chosen to visualise the distribution of the different groundwaters types and their relation to the major transmissive deformation zones which characterise the SFR site (cf. Figures 7-2 to 7-4). Attention has been given to the distribution of the different groundwater types along each borehole which has been discussed in Section 6.6. Figure 7-2 provides the general setting to the SFR site showing the dominance of the vertical deformation zones 3, 6 and 8 and their important hydraulic intersections with the equally dominant subhorizontal zone H2; zone 9a and b may also play a hydraulic role but this is still not clear. There is a good probability that H2 extends south-west eventually intersecting with the Singö deformation zone.

The hydrostructural properties of the SFR site have determined the distribution and degree of mixing of the different groundwater types, most of which have been introduced since the last deglaciation. These groundwaters (Local Baltic, Littorina type, Mixed transition type and Brackish glacial type) residing at shallow to intermediate depths (maximum elevation depth studied about –400 masl) are clearly indicated in Figures 7-2 and 7-3. The importance of the hydraulic connection with subhorizontal zone H2 can be seen in Figure 7.4 where most of the Littorina type groundwaters

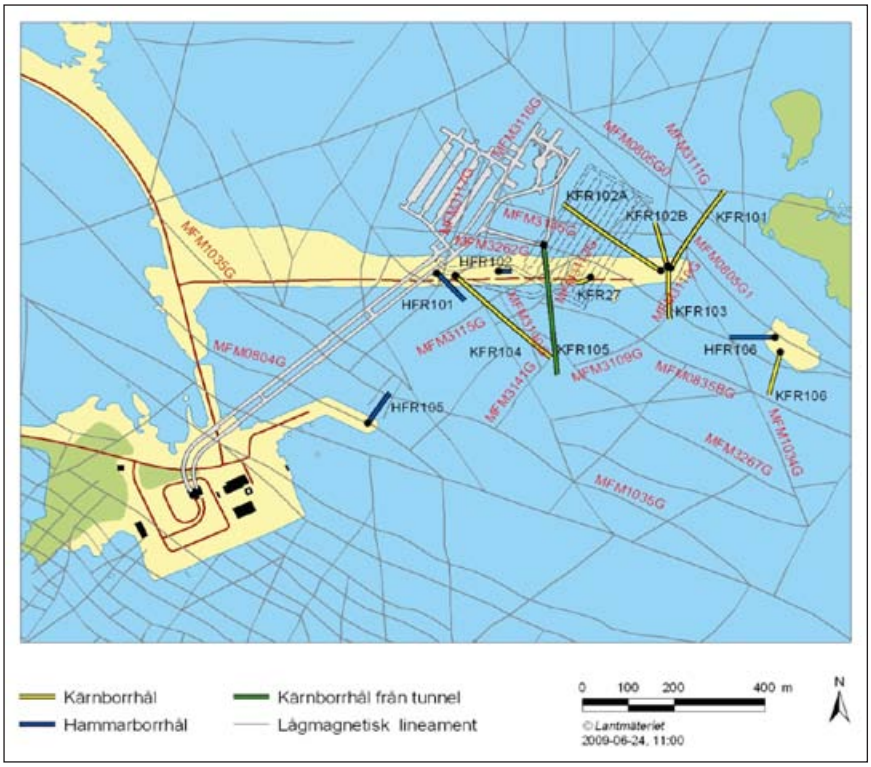

Figure 7-1. *SFR site/target area showing cross sections A and B in relation to the SFR waste storage facility and the series of drilled boreholes representing the SFR extension project. The 3D sections chosen are approximately parallel to section A viewed to the north-west.*

are present, together with some mixed transition and brackish glacial types. As discussed in Section 3.3.3, deglaciation meltwaters under high hydraulic pressure have penetrated at least to zone H2 via the transmissive intersecting vertical zones, but also to greater depths depending on the host rock hydraulic properties. These meltwaters underwent mixing with pre-existing groundwaters comprising old meteoric waters and more brackish types (i.e. to form brackish glacial types) at greater depths. During the subsequent Littorina transgression, density driven marine waters preferentially penetrated to H2 and partly displaced previously infiltrated last deglaciation meltwater and probably some residual dilute water of old meteoric character. This led to the Littorina Sea water undergoing degrees of dilution and also forming mixed transition types with the brackish glacial types. The strongest Littorina signatures seem to have been preserved at depth (–115 and –140 masl) in the steeply dipping zones zone 3 and zone 8 and within or close to zone H2.

In recent time, since construction of the SFR, Baltic Sea waters have been infiltrating the SFR site area descending to shallow depths (cf. Figures 7-2 to 7-4) and mixing with near-surface Littorina type and possibly also brackish glacial type groundwaters.

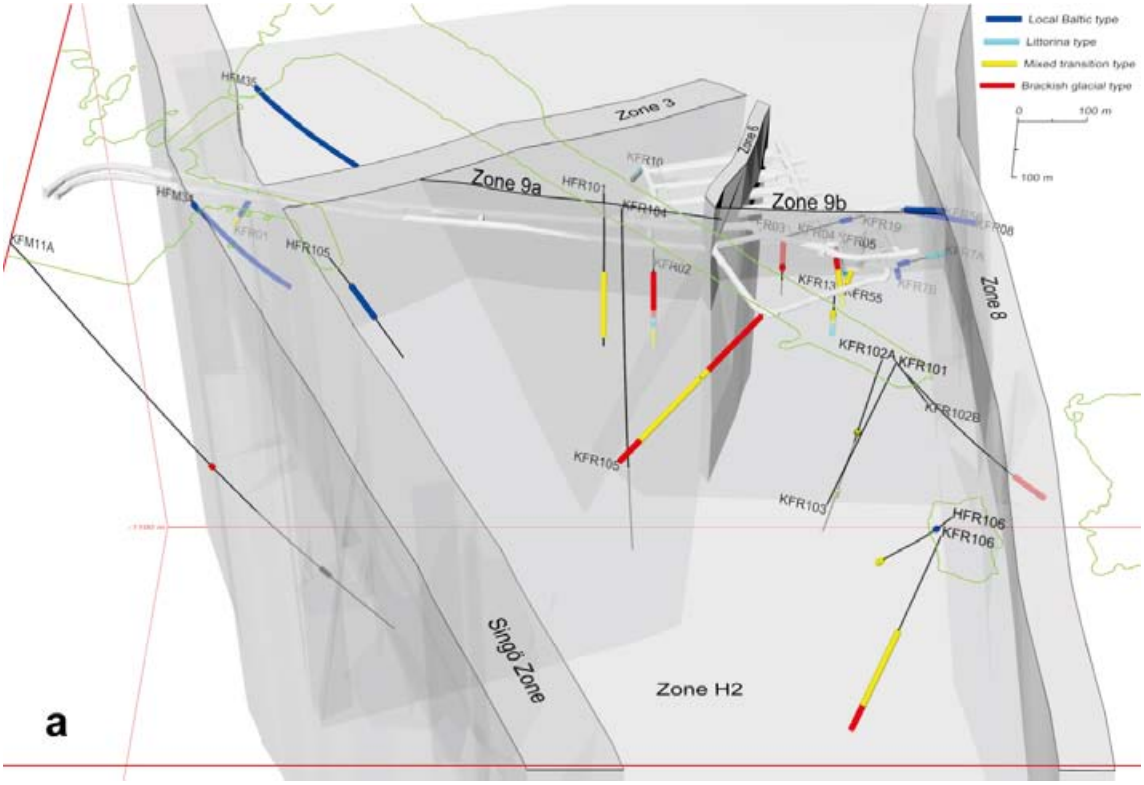

Figure 7-2. *3D presentation (viewed from south-east) of the groundwater type distribution in relation to major zones in the regional model volume. The overview shows all the boreholes included in the SFR model version 0.2. The early SFR boreholes, cf. Table 4-1, are represented by groundwater types observed from 2006 data. Note the decrease in colour intensity along the boreholes when viewed through a penetrated rock/deformation zone volume.*

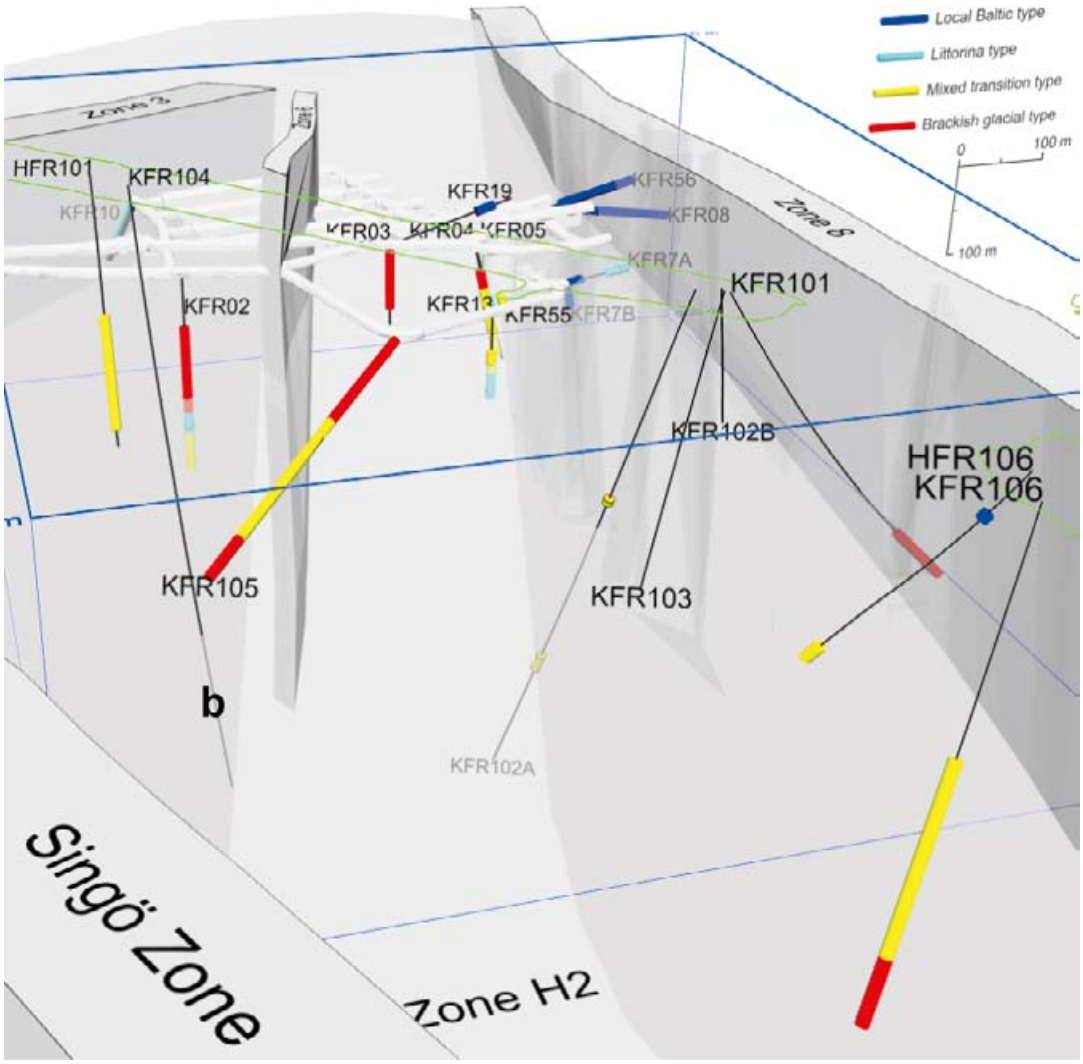

Figure 7-3. *3D presentation of the groundwater type distribution in relation to major zones in more detail and concentrated to the local model volume (basically the same view direction as in Figure 7-2). The thin blue line demarcates the 3D rock volume visualised. Zones 9a and 9b are omitted to improve clarity. The early SFR boreholes are represented by groundwater types observed from 2006 data, cf. Table 4-1. Note the decrease in colour intensity along the boreholes when viewed through a penetrated rock/deformation zone volume.*

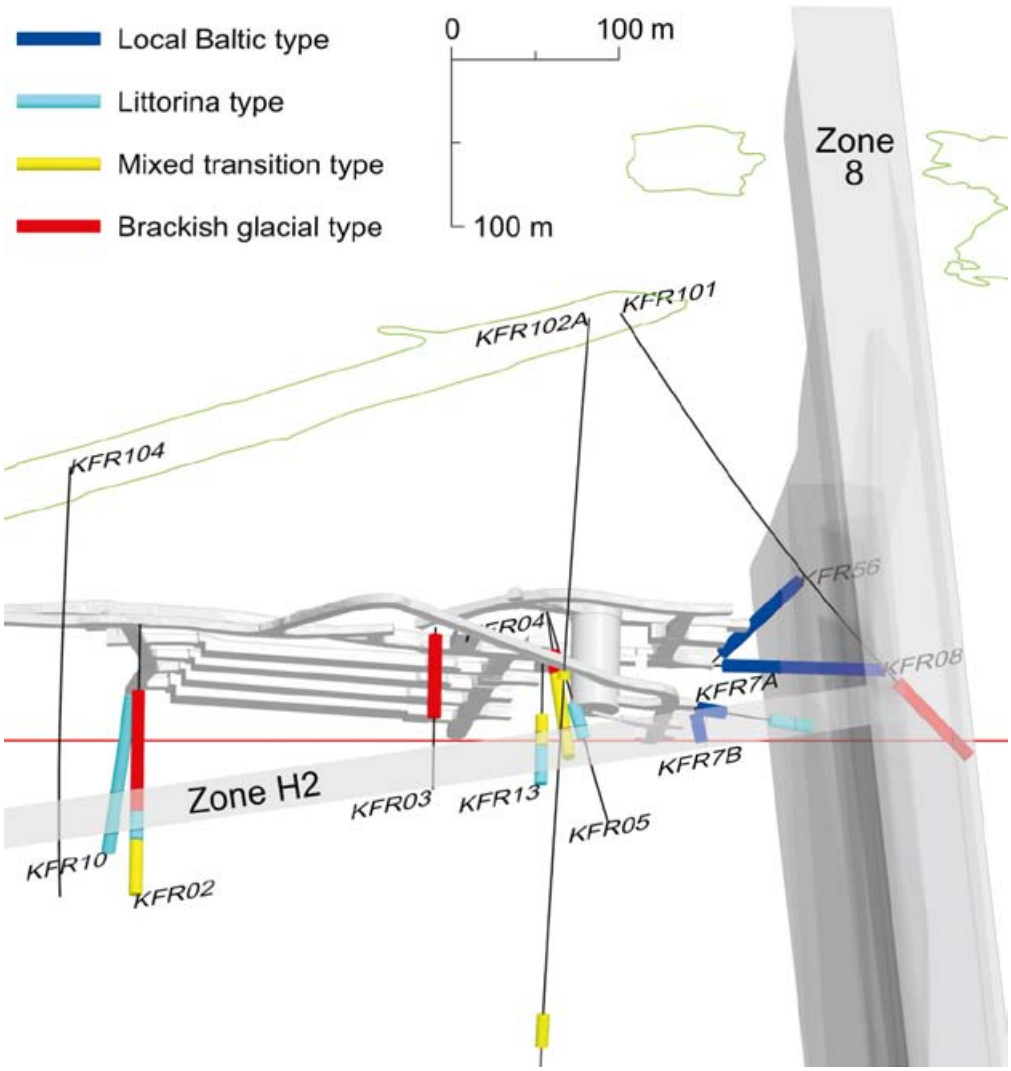

Figure 7-4. *3D presentation of the groundwater type distribution in relation to zone H2 and zone 8 (the viewpoint is from beneath and rotated to the east compared to the previous figures). The early SFR boreholes are represented by groundwater types observed from 2006 data, cf. Table 4.1. Note the decrease in colour intensity along the boreholes when viewed through a penetrated rock/deformation zone volume.*

8 Conclusions

8.1 Overall understanding

The data set for the SFR site descriptive model includes groundwater samples from old boreholes in the SFR facility and from new boreholes drilled for the SFR extension phase. Together, there are data representing 60 sections in 25 boreholes with samples covering depths down to –400 masl, with the majority of samples from –50 to –250 masl. The area is generally covered by the Baltic Sea with the exception of smaller islands and bankments. The groundwater composition is brackish and ranges from ~ 1,500 to 5,500 mgL^{-1} chloride. $d^{18}O$ varies from –7.5‰ down to almost –16‰ V-SMOW and is in this report used together with the large variation in magnesium content (30 mgL^{-1} to almost 300 mgL^{-1}) as an indicator of marine water. This indicates a large variation in the origin and residence time of the groundwaters despite the relatively small variation in salinity. A subdivision of the groundwaters into three major groups (origins) was made accordingly:

1) **Present Baltic** water with a Cl content of 2,500 to 3,500 mgL^{-1}, $d^{18}O$ at –9 to –7.5‰ V-SMOW and with strong marine signatures based on the Cl/Mg weight ratio and sulphate, potassium and the Br/Cl ratio. Tritium is also high (similar to the present Baltic Sea at the surface). This water is most common down to –100 masl but is found also in a few sections at about –150 masl. The inflow of Baltic Sea water has increased during the operation of the SFR facility due to draw down.
2) **Littorina type** water with a component of glacial water; Cl content is between 3,500 to 6,000 mgL^{-1} and $d^{18}O$ at –9.5 to –7.5‰ V-SMOW. The salinity is greater than the present Baltic Sea and chemical indicators such as Mg, SO_4 and Br/Cl ratio support a marine origin for the saline component. The slightly depleted $d^{18}O$ compared with the original Littorina Sea ($d^{18}O$ around –4.5 V-SMOW) indicate a significant component of glacial water probably from the last deglaciation. The Littorina type waters are commonly found at depths between –80 to –200 masl according to the present data set. In the nearby Forsmark area, however, Littorina-Glacial Waters are found down to 500–600 m depth.
3) **Brackish glacial** waters with a Cl content of 1,500 to 5,000 mgL^{-1} and $d^{18}O < –12.0$‰ V-SMOW. The marine signature is generally weak and the Br/Cl ratio deviates from that of marine waters. The brackish glacial waters (at depths > –100 msl) are the oldest present at the SFR and the amounts of post-glacial components are small.

A large number of samples cannot be defined by any of the three groups above because of varying degrees of mixing and therefore a forth group called **Transition type** water is used. Its presence is indicated from groundwater monitoring over the last two decades showing it becoming more frequent. This is probably a result of the changing hydrogeological conditions in the SFR area influenced by drawdown inflow to the tunnels. The transition type waters are found at depths from about 60 to 400 m.

The sequence of events and the possible mixing of different waters are summarised in Table 8-1.

Differences compared with the hydrochemistry at Forsmark:

- Importantly, there is no evidence of any input of modern meteoric water because the SFR is situated beneath the Baltic Sea.
- The magnesium contents in the sampled waters (30–300 mgL^{-1}) are all above the limit used within the Forsmark PLU (<25 mgL^{-1}) for the classification of non-marine brackish to saline waters. In fact, all of the samples except for one section in KFR101A are within the range of 70–300 mgL^{-1} Mg, which indicates that a marine input can be distinguished in most of the samples but to a very variable degree.
- Also, the bicarbonate contents (40 to 160 mgL^{-1}) are relatively high compared with the non-marine brackish waters at Forsmark, which are mostly below 25 mgL^{-1}.
- The most depleted $d^{18}O$ values (indicative of portions of glacial meltwater) are found in less transmissive fractures which differs from the Forsmark site where depleted values are found in more saline waters and at greater depths /cf. figures 6-1 e and 6-5 e/.

Table 8-1 Origin of groundwaters and sequence of events influencing their chemistry at SFR.

Origin of Groundwater	Approximate residence time	Depth	Type of structures	Comment
Present Baltic Sea	Modern water from the last 50 years based on tritium.	Down to 100 m depth.	Steeply dipping fracture zones with surface contact.	It is unclear if Baltic Sea water was present in the fracture zones before construction of the SFR tunnels.
Littorina Sea water	The Littorina maximum took place 4500 to 3000 BC.	80 to 220 m depth.	Most common in the larger fractures zones, especially subhorizontal zone H2 but also vertical zones 8 and 3.	The Littorina Sea water is mixed with preexisting glacial meltwaters in the fracture zones becoming more dilute (lower Cl) and with a significantly more depleted $d^{18}O$.
Glacial meltwater	This water is most probably from the last deglaciation which occurred at Forsmark ca 11,000 a ago.	The waters with the most depleted $d^{18}O$ values (indicative of glacial meltwater) are found at depths between 100 to 250 m.	Usually confined to fractures in the less transmissive parts of the bedrock.	The glacial meltwater has mixed with the preexisting brackish non-marine water producing some of the lowest Cl contents (1,600 mgL^{-1} Cl).
Non-marine brackish water	Older than last last deglaciation (>15,000 a)	This water is only found as relatively small portions mixed with the glacial meltwater and partly also with the brackish marine water of Littorina type.	Usually confined to the less transmissive parts of the bedrock.	The origin of the brackish non-marine water is unclear, but includes probably components of an old meteoric water and may also contain older glacial water, together with non-marine water of unknown age.

Redox conditions

The actual Eh measurements are very few (three values of –140 mV, –180 and –190 mV), as well as the samples analysed for sulphide. Fe(II) and Mn(II), in contrast, are frequently analysed and their contents support mildly reducing conditions in line with the present understanding of the groundwater system and indications from the few successful Eh measurements.

Uranium

Relatively high U contents (the majority of samples in the range 10 μgL^{-1} up to 140 μgL^{-1}) are found in the SFR samples, similar in content to some of the groundwaters at Forsmark. At both sites the increased uranium contents are associated with groundwaters with Eh values more positive than –190 mV but still reducing, and bicarbonate contents greater than 30 mgL^{-1}, once again supporting mildly reducing conditions in the SFR samples. In common with the Forsmark PLU, the probable source of the dissolved uranium is U phases precipitated in parts of the fracture system.

The carbon system

The fact that all samples from the SFR model volume contain groundwaters with bicarbonate contents greater than 30 mgL^{-1} and that all carbon isotope analyses on inorganic carbon showed the presence of radiocarbon (8 to 60 pmC), indicate that the major input to the carbon system has occurred after the deglaciation. The TOC/DOC content is generally between 1 to 4 mgL^{-1}. The carbon isotope signatures of the organic compounds are however not analysed.

8.1.1 Groundwater conditions special for the SFR

- The hydrogeochemical description shows clearly that there is a significant change in the groundwater composition towards increased Littorina infiltration in several boreholes at their intercepts with zone H2 (i.e. intercepts according to the early geological model version 0.1). It is obvious that this plane is substantially more transmissive than the bedrock volumes above and below and thereby supplies important groundwater flow pathways.
- There are several examples of sections with less saline groundwater located below sections with more saline water in the same borehole. These conditions, which are not usually observed in normal groundwater environments, provide strong indications of the preservation of very isolated groundwaters in parts of the less transmissive bedrock outside major zones. Similar observations have been reported from the detailed Onkalo investigations at Olkiluoto /Posiva 2009a, b/. An extreme borehole with this inverted salinity distribution is borehole KFR101. The diluted groundwater at the bottom of this borehole shows a chloride concentration significantly below that of the present Baltic Sea and even more below the salinity observed (from measured EC) a few hundred metres up in the same borehole. One possible explanation is the large variation in transmissivities between the major fracture zones and the less fractured rock in between. It is also probable that the transmissivity of the different fractures/fracture zones has varied through time, i.e. some fracture(s) may have had enhanced transmissivities restricted to the period of deglaciation.
- The more than twenty years of supervision of groundwater conditions in the SFR facility has allowed unique possibilities to observe and evaluate changes in the groundwater composition caused by drawdown effects from the SFR repository. Such information provides hydrogeological support to the hydrogeological site description and further emphasises that groundwater in bedrock volumes at some distance from major transmissive zones is preserved in low flow to stagnant hydraulic conditions.

8.2 Future issues and further modelling work

The interpretation and modelling work will continue in order to improve and refine the presented preliminary hydrogeochemical site description (version 0.2) and ultimately to produce the final version 1.0 for the SFR site. Additional approaches such as geochemical equilibrium calculations and M3 modelling (mixing calculations) will be carried out in order increase the understanding of the reaction and mixing processes in the groundwaters. Furthermore, the limited gas and microbe data will be treated and discussed in the hope that it may contribute to the general understanding of the site. The understanding of the previous groundwater history and the knowledge of the present groundwater conditions will be used to provide a description of future hydrogeochemical stability. The fracture mineral frequencies will be evaluated since fracture minerals contribute to the buffering capacities concerning pH and redox (i.e. providing reducing capacity).

A closer integration with geology and hydrogeology will also be necessary in order to obtain consistency in the final model versions. The geological site description version 1.0 will be first in line of the final site descriptions to be completed and therefore considerations and adjustments to the deformation zone model, which is based also on the recent SFR extension boreholes, will be the first step in continuing the hydrogeochemical work. Equally, if not more important, is to integrate the hydrogeological flow model when completed in order to improve the description of the hydrogeological conditions at the site in terms of flow directions and distribution of hydraulic transmissivities. This will lead to a more in-depth understanding of the hydrochemistry and a more robust hydrogeochemical site description model and visualisation.

References

SKB's (Svensk Kärnbränslehantering AB) publications can be found at www.skb.se/publications

Alexeev S V, Alexeeva L P, 2003. Hydrogeochemistry of the permafrost zone in the central part of the Yakutian diamond-bearing province, Russia. Hydrogeology Journal, 11, pp 574–581.

Auqué L, Gimeno M J, Gómez J, Nilsson A-C, 2008. Potentiometrically measured Eh in groundwaters from the Scandinavian Shield. Applied Geochemistry, 23, pp 1820–1833.

Axelsson C-L, 1997. Data for calibration and validation of numerical models at SFR nuclear waste repository, Forsmark, Sweden. SKB R-98-48, Svensk Kärnbränslehantering AB.

Axelsson C-L, Mærsk Hansen L, 1997. Update of structural models at SFR nuclear waste repository, Forsmark, Sweden. SKB R-98-05, Svensk Kärnbränslehantering AB.

Berg C, 2010. Site investigation SFR. Hydrochemical sampling and analyses of groundwater in borehole KFR106. Results from two investigated borehole sections. SKB P-10-24, Svensk Kärnbränslehantering AB.

Björck S, 1995. A review of the history of the Baltic Sea, 13–8 ka. Quarternary International, 27, pp 19–40.

Bodén A, Lundin J, 2007. SFR kontrollprogram. Bergkontroll. Bergkontrollgruppens årsrapport 2006. Huvudrapport. Doknr 2448900-001, Vattenfall Power Consultant AB (in Swedish).

Carlsson, L, Carlsten, S, Sigurdsson, T, Winberg, A, 1985. Hydraulic modeling of the final repository for reactor waste (SFR). Compilation and conceptualization of available geological and hydrogeological data. SKB SFR 85-06, Svensk Kärnbränslehantering AB.

Christiansson R, Bolvede P, 1987. Byggnadsgeologisk uppföljning – Slutrapport. SKB SFR 87-03, Svensk Kärnbränslehantering AB (in Swedish).

Curtis P, Petersson J, Triumf C-A, Isaksson H, 2009. Site investigation SFR. Deformation zone modelling. Model version 0.1. SKB P-09-48, Svensk Kärnbränslehantering AB.

Drever J I, 1997. The geochemistry of natural waters: surface and groundwater environments. 3rd ed. Upper Saddle River, N.J.: Prentice Hall.

Follin S, Johansson P-O, Hartley L, Holton D, McCarthy R, Roberts D, 2007a. Updated strategy and test of new concepts for groundwater flow modelling in Forsmark in preparation of site descriptive modelling stage 2.2. SKB R-07-20, Svensk Kärnbränslehantering AB.

Follin S, Levén J, Hartley L, Jackson P, Joyce S, Roberts D, Swift B, 2007b. Hydrogeological characterisation and modelling of deformation zones and fracture domains, Forsmark modelling stage 2.2. SKB R-07-48, Svensk Kärnbränslehantering AB.

Follin S, Hartley L, Jackson P, Roberts D, Marsic N, 2008a. Hydrogeological conceptual model development and numerical modelling using CONNECTFLOW, Forsmark modelling stage 2.3. SKB R-08-23, Svensk Kärnbränslehantering AB.

Follin S, Stephens M B, Laaksoharju M, Nilsson A-C, Smellie J A T, Tullborg E-L, 2008b. Modelling the evolution of hydrochemical conditions in the Fennoscandian Shield during Holocene time using multidisciplinary information. Applied Geochemistry, 23, pp 2004–2020.

Fredén C (ed), 2002. Sveriges nationalatlas. Berg och Jord. Stockholm: SNA publishing (in Swedish).

Gimeno M J, Auqué L F, Gómez J B, Acero P, 2008. Water-rock interaction modelling and uncertainties of mixing modelling SDM-Site Forsmark. SKB R-08-86, Svensk Kärnbränslehantering AB.

Gustavsson E, Jönsson S, Ludvigson J-E, 2006. Forsmark site investigation. Pumping tests and flow logging. Boreholes HFM33, HFM34 and HFM35. SKB P-06-193, Svensk Kärnbränslehantering AB.

Hedenström A, Sohlenius G, Strömgren M, Brydsten L, Nyman H, 2008. Depth and stratigraphy of regolith at Forsmark. Site desprictive modelling, SDM-Site Forsmark. SKB R-08-07, Svensk Kärnbränslehantering AB.

Heginbottom J A, Dubreuil M A, Harker P A, 1995. Canada – Permafrost. In: National atlas of Canada. 5th ed. National Atlas Information Service, Natural Resources Canada, MCR 4177.

Holden B, Stotler R L, Frape S K, Ruskeeniemi T, Talikka M, Freifeld B M, 2009. High Lake permafrost comparison site: Permafrost phase IV. NWMO TR-2009-11, Nuclear Waste Management Organization, Canada.

Holmén J G, 2005. SFR-1. Inverse modelling of inflow to tunnels and propagation of estimated uncertainties to predictive stages. SKB R-05-74, Svensk Kärnbränslehantering AB.

Holmén J G, Stigsson M, 2001a. Modelling of future hydrogeological conditions at SFR. SKB R-01-02, Svensk Kärnbränslehantering AB.

Holmén J G, Stigsson M, 2001b. Details of predicted flow in deposition tunnels at SFR, Forsmark. SKB R-01-21, Svensk Kärnbränslehantering AB.

Jönsson S, Harrström J, Ludvigson J-E, Nilsson A-C, 2008. Site investigation SFR. Hydraulic tests, flow logging and hydrochemical sampling. Boreholes HFR101, HFR102 and HFR105. SKB P-08-87, Svensk Kärnbränslehantering AB.

Kukkonen I T, Šafanda J, 2001. Numerical modelling of permafrost in bedrock in northern Fennoscandia during the Holocene. Global and Planetary Change, 29, pp 259–273.

Laaksoharju M, Gurban I, 2003. Groundwater chemical changes at SFR in Forsmark. SKB R-03-03, Svensk Kärnbränslehantering AB.

Laaksoharju M, Smellie J, Tullborg E-L, Gimeno M, Hallbek L, Molinero J, Waber N, 2008. Bedrock hydrogeochemistry Forsmark. Site descriptive modeling, SDM-Site Forsmark. SKB R-08-47, Svensk Kärnbränslehantering AB.

Lindquist A, Nilsson K, 2010. Site investigation SFR. Hydrochemical characterisation of groundwater in borehole KFR105. Results from five investigated borehole sections. SKB P-10-02, Svensk Kärnbränslehantering AB.

Nilsson A-C, 2009. Site investigation SFR. Presentation and evaluation of hydrogeochemical data from SFR-boreholes, 1984–2007. SKB P-09-45, Svensk Kärnbränslehantering AB.

Nilsson A-C (ed), Berg C, Jönsson S, Harrström J, Thur P, Borgiel M, Qvarfordt S, 2010. Forsmark site investigation. Hydrochemical monitoring of groundwaters and surface waters. Results from water sampling in the Forsmark area, January 2009–December 2009. SKB P-10-40, Svensk Kärnbränslehantering AB.

Nilsson G, 2009. Site investigation SFR. Drilling of the cored borehole KFR105. SKB P-09-41, Svensk Kärnbränslehantering AB.

Odén M, 2009. Site investigation SFR. Hydrogeological modelling at SFR using DarcyTools. Site description SFR version 0.0. SKB P-08-94, Svensk Kärnbränslehantering AB.

Olofsson I, Simeonov A, Stephens M, Follin S, Nilsson A-C, Röshoff K, Linberg U, Lanaro F, Fredriksson A, Persson L, 2007. Site descriptive modeling Forsmark, stage 2.2. A fracture domain concept as a basis for the statistical modelling of fractures and minor deformation zones, and interdisciplinary coordination. SKB R-07-15, Svensk Kärnbränslehantering AB.

Pitkänen P, Luukkonen A, Ruotsalainen P, Leino-Forsman H, Vuorinen U, 1999. Geochemical modelling of groundwater evolution and residence time at the Olkiluoto site. Posiva 98-10, Posiva Oy, Finland.

Pitkänen P, Partamies S, Luukkonen A, 2004. Hydrogeochemical interpretation of baseline groundwater conditions at the Olkiluoto site. Posiva 2003-07, Posiva Oy, Finland.

Posiva, 2009a. Olkilouto site description 2008, Part 1. Report 2009-1, Posiva Oy, Finland .

Posiva, 2009b. Olkilouto site description 2008, Part 2. Report 2009-2, Posiva Oy, Finland.

Påsse T, 1997. A mathematical model of past, present and future shore level displacement of Fennoscandia. SKB TR 97-28, Svensk Kärnbränslehhantering AB.

Sandström B, Tullborg E-L, Smellie J, MacKenzie A B, Suksi J, 2008. Fracture mineralogy of the Forsmark site. SDM-Site Forsmark. SKB R-08-102, Svensk Kärnbränslehantering AB.

Sigurdsson T, 1987. Bottenundersökning av ett område ovanför SFR, Forsmark. SKB SFR 87-07, Svensk Kärnbränslehantering AB (in Swedish).

Smellie J, Tullborg E-L, Nilsson A-C, Gimeno M, Sandström B, Waber N, Gascoyne M, 2008. Explorative analysis of major components and isotopes SDM-Site Forsmark. SKB R-08-84, Svensk Kärnbränslehantering AB.

Stephens M B, Fox A, La Pointe P, Simeonov A, Isaksson H, Hermanson J, Öhman J, 2007. Geology Forsmark. Site descriptive modeling, Forsmark stage 2.2. SKB R-07-45, Svensk Kärnbränslehantering AB.

Svensson U, 1996. SKB Palaeohydrogeological programme. Simulations of regional groundwater flows, as forced by glaciation cycles. SKB Utveckling Progress Report U-96-35, Svensk Kärnbränslehantering AB.

Svensson U, Follin, S, 2009. Groundwater flow modelling of the excavation and operation periods – SR-Site Forsmark. SKB R-09-19, Svensk Kärnbränslehantering AB.

Söderbäck B (ed), 2008. Geological evolution, palaeoclimate and historical development of the Forsmark and Laxemar-Simpevarp areas. Site descriptive modeling, SDM-Site. SKB R-08-19, Svensk Kärnbränslehantering AB.

Ruskeeniemi T, Paananen M, Ahonen L, Kaija J, Kuivamäki A, Frape S, Morén L, Degnan P, 2002. Permafrost at Lupin: report of phase I. Report YST-112, Geological Survey of Finland, Nuclear Waste Disposal Research.

Ruskeeniemi T, Ahonen L, Paananen M, Frape S, Stotler R, Hobbs M, Kaija J, Degnan P, Blomqvist R, Jensen M, Lehto K, Morén L, Puigdomènech I, Snellman M, 2004. Permafrost at Lupin: report of phase II. Report YST-119, Geological Survey of Finland, Nuclear Waste Disposal Research.

SKB, 2008a. Geovetenskapligt undersökningsprogram för utbyggnad av SFR. SKB R-08-67, Svensk Kärnbränslehantering AB (in Swedish).

SKB, 2008b. Bedrock hydrogeochemistry Forsmark. Site descriptive modelling SDM-Site Forsmark. SKB R-08-47, Svensk Kärnbränslehantering AB.

Tarasov L, Peltier W R, 2007. The coevolution of continental ice cover and permafrost extent over the last glacial-interglacial cycle in North America. Journal of Geophysical Research, 112, F02S08, doi:10.1029/2006JF000661.

Thur P, Nilsson K, 2009a. Site investigation SFR. Hydrogeochemical characterisation of groundwater in borehole KFR101 and results from water sampling and analyses in boreholes KFR02, KFR7A, KFR08 and KFR56. Sampling during winter 2008–2009. SKB P-09-53, Svensk Kärnbränslehantering AB.

Thur P, Nilsson K, 2009b. Site investigation SFR. Hydrogeochemical characterisation of groundwater in borehole KFR102A. Results from water sampling and analyses during March 2009. SKB P-09-50, Svensk Kärnbränslehantering AB.

Thur P, Jönsson S, Harrström J, Ludvigson J-E, 2009. Site investigation SFR. Hydraulic tests, flow logging and chemical sampling. Borehole HFR106. SKB P-09-54, Svensk Kärnbränslehantering AB.

Tröjbom M, Söderbäck B, Johansson P-O, 2007. Hydrochemistry in surface water and shallow groundwater. Site descriptive modelling, SDM-Site Forsmark SKB R-07-55, Svensk Kärnbränslehantering AB.

Upstill-Goddard R C, Elderfield H, 1988. The role of diagenesis in the estuarine budgets of iodine and bromine. Continental Shelf Research, 8, pp 405–430.

Waber H N, Gimmi T, Smellie J A T, deHaller A, 2009. Porewater in the rock matrix. Site descriptive modelling, SDM-Site Laxemar. SKB R-08-112, Svensk Kärnbränslehantering AB.

Westman P, Wastegård S, Schoning K, Gustafsson B, 1999. Salinity change in the Baltic Sea during the last 8,500 years: evidence, causes and models. SKB TR-99-38, Svensk Kärnbränslehantering AB.

Öhman J, Follin S, 2010. Site investigation SFR. Hydrogeological modelling of SFR. Data review and parameterisation of model version 0.1. SKB P-09-49, Svensk Kärnbränslehantering AB.